Examination of animal gut microbiota and mercury reveals the importance of diet in this relationship

Galen Guo

Thesis submitted to the University of Ottawa
in partial Fulfillment of the requirements for the
Doctorate in Philosophy degree in Biology

Department of Biology
Faculty of Science
University of Ottawa

Abstract

Methylmercury (MeHg) is a global pollutant that can bioaccumulate and biomagnify along the aquatic food chain, causing adverse outcomes in humans and wildlife. Effective biomonitoring programs are needed to identify high exposure populations and to develop proper mitigation strategies. However, biomonitoring results showed high inter-individual variability in the relationship between MeHg exposure and body burden. Moreover, the gut microbiota can potentially play a role in MeHg transformations, and it is widely believed that the gut microbiota may be the underlying reason for the variability between and within a population. However, the microbially-mediated mechanisms of Hg transformation in the gastrointestinal environment is poorly understood. The overarching goal of my thesis is to investigate the role of gut microbiota in MeHg transformation in human, and the relationship between environmental pollutants and the gut microbiota of sentinel species such as river otters (*Lontra canadensis*) and seabirds (Arctic Tern [*Sterna paradisaea*], Black Guillemot [*Cepphus grille*], Common Eider [*Somateria mollissima*], Double-crested Cormorant [*Phalacrocorax auratus*], and Leach's Storm Petrel [*Oceanodroma leucorhoa*]). My thesis consists of four research papers. In the first paper, I discovered that the gut microbiota`s ability to demethylate MeHg is significantly enhanced by altering the diet. In my second paper, I discovered a novel MeHg degradation pathway. In the third and fourth papers, I explored the effect of Hg and other environmental contaminant exposure on river otters and seabirds gut microbial community structures and found a relationship between prey selection and diet to the gut microbial structure. In conclusion, my thesis explores the relationship between diet, prey selection, environment contaminants and the humans and wildlife gut microbiota and contributes to understanding the gut microbiota's role in biomonitoring of ecosystem and human health.

Résumé

Le méthylmercure (MeHg) est un polluant mondial qui peut se bioaccumuler et se bioamplifier le long de la chaîne alimentaire aquatique, entraînant des effets néfastes chez les humains et la faune. Des programmes de biosurveillance efficaces sont nécessaires pour identifier les populations fortement exposées et pour développer des stratégies d'atténuation appropriées. Cependant, les résultats de la biosurveillance ont montré une forte variabilité interindividuelle dans la relation entre l'exposition au MeHg et la charge corporelle. De plus, le microbiote intestinal peut potentiellement jouer un rôle dans les transformations du MeHg, et il est largement admis que le microbiote intestinal peut être la cause de la variabilité entre et au sein d'une population. Cependant, les mécanismes causant la transformation microbienne du Hg dans l'environnement gastro-intestinal sont mal compris. L'objectif primordial de ma thèse est d'étudier le rôle du microbiote intestinal dans la transformation du MeHg chez l'homme, et la relation entre les polluants environnementaux et le microbiote intestinal d'espèces sentinelles telles que la loutre de rivière (Lontra canadensis) et les oiseaux de mer (Sterne arctique [Sterna paradisaea]) , Guillemot noir [Cepphus grille], Eider à duvet [Somateria mollissima], Cormoran à aigrettes [Phalacrocorax auratus] et Pétrel orageux de Leach [Oceanodroma leucorhoa]). Ma thèse se compose de quatre articles de recherche. Dans le premier article, j'ai découvert que la capacité du microbiote intestinal à déméthyler MeHg est considérablement améliorée en modifiant le régime alimentaire. Dans mon deuxième article, j'ai découvert une nouvelle voie de dégradation du MeHg. Dans le troisième et le quatrième articles, j'ai exploré l'effet de l'exposition au Hg et à d'autres contaminants environnementaux sur les structures microbiennes intestinales des loutres de rivière et des oiseaux de mer et j'ai trouvé une relation entre la sélection des proies et le régime alimentaire sur la structure microbienne intestinale. En conclusion, ma thèse explore la relation entre l'alimentation, la sélection des proies, les contaminants de l'environnement et le microbiote intestinal des humains et de la faune et contribue à comprendre le rôle du microbiote intestinal dans la biosurveillance de l'écosystème et de la santé humaine.

Acknowledgements

First and foremost, I would like to express my sincere gratitude to my supervisors Dr. Laurie Chan and Dr. Alexandre Poulain. I am deeply grateful for the mentorship, time, and resources you have provided me the past few years. I will always admire your perseverance and commitment to your work. Laurie, I will always cherish the lunch hour talk we have as it provided some sort of normalcy during this hectic Ph.D, as well as your wisdom you have shared with me. Alex, thank you for showing what true work-life balance is and what it means. I cannot thank you both enough.

Second, I would like to thank my labmates in the Chan lab and Poulain lab. Thank you for the time you offered listening to my talk even though its widely different to anything you do (a bit less to Poulain lab). A special and heartfelt thanks to Dr. Emmanuel Yumvihoze. I appreciate the brainstorming sessions, your continual support and technical expertise throughout my Ph.D. A special thank you to Kayla Greydanus to help me navigate the bureaucratic part, if it weren't for your help, I would probably still be waiting for a refund. Lastly, a big thank you to all the undergraduate students I supervised for the past four years. Your help was immense, and I much appreciate the opportunity to mentor you.

My family and friend, thank you for your patience and support through these tumultuous times. I am also sorry for plugging science story in every discussion we have. But I will keep doing so. Special thank you to my mom, your unwavering support and sacrifices [特别感谢我的妈妈, 您的坚定支持和牺牲。]

Most importantly, a heartful thanks to my wife, Maggie. I would have never pursued and accomplished this much without your guidance. You have made sacrifices and provided an immense emotional support. For that, I will always be in your debt.

Dedication

In loving memory of my dad, Ming Qi

Thank you

为了纪念我的父亲，郭铭祺

谢谢

Table of Contents

List of Figures

List of tables

Chapter 1: General introduction

1.1 Rationale

Mercury (Hg) is one of the most toxic metals in the environment. The organic form, methylmercury (MeHg) is a potent neurotoxicant of particular concern as it can be bioaccumulated and bioamplified along the food chain [1]. Therefore, higher trophic predatory seabirds and marine mammals have higher levels of MeHg [2–4]. Global MeHg contamination poses a critical health risk to wildlife and human populations who rely on fish and seafood for sustenance [1]. Based on the current knowledge of MeHg toxicodynamic, the World Health Organization and The Food and Agriculture Organization still recommends fish consumption among the general population. The health benefits outweigh the potential risk associated with MeHg toxicity [5–7]. There is growing evidence that the gut microbiota can influence the bioavailability of MeHg [8,9]. The role of the gut microbiota is currently not considered in toxicodynamic models predicting exposure to MeHg [1]. Moreover, it is unclear how diet (an important factor influencing the gut microbiota structure and function) can alter gut microbiota ability to biotransform MeHg. It elucidates an important challenge in Hg exposure modelling: interindividual variability.

Hg is a global pollutant emitted from natural sources (volcanoes, hydrothermal vents) and anthropogenic sources (small-scale artisanal mines, coal combustion) [10]. Gaseous Hg can remain in the atmosphere for up to a year and enter freshwater and marine ecosystems through wet and dry deposition [10]. Thus, since the Industrial Revolution, global ocean Hg has triple above the aphotic zone [11], and increased Hg concentration was found in freshwater fish populations [12]. Due to Hg's bioaccumulative properties, marine wildlife is at a higher risk of Hg associated adverse

effects. However, current knowledge on wildlife Hg exposure is insufficient to determine the impact and future impact on wildlife health due to elevated Hg exposure [13].

1.2 Human gut microbiome

The gut microbiota (microbes within the gut environment) plays an essential role in digestion [14], our immune system [15], and possibly protection against heavy metals [16,17]. The gastrointestinal tract harbours greater than 10^{12} microorganisms per ml of luminal content and more than 5 million unique genes, making the gut microbiota a diverse and dense microbial community [18]. This microbial ecosystem is highly dynamic and shaped by environmental factors such as diet, drug intake, contaminant exposure and intrinsic factors such as sex, age, and host genetics [19–21]. Moreover, recent studies have shown the importance of Eukaryote (protozoan and fungi) on the gut microbiota structure and the host's immune system [22–24].

There is currently a debate about whether environmental variables or the host genetic makeup influence gut microbial community structure and function. Goodrich et al. [25] conducted a large twin-pairs (n = 416) study and shown that the host's genetic makeup affects the abundance of specific gut microbiota taxa. In contrast, Rothschild et al. [26], by examining the genotypes and microbiome data from 1,046 healthy Israeli individuals (distinct ancestral origins sharing a similar environment), argued the opposite; in their study, environmental factor dominated the genetic makeup of the host. A growing body of literature supports environmental factors as an essential contributor in shaping the gut microbiome community structure and function [26–29]. The gut microbiome (genes encoded by the gut microbiota) is a source of genetic and metabolic diversity across populations [30]. At birth, contact with our immediate environment influences the community

structure of the gut microbiome. Our lifestyle, immune system and diet shape our gut microbiota as we grow older [15,28,31,32].

Multiple studies have provided evidence suggesting that diet can alter the human gut microbiome and influence gut health [30,31,33]. A recent study performed a two-week food exchange with subjects from the same populations, where African Americans were given a high-fibre, low-fat African-style diet, and rural Africans were given a high-fat, low-fibre western-style diet. Compared with their usual diets, the food switch resulted in reciprocal changes i) in mucosal biomarkers of cancer risk and ii) in aspects of the microbiota and metabolites known to affect cancer risk. Both conclusions were illustrated by the increased saccharolytic fermentation and butyrogenesis and the suppressed secondary bile acid synthesis in the African Americans [34]. Other studies have compared gut microbiome community structures between individuals living in rural vs. urban environments and reported shifts in the dominant taxa ratio and speculated that the host's diet was one of the main contributing factors [31,35,36]. These studies highlighted the importance of diet in shaping and maintaining a healthy steady-state gut microbiome. Nonetheless, the importance of how diet influences the gut microbiome's ability to metabolize or biotransform heavy metals remains to be determined.

1.3 MeHg interindividual variability and the potential role of the gut microbiota

The body burden of MeHg is often measured by the concentration of total Hg in hair. However, there is a considerable variation between estimated MeHg oral intake and hair Hg concentration in many populations [37]. To estimate human exposure to MeHg, risk assessors use standard models that assume 90 to 100% of MeHg [38] and 7-15% of Hg [39] ingested is bioavailable. However, as Bradley et al. [9] discussed in their systematic review of 45 studies, overall absorption estimates

range from 12% to 79% for MeHg and 49% to 69% for inorganic divalent Hg(II). This discrepancy suggests the existence of unknown factors that are not currently considered in modelling MeHg exposure risk.

The origin of the food, cooking methods and other ingested micronutrients (e.g., selenium, Se) could potentially alleviate MeHg toxicity by reducing bioavailability and bioaccessibility [40,41]. Li et al. [8] have shown that age, body weight, gender, ethnicity, household income, and geographic regions only account for 32% of the total variance in measured hair Hg concentrations. The authors suggested that other factors, such as diet or the gut microbiota activity, might explain the remaining variance. Indeed, Rand et al. [42] conducted a feeding experiment, during which fish were fed to human volunteers, and reported a high degree of inter-individual variability in the MeHg biotransformation kinetics. They proposed that the gut microbiome can be a significant modulating factor for MeHg absorption. Later, Caito et al. [43] showed that individuals who received antibiotic therapy had decreased MeHg elimination rate, further suggesting the gut microbiome's role in eliminating MeHg.

There is currently a knowledge gap on the genetic determinants and microbial mechanisms involved in Hg's biotransformation in the gut environment. Although a great emphasis has been placed on the mechanisms that control the formation of MeHg, fewer studies have addressed the fate of MeHg after it is produced. Most of our knowledge of MeHg biotransformation was gathered from experiments performed outside the human gut (e.g., lake sediments, wetlands). Two pathways can usually be identified for bacterially mediated MeHg demethylation: (1) a reductive process, producing Hg^0 and CH_4 usually found in Hg-contaminated sites [44], and (2) an oxidative process producing Hg^{2+} and CO_2 in unpolluted sites [45–47]. The reductive process is mediated

through an enzyme encoded by the *mer*-operon (organomercurial-lyase pathway), allowing the microorganism to be Hg-resistant. It is believed that the oxidative demethylation process occurs through the co-metabolism of MeHg and small organic compounds [45]. However, the enzymatic pathway is unknown. Finally, demethylation of MeHg by methanotrophs (CH_4-consuming microbes) was inhibited by methanol [48]. It probably indicates C1-metabolizing microaerobes' involvement in controlling the degradation of MeHg in environmental samples. The mechanisms of MeHg degradation in the human gut remain unknown.

Hg biotransformation in the gut environment is mainly unexplored. Few studies have reported that fish and zooplankton's guts can potentially methylate Hg [49,50], and the gut of rat and marine fish can demethylate MeHg [51–55]. The human gut does not appear to be a hotspot for MeHg production [56] but appears suitable for MeHg degradation [57]. Genes involved in Hg methylation (*hgcA* and *hgcB*) were undetected in healthy human individuals' gut microbiome [56,58]. However, genes involved in Hg and MeHg detoxification, encoded by the *mer*-operon, were detected [59,60]. The nature and importance of the microbial pathways involved in MeHg biotransformation remain a major gap in our knowledge, possibly limiting our ability to manage MeHg exposure through the diet.

1.4 Sentinel species gut microbiome

Sentinel species are organisms sensitive to environmental changes and are used by researchers to detect risks to humans by providing early warning of danger [61]. Sentinel species are designed to reveal and to monitor environmental contamination and the bioavailability of contaminants. The main criteria for a sentinel species are: (1) it has a measurable response to the substance in question, (2) it has a small and discrete home range that overlaps with the area to monitor and (3) it can be

easily captured and enumerated [62]. Thus, many sentinel species are top predators of their respective habitat.

Due to the bioaccumulative properties of MeHg, it is assumed that top predators (especially piscivorous animals) are at the highest risk for increased MeHg exposure and Hg related health effects [63]. Recent studies have documented deleterious health effects in piscivorous wildlife that are exposed to environmentally relevant levels of MeHg [64,65]. In this thesis, I explored the relationship between Hg and the gut microbiome of sentinel species in freshwater and marine environments. I selected the river otter (*Lontra canadensis*) and seabirds (including the Arctic Tern [*Sterna paradisaea*], the Black Guillemot [*Cepphus grylle*], the Common Eider [*Somateria mollissima*], the Double-crested Cormorant [*Phalacrocorax auritus*] and the Leach's Storm-Petrel [*Oceanodroma leucorhoa*]) as sentinel species for freshwater and marine ecosystem health. However, no studies investigated the effect of Hg and MeHg on the gut microbiome of those predators.

1.5 The gut microbiota as biomarkers of ecosystem health

Environmental factors such as diet and contaminants play a significant role in the composition of the human gut microbiome [26]. I hypothesized that the same correlation could be observed in the gut microbiome of river otters and seabirds. Coolon et al. [66] observed differences in assemblages of rodent's gut taxonomy in response to contamination. Similarly, an *in vitro* experiment where zebrafish were chronically exposed to titanium dioxide nanoparticle and bisphenol A altered the gut microbiome composition and decreased commensal bacteria's abundance present [67]. Currently, there is no study on the gut microbiome of river otters. As for seabirds, the avian gut microbiota generally has a conserved group of core taxa (Firmicutes, Proteobacteria, Actinobacteria and

Bacteroidetes) [68–71] that is mostly influenced by environmental pressure exhibited by the host's habitat and diet [72–75]. Moreover, as more species are suffering population decline due to anthropogenic impact, non-invasive biomarkers' development is crucial. My goal is to investigate the relationship between Hg exposure and river otters and seabirds' gut microbiota. Moreover, I explored the potential of using alterations in the gut microbiota structure in the river otter as a biomarker of early biological effect and Hg presence.

1.6 Thesis objectives

My thesis was organized into two major sections. The first section determined the effect of diet on the human gut microbiome's ability to transform Hg and the mechanism of microbial MeHg demethylation (Chapters 2 and 3). The second section grouped studies on the relationship between Hg and the gut microbial structure of sentinel species (Chapters 4 and 5). All chapters were written as standalone manuscripts. I concluded the thesis with Chapter 6, summarizing my research contributions, limitations, and future recommendations on the importance of incorporating gut microbiology in the field of ecotoxicology.

My thesis aimed to understand the effect of Hg and other inorganic contaminants on the human and sentinel species gut microbiome. Overall, this thesis investigated the mechanism of the human gut microbiota MeHg demethylation caused by the protein and contaminant exposure effect on the gut microbiome of sentinel species (river otters and seabirds). My thesis aimed to fill a gap in understanding the bi-directional influence between contaminants and the gut microbiome of an organism. Furthermore, I aimed to provide a framework for developing a biomarker for early biological effects on wildlife in aquatic ecosystems.

The objectives in Chapters 2 and 3 were to elucidate the effect of dietary nutritional contents (carbohydrate, protein) on the gut microbial structure and role in Hg transformation, and determine part of the mechanism involved in Hg transformation. Earlier studies looking at rodent models have observed a significant decrease in MeHg uptake due to the gut microbiome [76,77]. However, none have offered any potential mechanism underlying the excretion of MeHg. With the advance in sequencing technologies and computational analyses, studying the gut microbiome has become more affordable and powerful. This exploratory study determined if human gut microbiota has an innate ability to biotransform Hg and if dietary changes can alter the gut microbial structure and increase MeHg degradation. I hypothesize that dietary changes can increase the gut microbial ability to demethylate MeHg. In Chapter 2, I developed an experimental set-up that is reproducible by ensuring the fecal microbial structure remained functionally and taxonomically undisturbed. Then, I identified a human candidate gut microbiota capable of MeHg degradation and quasi-complete degradation of MeHg with protein in the medium. I tested and found that known demethylator in soil and sediment environments were not responsible for MeHg demethylation observed in the human gastrointestinal environment [45,48]. Lastly, I identified a novel microbial pathway involved in MeHg degradation in the human gut environment using comparative metagenomic analyses.

Chapter 4 observed the effect of increased environmental pressure on the river otter gut microbial structure. River otters are sentinel species for freshwater ecosystems [78]. The assessment of river otter health is a good indicator of the health of all organisms living within the same ecosystem. A better understanding of regional anthropogenic impact can help with conservation efforts on wildlife and the ecosystem. In return, this effort can help protect the human population

who relies on the availability of a clean environment for sustainability. I expect that river otter microbial diversity is significantly disturbed due to higher contaminant exposure from oil sands surface mining.

The objective in Chapter 5 was to build on the previously established framework in Chapter 4 and determine the role of prey ecology on the relationship between the gut microbiota of seabird and Hg exposure. I chose seabirds because it is a sentinel species in the marine ecosystem [79]. Moreover, each seabird species has evolved to prey on a different niche in the ocean [80]. I determined the relationship between each seabird prey ecology on their gut microbial structure by observing different seabird species. I expect seabird's gut microbial community to correlated with trophic consumption and Hg.

1.7 Reference Cited

1. Eagles-Smith, C. A. *et al.* Modulators of mercury risk to wildlife and humans in the context of rapid global change. *Ambio* **47**, 170–197 (2018).

2. Keller, R. H., Xie, L., Buchwalter, D. B., Franzreb, K. E. & Simons, T. R. Mercury bioaccumulation in Southern Appalachian birds, assessed through feather concentrations. *Ecotoxicology* **23**, 304–316 (2014).

3. Hosseini, M., Nabavi, S. M. B. & Parsa, Y. Bioaccumulation of trace mercury in trophic levels of benthic, benthopelagic, pelagic fish species, and sea birds from Arvand River, Iran. *Biol. Trace Elem. Res.* **156**, 175–180 (2013).

4. Rimmer, C. C., Miller, E. K., McFarland, K. P., Taylor, R. J. & Faccio, S. D. Mercury bioaccumulation and trophic transfer in the terrestrial food web of a montane forest. *Ecotoxicology* **19**, 697–709 (2010).

5. Starling, P., Charlton, K., McMahon, A. & Lucas, C. Fish Intake during Pregnancy and Foetal Neurodevelopment—A Systematic Review of the Evidence. *Nutrients* **7**, 2001–2014 (2015).

6. World Health Organization. Mercury and health (Fact sheet No. 361). (2013). Available at: http://www.who.int/mediacentre/factsheets/fs361/en/. (Accessed: 1st November 2015)

7. Food and Agriculture Organization of the United Nations & World Health Organization. *Report of the Joint FAO/WHO Expert Consultation on the Risks and Benefits of Fish Consumption : Rome, 25-29 January 2010.* (Food and Agriculture Organization of the United Nations, 2011).

8. Li, M. *et al.* Insights from mercury stable isotopes into factors affecting the internal body burden of methylmercury in frequent fish consumers. *Elem. Sci. Anthr.* **4**, 000103 (2016).

9. Bradley, M., Barst, B. & Basu, N. A Review of Mercury Bioavailability in Humans and Fish. *Int. J. Environ. Res. Public Health* **14**, 169 (2017).

10. Obrist, D. *et al.* A review of global environmental mercury processes in response to human

and natural perturbations: Changes of emissions, climate, and land use. *Ambio* **47**, 116–140 (2018).

11. Lamborg, C. H. *et al.* A global ocean inventory of anthropogenic mercury based on water column measurements. *Nature* **512**, 65–68 (2014).

12. Chételat, J. *et al.* Mercury in freshwater ecosystems of the Canadian Arctic: Recent advances on its cycling and fate. *Science of the Total Environment* **509**–**510**, 41–66 (2015).

13. Scheuhammer, A. *et al.* Recent progress on our understanding of the biological effects of mercury in fish and wildlife in the Canadian Arctic. *Science of the Total Environment* **509**–**510**, 91–103 (2015).

14. Ley, R. E. *et al.* Obesity alters gut microbial ecology. *Proc. Natl. Acad. Sci. U. S. A.* **102**, 11070–5 (2005).

15. Purchiaroni, F. *et al.* The role of intestinal microbiota and the immune system. *Eur. Rev. Med. Pharmacol. Sci.* **17**, 323–333 (2013).

16. Laird, B., Van De Wiele, T., Corriveau, M., Jamieson, H. & Siciliano, S. Evaluation of the Bioaccessibility of Metals and Metalloids in Eastern Canadian Mine Tailings Using an in Vitro Gastrointestinal Model, the Simulator of the Human Intestinal Microbial Ecology (Shime). *Epidemiology* **17**, (2006).

17. Laird, B. D., Shade, C., Gantner, N., Chan, H. M. & Siciliano, S. D. Bioaccessibility of mercury from traditional northern country foods measured using an in vitro gastrointestinal model is independent of mercury concentration. *Sci. Total Environ.* **407**, 6003–8 (2009).

18. Spanogiannopoulos, P., Bess, E. N., Carmody, R. N. & Turnbaugh, P. J. The microbial pharmacists within us: a metagenomic view of xenobiotic metabolism. *Nat. Rev. Microbiol.* **14**, 273–287 (2016).

19. Maslowski, K. M. & Mackay, C. R. Diet, gut microbiota and immune responses. *Nat. Immunol.* **12**, 5–9 (2011).

20. Lu, K., Mahbub, R. & Fox, J. G. Xenobiotics: Interaction with the Intestinal Microflora.

ILAR J. **56**, 218–27 (2015).

21. Ley, R. E. *et al.* Evolution of mammals and their gut microbes. *Science (80-.).* **320**, 1647–1651 (2008).

22. Laforest-Lapointe, I. & Arrieta, M.-C. Microbial Eukaryotes: a Missing Link in Gut Microbiome Studies. *mSystems* **3**, (2018).

23. Huffnagle, G. B. & Noverr, M. C. The emerging world of the fungal microbiome. *Trends in Microbiology* **21**, 334–341 (2013).

24. Arrieta, M. C. *et al.* Associations between infant fungal and bacterial dysbiosis and childhood atopic wheeze in a nonindustrialized setting. *J. Allergy Clin. Immunol.* **142**, 424-434.e10 (2018).

25. Goodrich, J. K. *et al.* Human genetics shape the gut microbiome. *Cell* **159**, 789–99 (2014).

26. Rothschild, D. *et al.* Environment dominates over host genetics in shaping human gut microbiota. *Nature* (2018). doi:10.1038/nature25973

27. Cotillard, A. *et al.* Dietary intervention impact on gut microbial gene richness. *Nature* **500**, 585–588 (2013).

28. David, L. A. *et al.* Diet rapidly and reproducibly alters the human gut microbiome. *Nature* **505**, 559–63 (2014).

29. Wu, G. D. *et al.* Linking long-term dietary patterns with gut microbial enterotypes. *Science* **334**, 105–8 (2011).

30. Yatsunenko, T. *et al.* Human gut microbiome viewed across age and geography. *Nature* **486**, 222–7 (2012).

31. De Filippo, C. *et al.* Impact of diet in shaping gut microbiota revealed by a comparative study in children from Europe and rural Africa. *Proc. Natl. Acad. Sci. U. S. A.* **107**, 14691–6 (2010).

32. Tremaroli, V. & Bäckhed, F. Functional interactions between the gut microbiota and host

metabolism. *Nature* **489**, 242–9 (2012).

33. Schnorr, S. L. *et al.* Gut microbiome of the Hadza hunter-gatherers. *Nat. Commun.* **5**, 32–46 (2014).

34. O'Keefe, S. J. D. *et al.* Fat, fibre and cancer risk in African Americans and rural Africans. *Nat. Commun.* **6**, 6342 (2015).

35. Gorvitovskaia, A., Holmes, S. P. & Huse, S. M. Interpreting Prevotella and Bacteroides as biomarkers of diet and lifestyle. *Microbiome* **4**, 15 (2016).

36. Tyakht, A. V. *et al.* Human gut microbiota community structures in urban and rural populations in Russia. *Nat. Commun.* **4**, e132 (2013).

37. Canuel, R. *et al.* New evidence on variations of human body burden of methylmercury from fish consumption. *Environ. Health Perspect.* **114**, 302–6 (2006).

38. Aberg, B. *et al.* Metabolism of Methyl Mercury (203 Hg) Compounds in Man. *Arch. Environ. Heal. An Int. J.* **19**, 478–484 (1969).

39. Miettinen, J. K. Absorption and elimination of dietary (Hg++) and methylmercury in man. in *Mercury, Mercurial, and Mercaptans* (eds. Miller, M. W. & Clarkson, T. W.) 233–246 (1973).

40. Ouédraogo, O. & Amyot, M. Effects of various cooking methods and food components on bioaccessibility of mercury from fish. *Environ. Res.* **111**, 1064–9 (2011).

41. Ralston, N. V. C. & Raymond, L. J. Dietary selenium's protective effects against methylmercury toxicity. *Toxicology* **278**, 112–23 (2010).

42. Rand, M. D. *et al.* Methods for Individualized Determination of Methylmercury Elimination Rate and De-Methylation Status in Humans Following Fish Consumption. *Toxicol. Sci.* **149**, 385–395 (2016).

43. Caito, S. W. *et al.* Editor's Highlight: Variation in Methylmercury Metabolism and Elimination Status in Humans Following Fish Consumption. *Toxicol. Sci.* **161**, 443–453 (2018).

44. Barkay, T., Miller, S. M. & Summers, A. O. Bacterial mercury resistance from atoms to ecosystems. *FEMS Microbiol. Rev.* **27**, 355–84 (2003).

45. Oremland, R. S., Culbertson, C. W. & Winfrey, M. R. Methylmercury decomposition in sediments and bacterial cultures: involvement of methanogens and sulfate reducers in oxidative demethylation. *Appl. Environ. Microbiol.* **57**, 130–7 (1991).

46. Martín-Díaz, M. L., Jiménez-Tenorio, N., Sales, D. & Delvalls, T. A. Accumulation and histopathological damage in the clam Ruditapes philippinarum and the crab Carcinus maenas to assess sediment toxicity in Spanish ports. *Chemosphere* **71**, 1916–27 (2008).

47. Kronberg, R.-M., Schaefer, J. K., Björn, E. & Skyllberg, U. Mechanisms of Methyl Mercury Net Degradation in Alder Swamps: The Role of Methanogens and Abiotic Processes. *Environ. Sci. Technol. Lett.* acs.estlett.8b00081 (2018). doi:10.1021/acs.estlett.8b00081

48. Lu, X. *et al.* Methylmercury uptake and degradation by methanotrophs. *Sci. Adv.* **3**, e1700041 (2017).

49. Wang, R., Feng, X.-B. & Wang, W.-X. In Vivo Mercury Methylation and Demethylation in Freshwater Tilapia Quantified by Mercury Stable Isotopes. *Environ. Sci. Technol.* **47**, 7949–7957 (2013).

50. Gorokhova, E., Soerensen, A. L. & Motwani, N. H. Mercury-methylating bacteria are associated with zooplankton: a proof-of-principle survey in the Baltic Sea. *bioRxiv* 279976 (2018). doi:10.1101/279976

51. Urano, T., Iwasaki, A., Himeno, S., Naganuma, A. & Imura, N. Absorption of methylmercury compounds from rat intestine. *Toxicol. Lett.* **50**, 159–64 (1990).

52. Rowland, I. R., Robinson, R. D. & Doherty, R. A. Effects of diet on mercury metabolism and excretion in mice given methylmercury: role of gut flora. *Arch. Environ. Heal. An Int. J.* **39**, 401–8 (1984).

53. Rowland, I. R., Mallett, A. K., Flynn, J. & Hargreaves, R. J. The effect of various dietary fibres on tissue concentration and chemical form of mercury after methylmercury exposure in mice. *Arch. Toxicol.* **59**, 94–98 (1986).

54. Nakamura, I., Hosokawa, K., Tamura, H. & Miura, T. Reduced mercury excretion with feces in germfree mice after oral administration of methyl mercury chloride. *Bull. Environ. Contam. Toxicol.* **17**, 528–33 (1977).

55. Wang, X., Wu, F. & Wang, W.-X. In Vivo Mercury Demethylation in a Marine Fish (Acanthopagrus schlegeli). *Environ. Sci. Technol.* **51**, 6441–6451 (2017).

56. Podar, M. *et al.* Global prevalence and distribution of genes and microorganisms involved in mercury methylation. *Sci. Adv.* **1**, e1500675–e1500675 (2015).

57. Rowland, I. R. Interactions of the Gut Microflora and the Host in Toxicology. *Toxicol. Pathol.* **16**, 147–153 (1988).

58. Gilmour, C. C. *et al.* Mercury methylation by novel microorganisms from new environments. *Environ. Sci. Technol.* **47**, 11810–20 (2013).

59. Osborn, A. M., Bruce, K. D., Strike, P. & Ritchie, D. A. Distribution, diversity and evolution of the bacterial mercury resistance (mer) operon. *FEMS Microbiol. Rev.* **19**, 239–62 (1997).

60. Rothenberg, S. E. *et al.* The role of gut microbiota in fetal methylmercury exposure: insights from a pilot study. *Toxicol. Lett.* **242**, 60–67 (2016).

61. Bossart, G. D. Marine mammals as sentinel species for oceans and human health. *Vet. Pathol.* **48**, 676–690 (2011).

62. National Research Council (US). Committee on Animals as Monitors of Environmental Hazards. Animals as Sentinels of Environmental Health Hazards. Concepts and Definitions. in *Animals as Sentinels of Environmental Health Hazards* (National Academies Press (US), 1991).

63. Wiener, J. G., Krabbenhoft, D. P., Heinz, G. H. & Scheuhammer, A. M. Ecotoxicology of mercury. in *Handbook of Ecotoxicology* (eds. Hoffman, D. J., Rattner, B. A., Burton, G. A. & Cairns, J.) 409–463 (2003).

64. Scheuhammer, A. M. & Sandheinrich, M. B. Recent advances in the toxicology of methylmercury in wildlife. *Ecotoxicology* **17**, 67–68 (2008).

65. Depew, D. C., Burgess, N. M. & Campbell, L. M. Spatial Patterns of Methylmercury Risks to Common Loons and Piscivorous Fish in Canada. *Environ. Sci. Technol.* **47**, 13093–13103 (2013).

66. Coolon, J. D., Jones, K. L., Narayanan, S. & Wisely, S. M. Microbial ecological response of the intestinal flora of Peromyscus maniculatus and P. leucopus to heavy metal contamination. *Mol. Ecol.* **19**, 67–80 (2010).

67. Chen, L. *et al.* Dysbiosis of gut microbiota by chronic coexposure to titanium dioxide nanoparticles and bisphenol A: Implications for host health in zebrafish. *Environ. Pollut.* **234**, 307–317 (2018).

68. Dewar, M. L., Arnould, J. P. Y., Krause, L., Dann, P. & Smith, S. C. Interspecific variations in the faecal microbiota of Procellariiform seabirds. *FEMS Microbiol. Ecol.* **89**, 47–55 (2014).

69. Dewar, M. L. *et al.* Microbiota of little penguins and short-tailed shearwaters during development. *PLoS One* **12**, e0183117 (2017).

70. Fuirst, M., Veit, R. R., Hahn, M., Dheilly, N. & Thorne, L. H. Effects of urbanization on the foraging ecology and microbiota of the generalist seabird Larus argentatus. *PLoS One* **13**, e0209200 (2018).

71. Waite, D. W. & Taylor, M. W. Exploring the avian gut microbiota: Current trends and future directions. *Frontiers in Microbiology* **6**, (2015).

72. Wu, Y. *et al.* Habitat environments impacted the gut microbiome of long-distance migratory swan geese but central species conserved. *Sci. Rep.* **8**, 1–11 (2018).

73. Lucas, F. S. & Heeb, P. Environmental factors shape cloacal bacterial assemblages in great tit *Parus major* and blue tit *P. caeruleus* nestlings. *J. Avian Biol.* **36**, 510–516 (2005).

74. Hird, S. M., Carstens, B. C., Cardiff, S. W., Dittmann, D. L. & Brumfield, R. T. Sampling locality is more detectable than taxonomy or ecology in the gut microbiota of the brood-parasitic Brown-headed Cowbird (Molothrus ater). *PeerJ* **2014**, e321 (2014).

75. Grond, K. *et al.* Composition and Drivers of Gut Microbial Communities in Arctic-Breeding Shorebirds. *Front. Microbiol.* **10**, 2258 (2019).

76. Norseth, T. Biliary excretion and intestinal reabsorption of mercury in the rat after injection of methyl mercuric chloride. *Acta Pharmacol. Toxicol. (Copenh).* **33**, 280–288 (1973).

77. Rowland, I. R., Davies, M. J. & Evans, J. G. Tissue Content of Mercury in Rats Given Methylmercuric Chloride Orally: Influence of Intestinal Flora. *Arch. Environ. Heal. An Int. J.* **35**, 155–160 (1980).

78. Peterson, E. K. & Schulte, B. A. Impacts of Pollutants on Beavers and Otters with Implications for Ecosystem Ramifications. *J. Contemp. Water Res. Educ.* **157**, 33–45 (2016).

79. Hazen, E. L. *et al.* Marine top predators as climate and ecosystem sentinels. *Front. Ecol. Environ.* **17**, 565–574 (2019).

80. Croxall, J. P. *et al.* Seabird conservation status, threats and priority actions: A global assessment. *Bird Conserv. Int.* **22**, 1–34 (2012).

Chapter 2: Monomethylmercury degradation by the human gut microbiota is stimulated by protein amendments

G. Guo, E. Yumvihoze, A.J. Poulain and H.M. Chan*

Department of Biology, Faculty of Science, University of Ottawa, Ottawa, Canada K1N 9B4

This manuscript was originally published as:

G Guo, E Yumvihoze, AJ Poulain, HM Chan. Monomethylmercury degradation by the human gut microbiota is stimulated by protein amendments. *The Journal of Toxicological Sciences*, **2018**, *43*, (12). 717-725.

2.1 **Abstract**

Monomethylmercury (MMHg) is a potent neurotoxicant that can be bioaccumulated and biomagnified through trophic levels. Human populations whose diets contain MMHg are at risk of MMHg toxicity. The gut microbiota was identified as a potential factor causing variation in MMHg absorption and body burden. However, little is known about the role of gut microbiota on Hg transformations. We conducted a series of *in vitro* experiments to study the effects of dietary nutrient change on Hg metabolism and the human gut microbiota using anoxic fecal slurry incubations. We used stable Hg isotope tracers to track MMHg production and degradation and characterized the microbiota using high throughput sequencing of the 16S rRNA gene. We show that the magnitude of MMHg degradation is individual dependent and rapidly responds to changes in nutrient amendments, leading to complete degradation of the MMHg present. Although the mechanism involved remains unknown, it does not appear to involve the well-known *mer* operon. Our data are the first to show a nutrient dependency on the ability of the simulated human gut microbiota to demethylate MMHg. This work provides much-needed insights into individual variations in Hg absorption and potential toxicity.

Keywords: gut microbiome, monomethylmercury, metabolism, mercury, diet, protein

2.2 Introduction

Global mercury (Hg) pollution leads to an increase in monomethylmercury (MMHg) levels in fish and seafood and poses a health risk to human consumers (Mergler *et al.*, 2007). The World Health Organization and the Food and Agriculture Organization recommend the consumption of fish as its health benefits outweigh the potential risk associated with MMHg toxicity (Food and Agriculture Organization of the United Nations. and World Health Organization., 2011; Starling *et al.*, 2015). To set these guidelines, the body burden of MMHg is often estimated by measuring Hg concentration in hair. However, there is considerable variation between the estimated MMHg oral intake and hair Hg concentrations in most populations tested (Canuel *et al.*, 2006). To estimate human exposure to MMHg, risk assessors often use

standard models that assume that 90 to 100% of MMHg (Aberg *et al.*, 1969) and 7-15% of Hg (Miettinen, 1973) ingested is bioavailable. However, experimental evidence suggests that absorption estimates range from 12% to 79% for MMHg and 49% to 69% for inorganic divalent (Hg^{II}) (Bradley *et al.*, 2017). This discrepancy points to the existence of unidentified factors that are currently not considered in modelling the oral intake and body burden of MMHg.

The mechanism of absorption of MMHg from the intestine has been well documented (Naganuma *et al.*, 1991). MMHg has a much higher absorption rate than Hg^{II} (Bridges and Zalups, 2010). Therefore, the demethylation of MMHg in the gastrointestinal tract will decrease its absorption. The origin of the food, cooking methods and co-ingested micronutrients (e.g., selenium, fruit fibres) can potentially alleviate MMHg toxicity by reducing its bioavailability and bioaccessibility (Passos *et al.*, 2007; Ralston and Raymond, 2010; Ouédraogo and Amyot, 2011). Li et al (2016) have shown that age, body weight, gender, ethnicity, household income, and geographic regions only account for 32% of the total variance measured in hair Hg concentrations. The authors suggested that other factors such as diet or the activity of the gut microbiota might explain the remaining variance. Rand et al. (2016) reported a high degree of inter-individual variability in the MMHg biotransformation kinetics during a feeding experiment and proposed that the gut microbiome can be a significant modulating factor for MMHg absorption. Later, Caito et al. (2018) showed that individuals who received antibiotic therapy had lower MMHg elimination rates than untreated individuals, highlighting the importance of gut microbiota in the elimination of MMHg.

Hg biotransformation in the gut environment is largely unexplored. Few studies have reported that the gut of fish and zooplankton can potentially methylate Hg (Wang *et al.*, 2013; Gorokhova *et al.*, 2018) and the gut of rat and marine fish can demethylate MMHg (Nakamura *et al.*, 1977; Rowland *et al.*, 1984; Urano *et al.*, 1990; Wang *et al.*, 2017). The human gut does not appear to be a hotspot for MMHg production (Podar *et al.*, 2015) but appears suitable for MMHg degradation (Rowland, 1988). Genes involved in Hg methylation (*hgcA* and *hgcB*) were not detected in the gut microbiome of healthy human individuals

(Gilmour *et al.*, 2013; Podar *et al.*, 2015). However, genes involved in MMHg demethylation, encoded by the *mer* operon were detected (Osborn *et al.*, 1997; Rothenberg *et al.*, 2016).

There is a knowledge gap on the genetic determinants and microbial mechanisms involved in the biotransformation of Hg in the gut environment. Although a great emphasis has been placed on the mechanisms that control the formation of MMHg in sediments and soils, fewer studies have addressed the fate of MMHg after it is produced. Most of our knowledge of MMHg biotransformation was gathered from experiments performed outside the human gut (e.g., lake sediments, wetlands). Two pathways can usually be identified for bacterially mediated MMHg demethylation: (1) a reductive process, producing Hg^0 and CH_4 usually found in Hg-contaminated sites (Barkay *et al.*, 2003), and (2) an oxidative process producing Hg^{II} and CO_2 (Oremland *et al.*, 1991; Martín-Díaz *et al.*, 2008; Kronberg *et al.*, 2018). The reductive process is mediated through an enzyme encoded by the *mer*-operon (organomercurial-lyase pathway) allowing microorganisms to be Hg-resistant. Oxidative demethylation possibly occurs via co-metabolism of MMHg and small organic compounds (Oremland *et al.*, 1991), but the mechanism remains unknown. Recently, lab experiments using pure cultures have identified MMHg degradation by (micro)aerobic methanotrophs (e.g., CH_4-consuming microbes) (Lu *et al.*, 2017).

Because diet can affect the ecology of the gut microbiota (Singh *et al.*, 2017), it is possible that nutrient intake from different diets can control the rate of MMHg degradation by affecting the gut microbiota community structure. Using an *in vitro* model, we manipulated the nutrient composition of fecal slurries prepared from two healthy human individuals and tracked MMHg production and degradation using stable Hg isotopes. Changes in microbial community structure were assessed using high throughput sequencing of 16S rRNA gene amplicon. We hypothesize that changes in the structure and function of the gut microbiota community induced by changes in dietary nutrient intake can affect the demethylation rate of MMHg.

2.3 Material and method

2.3.1 Ethics

Ethics application (H09-17-12) was reviewed and approved by the Research Ethics Board at the University of Ottawa. No information from participants was collected for this study.

2.3.2 Fecal collection and incubation set-up

Fresh fecal samples (< 1-hr old) collected from two healthy human volunteers were used as a proxy for distal gut microbiota. The volunteers had no history of gastrointestinal disorders, have consumed no antibiotics in the past six months, or any probiotics in the form of pills or food products in the last month. Feces were collected from two individuals in plastic commode provided. All manipulations were conducted under a nitrogen atmosphere devoided of oxygen in a Bactron anaerobic chamber (ShelLab). The fecal slurry was prepared by diluting 1-part fecal sample, 9-part degassed PBS prepared at pH 7.0. Fecal slurries were mechanically shaken and mixed in 100 ml glass bottle, in a 1:10 ratio with the respective medium: balanced (basal medium) (Olano-Martin *et al.*, 2000), protein-rich (basal medium + 20g.L^{-1} peptone) and carbohydrate-rich (basal medium + 10g.L^{-1} glucose). Bottles were spiked with stable isotope enriched MM^{198}Hg and ^{199}Hg isotopes are added to the mix to measure Hg methylation and demethylation using LC-ICP-MS. This ratio was chosen to reflect that of MMHg:Hg in the gut environment. Final concentrations were [MMHg]=10 ng.g^{-1} and [Hg^{II}] = 1 ng.g^{-1}, and were lower than levels typically found in fish meal. All treatments were performed in biological triplicates. Serum bottles containing the samples were crimped to ensure anaerobic conditions and wrapped in aluminum foil to limit light exposure. Bottles were placed in a shaking incubator at 37°C. Bottles were sampled at t = 0, 12, 24, 36 and 48h for Hg transformation analysis and t = 0 and 48h for microbial analysis. Samples were stored in 15 ml falcon tubes kept at -20°C for microbial community analysis and in small 7 ml scintillation vial kept at -80°C for Hg isotope analysis.

2.3.3 Probiotic and transfer experiment

Sutterella parvirubra (DSMZ-19354) and *Acidaminococcus intestini* (DSMZ-21505) were commercially obtained from the DSMZ to test for their demethylation potential. Both strains were grown as per DSMZ cultivation conditions. Strains were tested for their methylation and demethylation potential in the balanced medium. In another series of experiments, *Sutterella parvirubra* or *Acidaminococcus instestini* were added to Individual B fecal slurry to test for their potential to induce a demethylation phenotype. Finally, to test the effect of transferring the gut microbiota of Individual A into individual B, fecal slurry preparation of Individuals A and B was added in 1:1 (5 ml of Individual A and 5 ml of Individual B) and 1:2 (3.3 ml of Individual A and 6.7 ml of Individual B) ratio.

2.3.4 Hg analyses

Samples were prepared according to the modified protocol outlined by Batista et al. (2011). All analysis and Hg isotope separation were performed on an Agilent LC-ICP-MS system. Chromatographic separation of isotope $MM^{198}Hg$ (demethylation tracer), ^{199}Hg (methylation tracer), ^{201}Hg (internal standard), and ^{202}Hg (ambient) was performed using a mobile phase consisting of 0.05% v/v mercaptoethanol, 0.4% m/v L-cysteine and 0.06M ammonium acetate on Agilent 1200 Infinity LC system consisting of a 1260 Isocratic pump and 1260 Autosampler. The LC system was connected to the Agilent 7700x ICP-MS via Peek tubing and equipped with a low flow Micro Mist Nebulizer and quartz, low-volume Scott-type double-pass spray chamber. All calculations for quantifying excess of $MM^{199}Hg$ and $MM^{198}Hg$ were made according to Hintelmann and Evans (1997). Additional information can be found in supporting methods.

2.3.5 Microbial community analysis using 16S rRNA gene amplicon metagenomic

DNA was extracted using the PowerSoil® DNA Isolation Kit (Mo Bio Laboratories, Carlsbad, CA). Sequencing was performed by Molecular Research LP (Shallowater, TX), which amplified DNA using a two-step PCR targeting the V4 hypervariable region of the 16S rRNA gene using the primer 515f (forward:

GTGYCAGCMGCCGCGGTAA) and 806r (reverse: GGACTACNVGGGTWTCTAAT). A negative control of our DNA extraction kit was performed using PBS 1X as a sample. We were not able to obtain an amplicon and no band was observed on a gel electrophoresis; samples were sent to the sequencing facility which was also unable to reliably generate amplicons for sequencing.

Amplicon sequence datasets were analyzed using the Quantitative Insights into Microbial Ecology (QIIME) pipeline (Caporaso *et al.*, 2010a). The data was quality filtered using QIIME default parameters (quality score = 25, min length = 200, max length = 1000). Additional quality filtering and operational taxonomic unit (OTU) clustering were performed the UCHIME algorithm to identify chimera sequences for removal against the Gold databases. Remaining sequences were clustered into OTU (97% identity) using Closed reference OTU picking with UCLUST to form the representative dataset. Taxonomical classification of the representative dataset was performed using Ribosomal Database Project's classifier against the SILVA database as a reference using the default settings (DeSantis *et al.*, 2006). The representative sequences for each OTU were aligned using PyNAST (Caporaso, *et al.*, 2010b). The Hg tracer did not alter the fecal microbial community structure (Figure 2.2).

2.3.6 Statistical analysis

All analyses were performed in R v. 3.3.2 (R Core Team 2017). Beta diversity, weighted Unifrac distances, were used to perform the principal coordinate analyses (PCoA) using the package Vegan (http://www.cran.r-project.org/package=vegan). Weighted Unifrac distance was chosen to account for the taxa abundance in the calculation of shared and unshared branch (Lopuzone et al. 2016). Data separation in the PCoA was tested using a permutational multivariate analysis of variance (PERMANOVA; function Adonis in the Vegan package). Hierarchical cluster analysis was performed using weight Unifrac distance dissimilarity matrix Two-way analyses of variance (ANOVA) with Tukey multiple comparisons were used

to evaluate differences in Hg methylation and demethylation potential between medium and incubation time.

2.4 Results and discussion

Using fecal slurry incubations, we conducted a series of experiments aiming to evaluate the potential for the gut microbiota to affect Hg speciation under different nutritional profiles for two healthy human adult individuals, referred to as Individuals A and B. At 48h post-incubation, $MM^{198}Hg$ levels in Individual A fecal slurries incubated in protein-rich medium were undetectable (Figure 2.1A, Figure A1; $p < 0.001$). In the balanced diet treatment, $MM^{198}Hg$ concentrations decreased by 52.5%. No significant decrease was observed in the carbohydrate-rich treatment (Figure 2.1A). Strikingly, MMHg degradation was muted in Individual B samples (Figure 2.1B; Figure A1). We did not observe significant production of $MM^{199}Hg$ in any of the treatments, supporting previous reports that the gut microbiota is not a hotspot for MMHg formation (Figure A2). Control abiotic experiments (balanced, carbohydrate- and protein-rich treatments amended with stable isotope) did not show changes in Hg isotope concentrations ($MM^{198}Hg$ and ^{199}Hg; Figure A3). These results suggest that i) the ability to degrade MMHg is individual dependent and ii) that protein amendments stimulate pathways that lead to MMHg degradation. All experiments were conducted in darkness, ruling out the possibility of abiotic demethylation of MMHg via photodegradation (Seller *et al.*, 1996).

Individuals A and B exhibited similar gut microbial community structures (Figure 2.1C, Figure 2.2), which were both dominated by Firmicutes and Bacteroidetes (> 80% in relative abundance), as expected from the gut microbiota of healthy human individuals (Ley *et al.*, 2008). The addition of Hg did not significantly affect the microbial community structure suggesting that the Hg tracer added did not significantly alter the gut microbiota community structure (Figure 2.2). Using PERMANOVA (Adonis), we are able to identify the incubation time (T0 vs T48) as a variable that significantly affected the microbial community structure in both individuals (Figure 2.1C; $p = 0.002$). Carbohydrate-rich medium post-

incubation also significantly shifted the microbial community structure that is different from the structure observed in the balanced and protein-rich medium (Figure 2.1C; $p = 0.007$). The carbohydrate-rich treatment promoted the growth of Actinobacteria whereas balanced and protein-rich media saw an increased abundance of phyla that were already dominating the gut microbial profile at T0. The carbohydrate-rich treatment also decreased baseline MMHg degradation rates observed in Individual A (Figure A1). One possible explanation for the absence of MMHg degradation in the carbohydrate treatment could be the production of compounds inhibiting MMHg degradation. Indeed, Lu et al. (2017) showed that C1 compounds could inhibit oxidative MMHg degradation. Further investigation is required to determine if the same process takes place in the human gut environment.

A more detailed analysis of the changes in the microbial community structure showed that Individual A exhibited a significant increase in Sutterellaceae and Acidaminococcaceae (0.44 → 15.34%) in the protein-rich medium after 48h of treatment that was not observed for Individual B (Table 2.1). Both bacterial families are known to be commensal of the human gut (D'Auria *et al.*, 2011; Morotomi *et al.*, 2011).

In a subsequent series of experiments, commercially obtained *Sutterella parvirubra* (DSMZ-19354) and *Acidaminococcus intestini* (DSMZ-21505) were tested for their MMHg degradation capabilities in balanced and protein-rich media. *A. intestini* incubated in protein-rich medium exhibited significantly higher demethylation rates than in the balanced medium. *S. parvirubra* did not show a significant change in MMHg degradation rates compare to control (Figure 2.3). When both strains were combined together (1:1 ratio), MMHg demethylation rate was significantly higher than control but much lower than what was observed in the fecal slurry experiments (0.14 $nM.g^{-1}.h^{-1}$ of $MM^{198}Hg$, vs 6.7 $nM.g^{-1}.h^{-1}$ of $MM^{198}Hg$, respectively; Figure 2.3).

The next experiment was to add *S. parvirubra* and *A. intestini* strains to fecal slurries collected from Individual B to test whether they would enhance the demethylation of MMHg. We did not observe

significant changes in MMHg metabolism with the addition of *S. parvirubra* or *A. intestini* in Individual B fecal slurries (Figure 2.4). These data suggest that MMHg demethylation does not result from the isolated activity of these two single strains. These results indicate that the increased abundance of these two strains in the demethylating individual likely reflects more complex changes within the gut microbial community. The enhanced degradation of MMHg as a result of protein addition could be explained by syntrophic interactions, in which microorganisms are linked via metabolic handoffs (Abreu and Taga, 2016; Anantharaman *et al.*, 2016). Syntrophic interactions have already been identified as important in the production of MMHg (Yu *et al.*, 2018) and deserve further investigations to evaluate their role in MMHg degradation.

Finally, to test whether the absence of MMHg degradation in Individual B was the result of a community-level inhibitory process, we performed a series of fecal mixing experiments. In these experiments, fecal samples from Individuals A (strong demethylator phenotype) and B (weak demethylator phenotype) were mixed in different ratio. We observed that degradation of MMHg was increasingly higher with increasing ratio of fecal samples from Individual A (Figure 2.5). These data suggest that the microbial community of Individual B did not inhibit the degradation of MMHg and that Individual A fecal samples consistently exhibit a microbial community that can be stimulated to enhance MMHg degradation *in vitro*. We tested for the presence of genes encoding for the *mer* operon to test if these genes were responsible for the higher demethylation capacity of the microbiota of Individual A. None of the *mer* operon genes that we targeted were present in the gut microbiota of either Individuals A or B (data not shown).

We cannot yet offer a convincing mechanism explaining the quasi-complete demethylation phenotype observed for Individual A in the presence of proteins. Nevertheless, these data are the first to show a nutrient dependency on the ability of the human gut microbiota to demethylate MMHg *in vitro*. We are currently gathering evidence testing how widespread this superdemethylation phenotype is at the human population level. This research contributes to the understanding of the roles that the gut microbiota and

nutrient intake have on Hg metabolism. Should a reproducible mechanistic relationship between diet, microbiota community structure and function, and MMHg demethylation phenotype be identified, this research could lead to a shift in how risk assessment is conducted.

2.5 Acknowledgements

Our work was funded by NSERC Discovery (AJP, HMC), Accelerator grant (AJP), CFI funding (AJP, HMC), Canada Research Chair (HMC) and an NSERC CREATE-REACT scholarship to GG. We are grateful to the participants of this study that have contributed fecal samples and for Poulain and Chan lab members for stimulating discussion. We would like to Morgan McMillan for her help with the analyses.

Author contribution statement: GG, HMC and AJP conceived and planned the experiments. GG carried out the experiment and data analysis. EY performed isotopic analysis. GG wrote the manuscript. All authors edited and provided comments to the final version of the manuscript

2.6 Reference cited

Aberg, B., Ekman, L., Falk, R., Greitz, U., Persson, G., and Snihs, J. (1969) Metabolism of Methyl Mercury (203 Hg) Compounds in Man. *Arch. Environ. Heal. An Int. J.* **19**: 478–484.

Abreu, N.A. and Taga, M.E. (2016) Decoding molecular interactions in microbial communities. *FEMS Microbiol. Rev.* **40**: 648–663.

Anantharaman, K., Brown, C.T., Hug, L.A., Sharon, I., Castelle, C.J., Probst, A.J., et al. (2016) Thousands of microbial genomes shed light on interconnected biogeochemical processes in an aquifer system. *Nat. Commun.* **7**: 13219.

Barkay, T., Miller, S.M., and Summers, A.O. (2003) Bacterial mercury resistance from atoms to ecosystems. *FEMS Microbiol. Rev.* **27**: 355–84.

Batista, B.L., Rodrigues, J.L., de Souza, S.S., Oliveira Souza, V.C., and Barbosa, F. (2011) Mercury speciation in seafood samples by LC–ICP-MS with a rapid ultrasound-assisted extraction procedure: Application to the determination of mercury in Brazilian seafood samples. *Food Chem.* **126**: 2000–2004.

Bradley, M., Barst, B., and Basu, N. (2017) A Review of Mercury Bioavailability in Humans and Fish. *Int. J. Environ. Res. Public Health* **14**: 169.

Bridges, C.C. and Zalups, R.K. (2010) Transport of Inorganic Mercury and Methylmercury in Target Tissues and Organs. *J. Toxicol. Environ. Heal. Part B* **13**: 385–410.

Caito, S.W., Jackson, B.P., Punshon, T., Scrimale, T., Grier, A., Gill, S.R., et al. (2018) Editor's Highlight: Variation in Methylmercury Metabolism and Elimination Status in Humans

Following Fish Consumption. *Toxicol. Sci.* **161**: 443–453.

Canuel, R., de Grosbois, S.B., Atikessé, L., Lucotte, M., Arp, P., Ritchie, C., et al. (2006) New evidence on variations of human body burden of methylmercury from fish consumption. *Environ. Health Perspect.* **114**: 302–6.

Caporaso, J.G., Bittinger, K., Bushman, F.D., DeSantis, T.Z., Andersen, G.L., and Knight, R. (2010) PyNAST: a flexible tool for aligning sequences to a template alignment. *Bioinformatics* **26**: 266–267.

Caporaso, J.G., Kuczynski, J., Stombaugh, J., Bittinger, K., Bushman, F.D., Costello, E.K., et al. (2010) QIIME allows analysis of high-throughput community sequencing data. *Nat. Methods* **7**: 335–336.

D'Auria, G., Galán, J.-C., Rodríguez-Alcayna, M., Moya, A., Baquero, F., and Latorre, A. (2011) Complete genome sequence of Acidaminococcus intestini RYC-MR95, a Gram-negative bacterium from the phylum Firmicutes. *J. Bacteriol.* **193**: 7008–9.

DeSantis, T.Z., Hugenholtz, P., Larsen, N., Rojas, M., Brodie, E.L., Keller, K., et al. (2006) Greengenes, a chimera-checked 16S rRNA gene database and workbench compatible with ARB. *Appl. Environ. Microbiol.* **72**: 5069–72.

Food and Agriculture Organization of the United Nations. and World Health Organization. (2011) Report of the Joint FAO/WHO Expert Consultation on the Risks and Benefits of Fish Consumption : Rome, 25-29 January 2010. Food and Agriculture Organization of the United Nations.

Gilmour, C.C., Podar, M., Bullock, A.L., Graham, A.M., Brown, S.D., Somenahally, A.C., et al.

(2013) Mercury methylation by novel microorganisms from new environments. *Environ. Sci. Technol.* **47**: 11810–20.

Gorokhova, E., Soerensen, A.L., and Motwani, N.H. (2018) Mercury-methylating bacteria are associated with zooplankton: a proof-of-principle survey in the Baltic Sea. *bioRxiv* 279976.

Hintelmann, H. and Evans, R.D. (1997) Application of stable isotopes in environmental tracer studies - Measurement of monomethylmercury (CH 3 Hg +) by isotope dilution ICP-MS and detection of species transformation. *Fresenius. J. Anal. Chem.* **358**: 378–385.

Kronberg, R.-M., Schaefer, J.K., Björn, E., and Skyllberg, U. (2018) Mechanisms of Methyl Mercury Net Degradation in Alder Swamps: The Role of Methanogens and Abiotic Processes. *Environ. Sci. Technol. Lett.* acs.estlett.8b00081.

Ley, R.E., Hamady, M., Lozupone, C., Turnbaugh, P.J., Ramey, R.R., Bircher, J.S., et al. (2008) Evolution of mammals and their gut microbes. *Science* **320**: 1647–51.

Li, M., von Stackelberg, K., Rheinberger, C.M., Hammitt, J.K., Krabbenhoft, D.P., Yin, R., and Sunderland, E.M. (2016) Insights from mercury stable isotopes into factors affecting the internal body burden of methylmercury in frequent fish consumers. *Elem. Sci. Anthr.* **4**: 000103.

Lopuzone, C., Hamady, M., and Knight, R. (2006). UniFrac – An online tool for comparing microbial community diversity in a phylogenetic context. BMC Bioinf. **7.** 371

Lu, X., Gu, W., Zhao, L., Farhan Ul Haque, M., DiSpirito, A.A., Semrau, J.D., and Gu, B. (2017) Methylmercury uptake and degradation by methanotrophs. *Sci. Adv.* **3**: e1700041.

Martín-Díaz, M.L., Jiménez-Tenorio, N., Sales, D., and Delvalls, T.A. (2008) Accumulation and histopathological damage in the clam Ruditapes philippinarum and the crab Carcinus maenas to assess sediment toxicity in Spanish ports. *Chemosphere* **71**: 1916–27.

Mergler, D., Anderson, H.A., Chan, L.H.M., Mahaffey, K.R., Murray, M., Sakamoto, M., and Stern, A.H. (2007) Methylmercury Exposure and Health Effects in Humans: A Worldwide Concern. *AMBIO A J. Hum. Environ.* **36**: 3–11.

Miettinen, J.K. (1973) Absorption and elimination of dietary (Hg++) and methylmercury in man. In, Miller,M.W. and Clarkson,T.W. (eds), *Mercury, Mercurial, and Mercaptans*. Springfield, IL, pp. 233–246.

Morotomi, M., Nagai, F., and Watanabe, Y. (2011) Parasutterella secunda sp. nov., isolated from human faeces and proposal of Sutterellaceae fam. nov. in the order Burkholderiales. *Int. J. Syst. Evol. Microbiol.* **61**: 637–643.

Naganuma, A., Tanaka, T., Urano, T., and Imura, N. (1991) Role of Glutathione in Mercury Disposition. In, *Advances in Mercury Toxicology*. Springer US, Boston, MA, pp. 111–120.

Nakamura, I., Hosokawa, K., Tamura, H., and Miura, T. (1977) Reduced mercury excretion with feces in germfree mice after oral administration of methyl mercury chloride. *Bull. Environ. Contam. Toxicol.* **17**: 528–33.

Olano-Martin, E., Mountzouris, K.C., Gibson, G.R., and Rastall, R.A. (2000) In vitro fermentability of dextran, oligodextran and maltodextrin by human gut bacteria. *Br. J. Nutr.* **83**: 247–55.

Oremland, R.S., Culbertson, C.W., and Winfrey, M.R. (1991) Methylmercury decomposition in

sediments and bacterial cultures: involvement of methanogens and sulfate reducers in oxidative demethylation. *Appl. Environ. Microbiol.* **57**: 130–7.

Osborn, A.M., Bruce, K.D., Strike, P., and Ritchie, D.A. (1997) Distribution, diversity and evolution of the bacterial mercury resistance (mer) operon. *FEMS Microbiol. Rev.* **19**: 239–62.

Ouédraogo, O. and Amyot, M. (2011) Effects of various cooking methods and food components on bioaccessibility of mercury from fish. *Environ. Res.* **111**: 1064–9.

Passos, C.J.S., Mergler, D., Fillion, M., Lemire, M., Mertens, F., Guimarães, J.R.D., and Philibert, A. (2007) Epidemiologic confirmation that fruit consumption influences mercury exposure in riparian communities in the Brazilian Amazon. *Environ. Res.* **105**: 183–193.

Podar, M., Gilmour, C.C., Brandt, C.C., Soren, A., Brown, S.D., Crable, B.R., et al. (2015) Global prevalence and distribution of genes and microorganisms involved in mercury methylation. *Sci. Adv.* **1**: e1500675–e1500675.

Ralston, N.V.C. and Raymond, L.J. (2010) Dietary selenium's protective effects against methylmercury toxicity. *Toxicology* **278**: 112–23.

Rand, M.D., Vorojeikina, D., van Wijngaarden, E., Jackson, B.P., Scrimale, T., Zareba, G., et al. (2016) Methods for Individualized Determination of Methylmercury Elimination Rate and De-Methylation Status in Humans Following Fish Consumption. *Toxicol. Sci.* **149**: 385–395.

Rothenberg, S.E., Keiser, S., Ajami, N.J., Wong, M.C., Gesell, J., Petrosino, J.F., and Johs, A. (2016) The role of gut microbiota in fetal methylmercury exposure: insights from a pilot study. *Toxicol. Lett.* **242**: 60–67.

Rowland, I.R. (1988) Interactions of the Gut Microflora and the Host in Toxicology. *Toxicol. Pathol.* **16**: 147–153.

Rowland, I.R., Robinson, R.D., and Doherty, R.A. (1984) Effects of diet on mercury metabolism and excretion in mice given methylmercury: role of gut flora. *Arch. Environ. Heal. An Int. J.* **39**: 401–8.

Seller, P., Kelly, C.A., Rudd, J.W.M., and MacHutchon, A.R. (1996) Photodegradation of methylmercury in lakes. *Nature* **380**: 694–697.

Singh, R.K., Chang, H.-W., Yan, D., Lee, K.M., Ucmak, D., Wong, K., et al. (2017) Influence of diet on the gut microbiome and implications for human health. *J. Transl. Med.* **15**: 73.

Starling, P., Charlton, K., McMahon, A., and Lucas, C. (2015) Fish Intake during Pregnancy and Foetal Neurodevelopment—A Systematic Review of the Evidence. *Nutrients* **7**: 2001–2014.

Urano, T., Iwasaki, A., Himeno, S., Naganuma, A., and Imura, N. (1990) Absorption of methylmercury compounds from rat intestine. *Toxicol. Lett.* **50**: 159–64.

Wang, H.-S., Xu, W.-F., Chen, Z.-J., Cheng, Z., Ge, L.-C., Man, Y.-B., et al. (2013) In vitro estimation of exposure of Hong Kong residents to mercury and methylmercury via consumption of market fishes. *J. Hazard. Mater.* **248**–**249**: 387–93.

Wang, X., Wu, F., and Wang, W.-X. (2017) In Vivo Mercury Demethylation in a Marine Fish (Acanthopagrus schlegeli). *Environ. Sci. Technol.* **51**: 6441–6451.

Yu, R.-Q., Reinfelder, J.R., Hines, M.E., and Barkay, T. (2018) Syntrophic pathways for microbial mercury methylation. *ISME J.* 1.

2.7 Tables and Figures

Table 2.1 - Table representing both taxa that increase in the MMHg degradation treatment and the relative proportion in other treatment. All values are relative proportion in percentage. (*) represent significant difference ($p < 0.001$). Acidaminococcaceae was not detected in Individual B.

		Balanced (%)	**Protein (%)**
Individual A	Sutterellaceae	0.08 → 0.33	0.22 → 7.87*
	Acidaminococcaceae	0.05 → 2.46*	0.23 → 7.87*
Individual B	Sutterellaceae	0.08 → 0.04	0.07 → 0.04
	Acidaminococcaceae	N/A	N/A

Figure 1

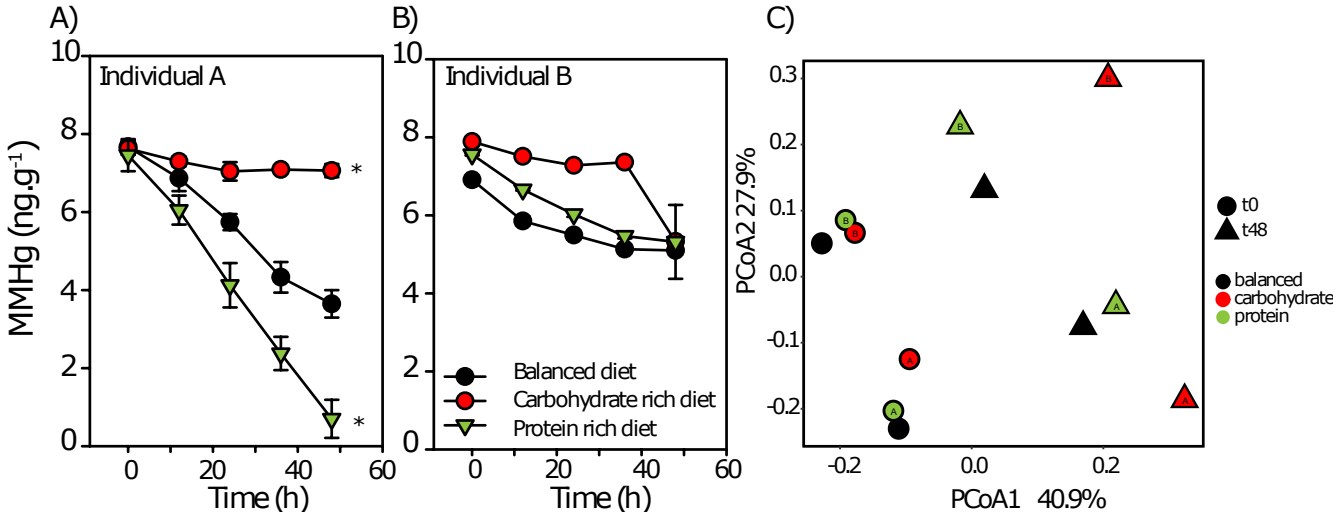

Figure 2.1– $MM^{198}Hg$ concentrations over time for Individuals A (A) and B (B). Fecal slurries from Individuals A and B were prepared in balanced medium, balanced medium enriched with carbohydrates or balanced medium enriched with proteins. (C) A principal coordinates analysis based on characterization of the overall fecal community structure for Individuals A and B. Weighted UniFrac metrics was calculated using QIIME to compute microbial β diversity. Sample dissimilarities were projected on a two-dimensional axis using principal coordinate analysis (PCoA). * indicates any significant difference between treatment and control.

Figure 2

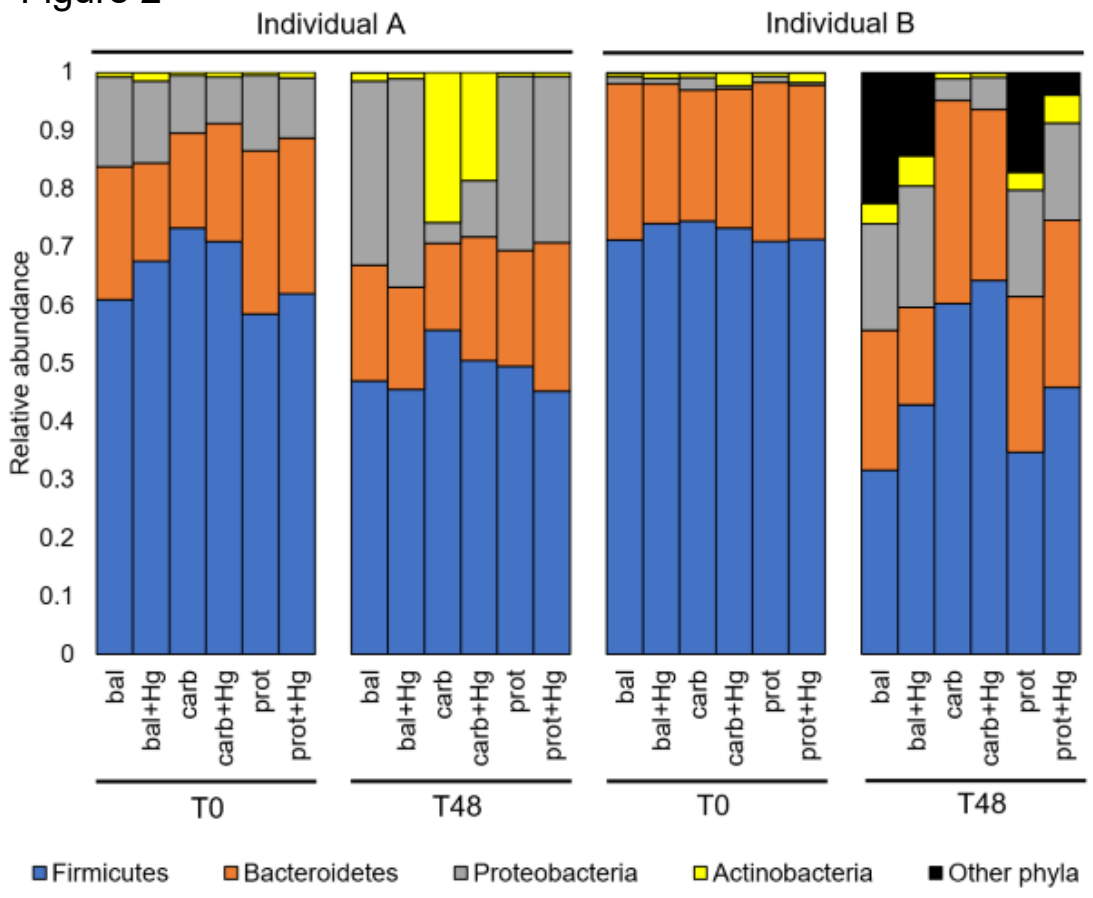

Individual A		simpson	shannon	evenness	Individual B		simpson	shannon	evenness
T0	bal	0.84	2.09	0.52	T0	bal	0.79	1.86	0.51
	bal+Hg	0.81	2.02	0.52		bal+Hg	0.78	1.84	0.49
	carb	0.84	2.09	0.52		carb	0.78	1.80	0.50
	carb+Hg	0.84	2.11	0.53		carb+Hg	0.78	1.83	0.50
	prot	0.81	1.98	0.51		prot	0.78	1.85	0.52
	prot+Hg	0.83	2.07	0.54		prot+Hg	0.79	1.85	0.51
T48	bal	0.87	2.25	0.57	T48	bal	0.83	1.97	0.61
	bal+Hg	0.68	1.49	0.42		bal+Hg	0.73	1.66	0.50
	carb	0.89	2.40	0.63		carb	0.84	2.10	0.65
	carb+Hg	0.86	2.17	0.57		carb+Hg	0.85	2.11	0.65
	prot	0.76	1.81	0.48		prot	0.77	1.79	0.54
	prot+Hg	0.88	2.36	0.62		prot+Hg	0.82	2.02	0.60

Figure 2.2 – (Top) Barplot showing relative abundance (phylum level) from the high-throughput 16S rRNA amplicon sequencing of the control experiment testing for the effect of the Hg tracer added. The table displays alpha diversity calculated for both Individuals at the family level. An ANOVA did not detect any significant differences.

Figure 3

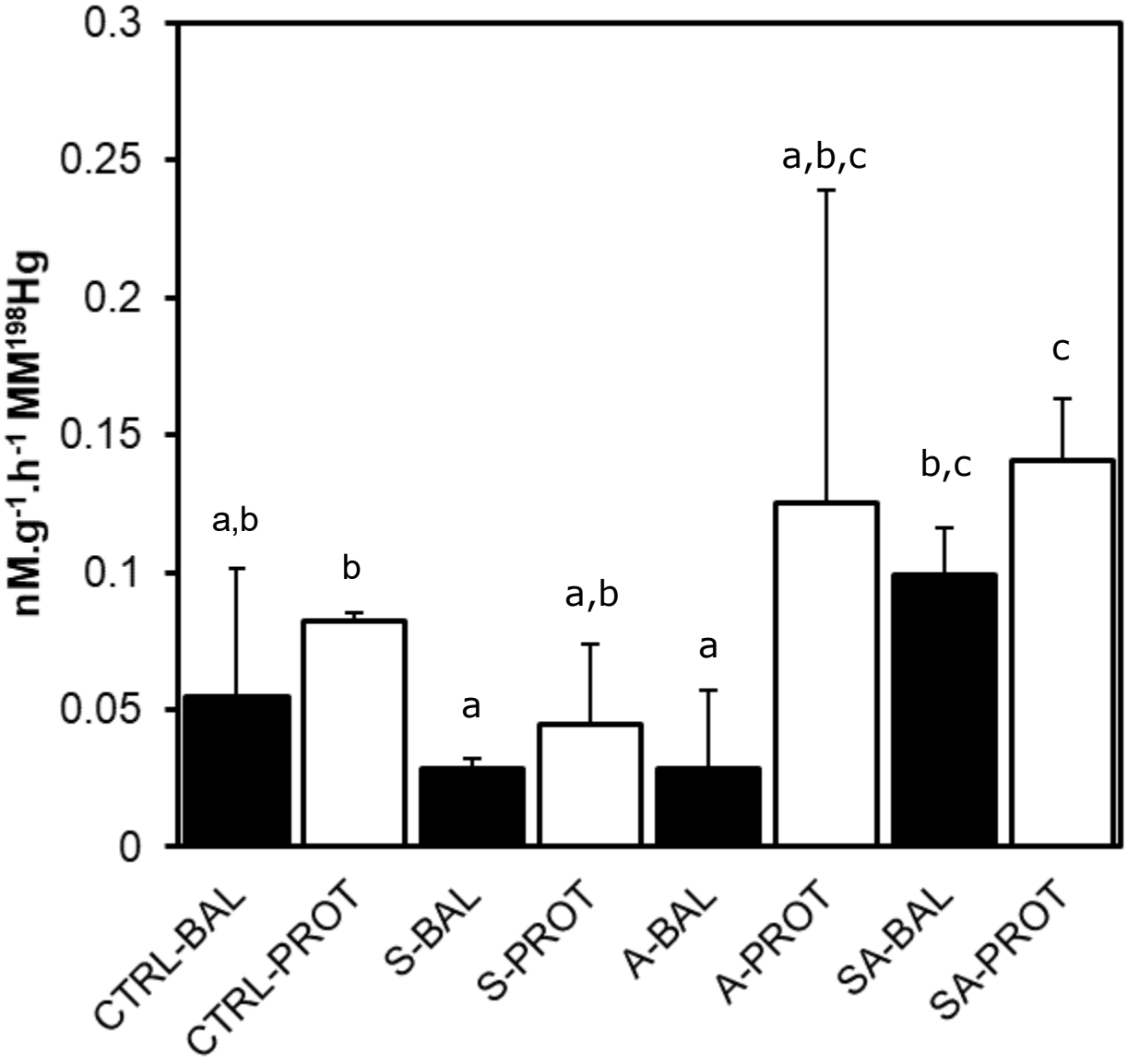

Figure 2.3 – Demethylation from pure culture *Sutterella parivubra* (S) and *Acidaminococcus intestini* (A) in balanced (BAL) and protein-rich (PROT) media. Control treatments consisted of media with no microbial amendments. Letters represent significant differences: (a) indicate significant differences between nutrient amendment added while (b) indicate significant differences between treatment and abiotic control (ANOVA and Tukey post-hoc; $p < 0.001$).

Figure 4

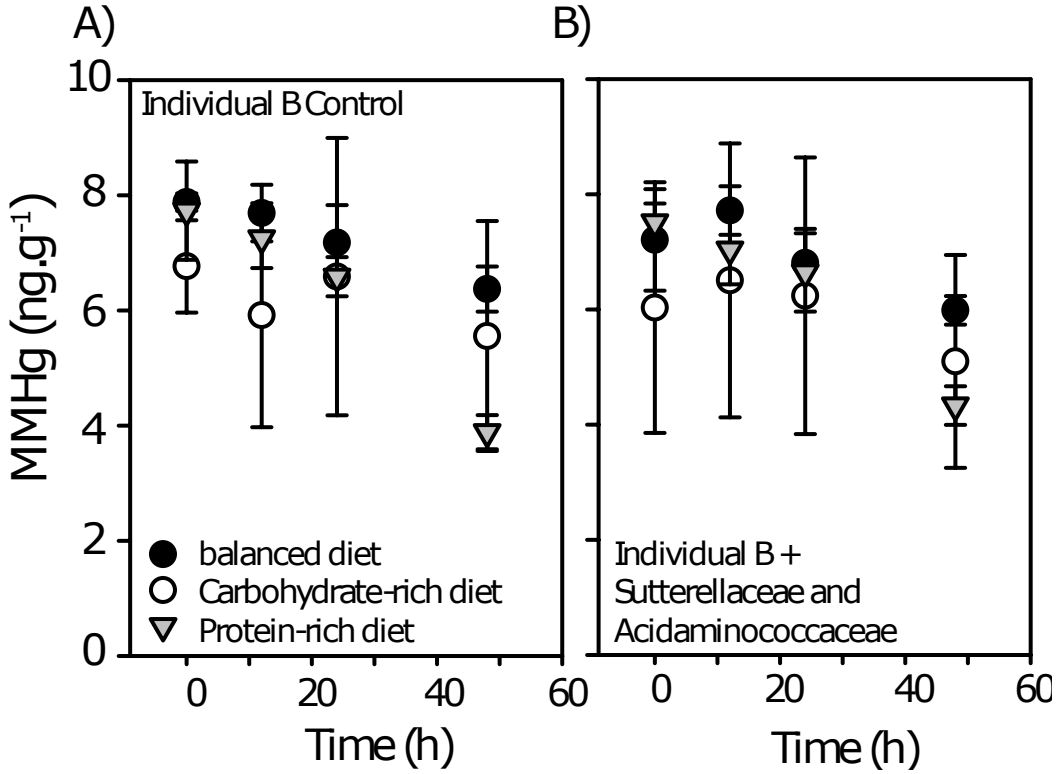

Figure 2.4 – $MM^{198}Hg$ concentrations over time for Individual B with (A) and, without (B) the addition of *S. parivubra* and *A. intestini*.

Figure 5

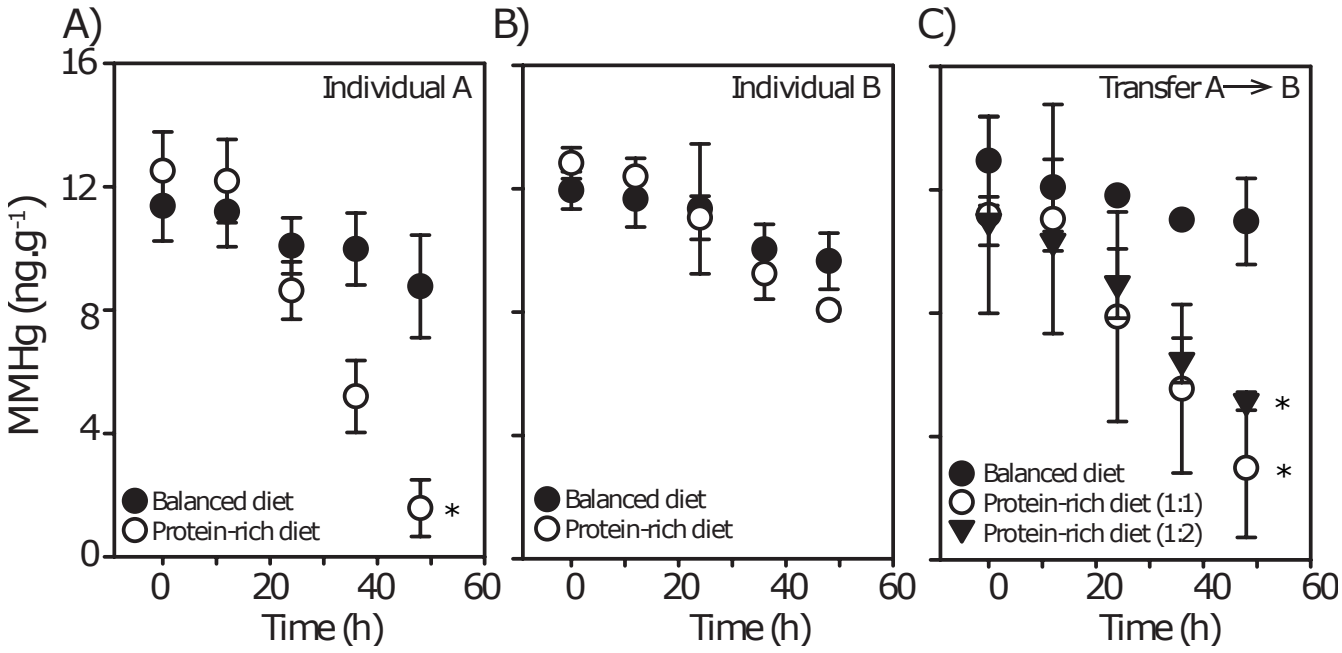

Figure 2.5 – $MM^{198}Hg$ concentrations over time for Individuals A (A), B (B) and a mix of Individuals A and B (1:1 and 1:2, A:B, respectively) (C) prepared in balanced medium and balanced medium amended with protein. Note that $MM^{199}Hg$ concentrations did not change across treatments suggesting the absence of methylation (Figure A3). * indicates any significant difference between treatment and control.

2.8 Supplemental tables and figures

Table A1 – All analysis and Hg isotope separation were performed on an Agilent LC-ICP-MS system. Instruments conditions are as followed:

LC conditions	
Column	Zorbax RX-C8 (5 µm x 250mm x 4.6mm id)
Mobile phase	0.05% v/v mercaptoethanol 0.4% m/v L-cysteine 0.06 M ammonium acetate
Flow rate	1ml/min
Injection volume	100ul
ICP-MS Conditions	
RF Power	1200 [W]
Plasma gas flow	15.0 L/min
Sampling depth	8.0mm
Nebulizer gas flow	1.0 [L/min]
Spray chamber temperature	2 [C]
Collision cell gas	He, 2.0 ml/min
Data acquisition mode and isotope monitored	Time-resolved analysis: m/z for ^{198}Hg,^{199}Hg,^{201}Hg and ^{202}Hg
Integration Time per Isotope	0.3 s
Energy Discrimination	4.5 [V]

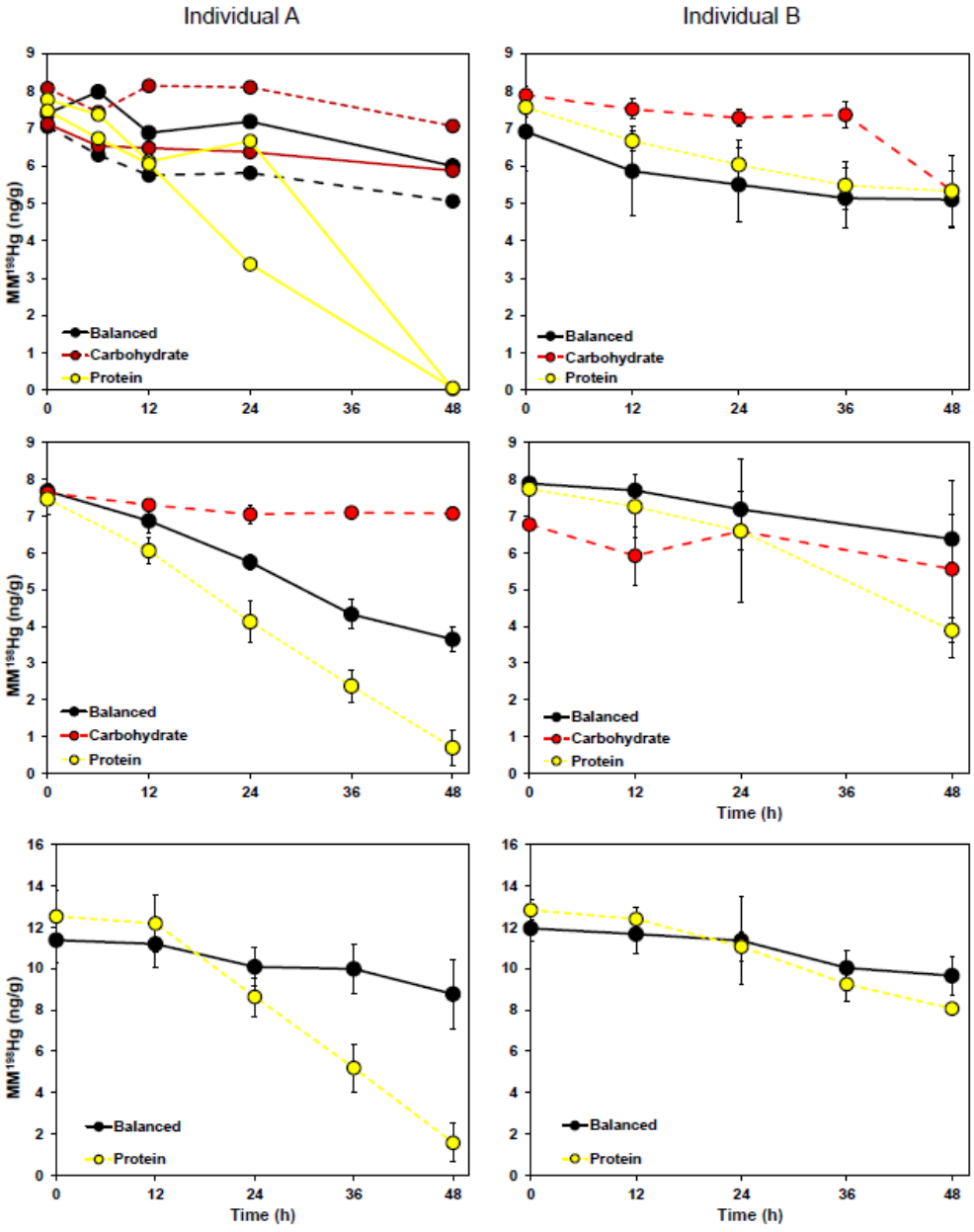

Figure A1 – Timeseries of batch experiment triplicates.Each replicate are biological replicates, fresh samples were collected prior to the experimentation. In all cases, protein-rich medium increase degradation of $MM^{198}Hg$ in Individual A while that phenotype was not observed in Individual B.

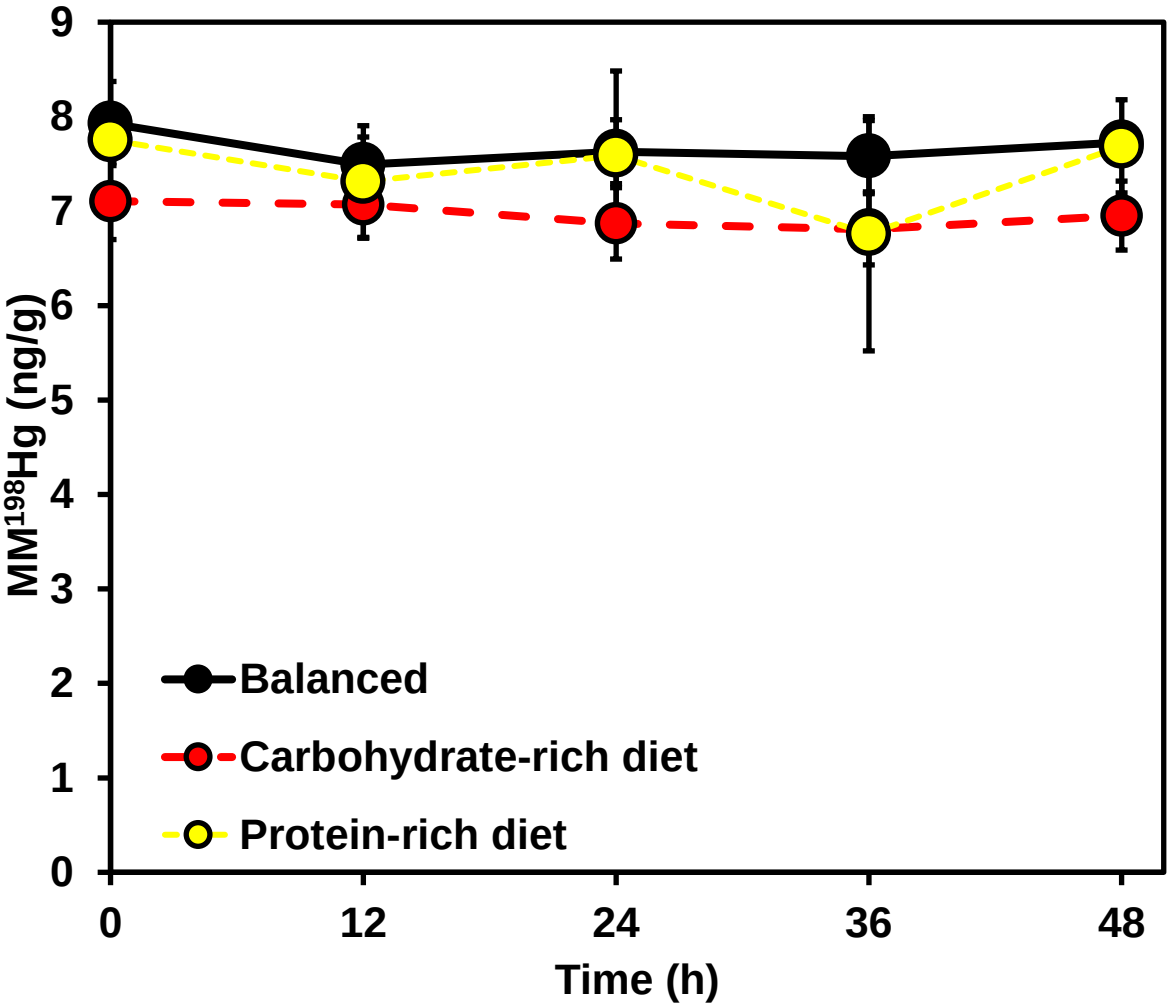

Figure A2 – Timeseries of the mesocosm set-up containing no fecal slurries (no microbial community) and incubated in parralell with the treatment mesocosms. The results shows no sign of $MM^{198}Hg$ degradation. The data suggests that there is no abiotic degradation (chemical or photodegradation) of $MM^{198}Hg$ from our experimental set-up.

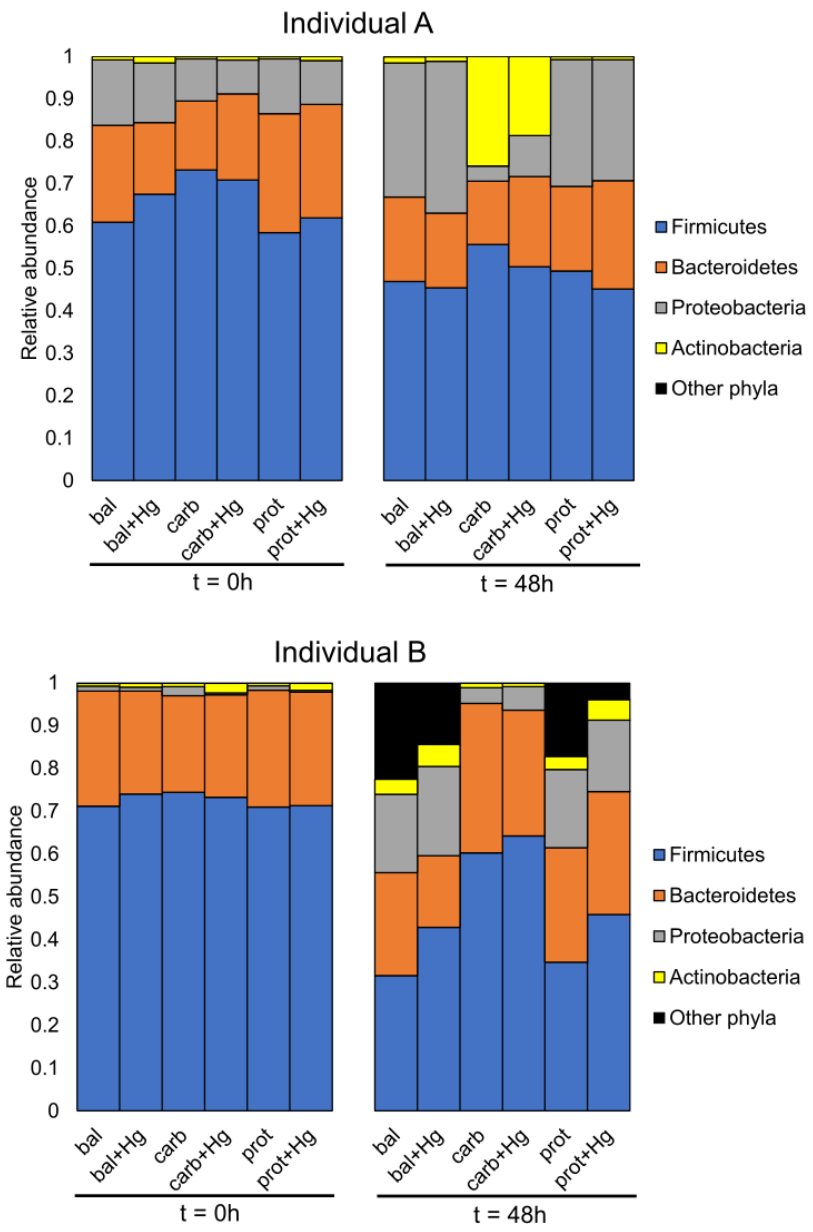

Figure A3 – Above barplot display relative abundance phylum level data from the 16S rRNA amplicon metagenomic sequencing the mesocosm experiment to test the toxicity of the Hg tracer added. At T0, the microbial community structure are the same regardless of addition of Hg tracer or medium. At T48, the addition of Hg does not significantly affect the microbial community structure at the phylum level.

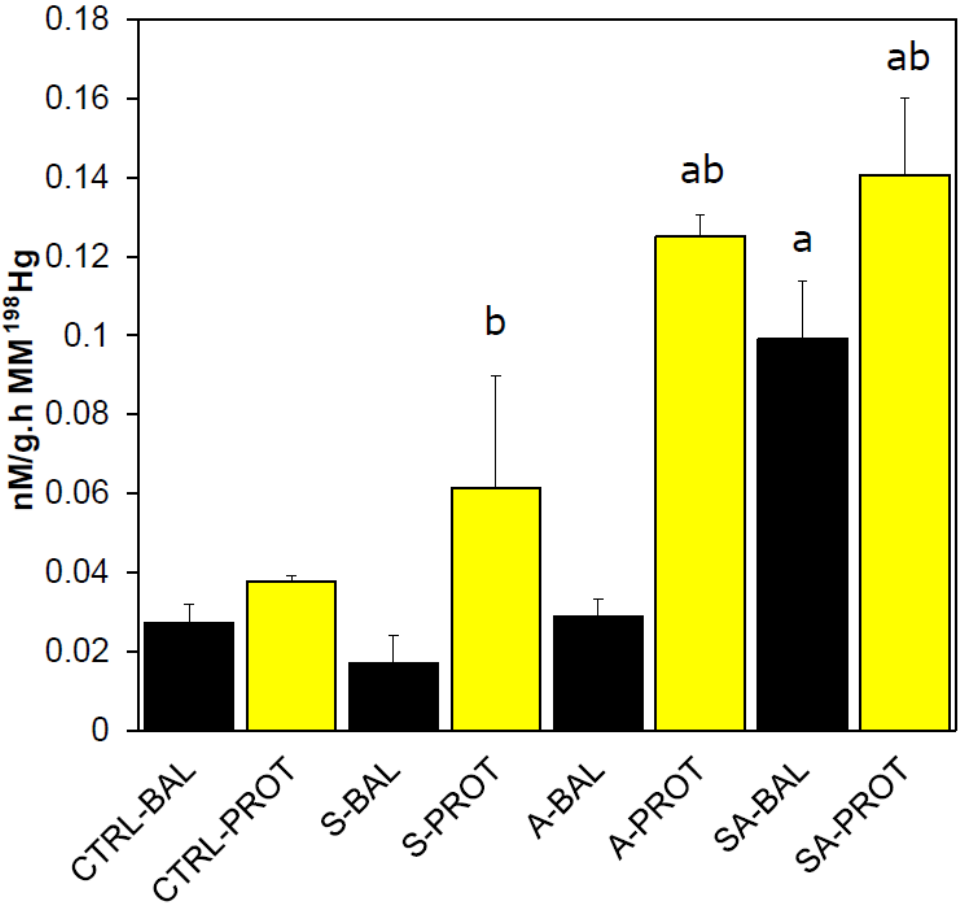

Figure A4 – Barplot representing demethylation rate from pure culture Sutterella parivubra (S) and Acidaminococcus intestini (A) in balanced (Bal) and protein-rich (Prot) medium. Control treatment consists of the sterile medium. (a) represent significant difference between control and treatment. (b) represent significant difference between balanced medium and protein-rich medium

Chapter 3: Shotgun metagenomic analysis reveals potential genetic determinants for methylmercury degradation in the human gut microbiome

Galen Guo, Hing Man Chan, Alexandre J Poulain

Affiliations:

Department of Biology, University of Ottawa, Ontario, Canada

This chapter is being prepared for submission to Toxicological Sciences

3.1 Abstract

Methylmercury (MeHg) is a global pollutant affecting the health of millions of people worldwide. The biotransformation of MeHg in the gastrointestinal tract has been shown to play an important role in MeHg toxicokinetics. However, the role of the gut microbiota is not known. In a previous study, we used batch culture experiments to show that *in vitro* MeHg degradation rates differed depending on the origin of the fecal samples (i.e., human donors), and, for one individual, was enhanced in the presence of proteins. In this follow-up study, we used comparative metagenomics to explore the potential mechanism underlying MeHg degradation in the gut microbiota. We compared the fecal microbiota metagenomes of two individuals, one known to yield virtually complete degradation of MeHg in the presence of protein within 48h and the other who did not. Using metagenome-assembled genomes, we identified a potential gene (*menG*) and associated pathway (menaquinone biosynthesis) that could be responsible for MeHg degradation. We speculate that MenG is a possible candidate catalyzing the transfer of the methyl group on MeHg to 2-demethylmenaquinol, forming menaquinol.

Keywords: Methylmercury, demethylation, gut microbiome, metagenome-assembled-genome, menG

3.2 Introduction

Methylmercury (MeHg) is a persistent environmental neurotoxicant that can be bioaccumulated and biomagnified in the food web [1]. Recent models project an increase in MeHg level in predatory fish due to overfishing and warming of ocean waters [2]. More than a third of the world population relies on seafood for nutrition. As such, proper biomonitoring of at-risk populations is crucial in understanding the extent of MeHg exposure and in employing proper consumption advisories and mitigation strategies. However, current biomonitoring methods have discovered large interindividual variability among subject tested, even those within the same population [3–5]. Several studies have reported that the gut microbiota could play a significant role in the absorption, metabolism and, ultimately, the bioavailability of MeHg [6–8]. Previous works have looked at the human gut microbiota role on MeHg degradation [7,9–13]; however, none have determined the mechanism(s) involved. Identifying microbial MeHg degradation mechanisms is essential in addressing interindividual variability and assessing the health risk associated with MeHg exposure. Identifying key genes and microbial taxa could be utilized as biomarkers for identifying sensitive or resistant sub-populations and eventually be developed into potential prophylaxis or treatment for MeHg toxicity.

Most of our current mercury demethylation knowledge is derived from other microbial habitats, particularly habitats outside the human body, such as freshwater or marine systems [14–16]. Currently, reductive and oxidative demethylation pathways have been described for microbial mediated demethylation. Microbes that carry out reductive demethylation typically possess the *mer* operon that encodes Hg binding, transport, reduction, and organomercury compounds' degradation proteins via the organomercury lyase MerB [17]. MerB catalyzes the protonation of the

C-Hg bond to oxidize Hg^{+} to Hg(II), which is subsequently reduced by MerA to Hg(0) that exits the microbial cells. Although it was identified in primates [18], *merA* has yet to be detected in the human gut environment [19,20]. Microbes capable of oxidative demethylation, mostly anaerobes, usually lack a dedicated MeHg detoxification machinery, such as that coded by the *mer* operon. It is believed that it relies on a co-metabolic process involving C1 compound metabolism resulting in the production of Hg(II) and CO_2 [14,15,21].

C1 compound metabolism and oxidative demethylation are thought to be the microbial guild's pathways such as sulfate-reducers and methanogens used to demethylate MeHg [14,15]. Sulfate-reducers and methanogens are commonly found within the gut environment [22,23]. However, no studies have linked these two microbial guilds with MeHg degradation in the human gut environment. A novel oxidative demethylation pathway was recently described in methanotrophs involving copper (Cu) metabolism and was dependent on the activity of methanol dehydrogenase [21]. Methanotrophs typically rely on the aerobic oxidation of methane to fulfil their carbon and energy needs; anaerobic pathways for MeHg degradation remain elusive.

High-throughput DNA sequencing of gene amplicons (e.g., 16S rRNA or *mcrA*) provides useful but limited information on microbial communities' structure and function [24 25,26]. In the last decade, community-wide genome-level analysis has helped improve both taxonomical and functional information on microbial assemblages [27,28]. By informing on the functional potential of non-culturable microbes, microbial metagenomic analyses offer useful context to generate new hypotheses to gain insights into the complex interplay of microbes with their environment [29,30]. In this study, we performed a comparative metagenomic analysis of fecal samples obtained from two individuals who have demonstrated the reproducible differential ability to degrade MeHg. We

previously explored the role of gut microbiota on MeHg speciation using *in vitro* fecal incubation experiments coupled to Hg stable isotope measurements [19]. We identified a strong demethylation phenotype leading to virtually complete degradation of MeHg in samples collected from one of the two volunteers in the presence of high concentrations of proteins (added as peptone in the assay medium). The phenotype observed could not be linked to any known pathways for which primers exist [19]. The goal of this study is to explore the mechanism of MeHg degradation by the gut microbiota. Here, we performed comparative shotgun metagenomic analyses of fecal samples collected from two individuals with contrasting demethylation phenotypes to explore the mechanisms of MeHg degradation and possibly identify the mechanism involved.

3.3 Materials and method

3.3.1 Ethics

Ethics application (H09-17-12) was reviewed and approved by the Research Ethics Board at the University of Ottawa. No personal information from participants was collected for this study.

3.3.2 Fecal collection and incubation setup

Fecal collection and incubation methods are described in Guo et al. [19] with a few modifications. Fresh fecal samples (< 1hr) were collected and quickly transported into an oxygen-deprived environment. Volunteers had no history of gastrointestinal disorders, had not consumed any antibiotics in the past six months or any probiotics in the last month. Feces were collected using a commode provided. Fecal slurries were prepared by diluting 1-part fecal sample, 9-part degassed PBS (1X, pH = 7.0). Fecal slurries were mixed in 100 ml serum glass bottle in a 1:10 ratio with the respective medium: balanced medium and peptone-enriched medium (10 g peptone + balanced

medium). MeHg chloride was added to measure the amount of MeHg degraded. Bottles were shaken (150 rpm) on a modified plate shaker in darkness and at 37ºC.

3.3.3 Inhibition assays

A series of assay was conducted using specific metabolic inhibitors to determine if sulfate reducers, methanogens or methanotrophs were involved in MeHg degradation in Individual A. MoO_4 (0.02 mM), BES (10 mM) and methanol (10 mM) was used as specific inhibitors of sulfate reducers, methanogens and methanotroph, respectively. Abiotic demethylation was examined using autoclaved bottles and bottles without fecal samples. All assays were performed in darkness, eliminating any photodegradation of organomercury [31,32].

3.3.4 Mercury extraction and analysis

Fecal slurries (1 g) were digested in HNO_3 (4 M) overnight (~ 16hr) in an incubator set at 55ºC. Then, 2 g of dichloromethane (DCM) was added to the acidified solution, shaken (330 RPM, 2 hr), centrifuged (3500 RPM, 10 mins) and phase-separated. L-cysteine (0.01M) was added to the DCM portion, shaken (330 RPM, 30 min), centrifuged (3500 RPM, 10 min) and phase separated. The L-cysteine portion (200 ul) was leached in a 3:1 solution of potassium bromide and copper sulfate, 300 ul DCM. It was then shaken (330 RPM, 45 min), centrifuged (3500 RPM, 10 min) and phase extracted. Samples were stored in small amber vials until ready for MeHg quantification by gas chromatography-CVAFS (GC-CVAFS).

3.3.5 Fecal DNA extraction, sequencing and data processing

Total DNA was extracted from Fecal slurries using the QIAGEN DNeasy PowerSoil Pro Kit as per instruction. The “Centre d’expertise et de services Génome Québec” (Québec, Canada)

prepared our libraries and sequenced using the Illumina HiSeq 4000 platform (PE100) with custom adaptors (read 1: AGA TCG GAA GAG CAC ACG TCT GAA CTC CAG TCA C, and read 2: AGA TCG GAA GAG CGT CGT GTA GGG AAA GAG TGT). The sequencing generated over 65.8 Gbp. Low quality reads, low-quality base at the end of reads, unpaired reads, and adaptors were removed using Trimmomatic v0.39 [33] using {PHRED33 | adapter.fa:3:26:10 | LEADING:3 | TRAILING:3 | SLIDINGWINDOW:4:15 | MINLEN:36}. FASTQC was used to assess the quality of our reads (https://www.bioinformatics.babraham.ac.uk/projects/fastqc/).

3.3.6 Bacterial functional profiling and reconstruction of bacterial genome

The demethylation phenotype observed in Individual A did not appear to match any of the currently known microbial pathways for MeHg degradation. A metagenomic approach was performed to identify taxa or pathways possibly associated with MeHg degradation in the gut microbiota, that would be differentially present in Individuals A and B. We compared shotgun sequencing data obtained from the gut microbiome of Individuals A and B at T0, T48 balanced medium, and T48 peptone-amended medium. More specifically, we performed a taxonomical and functional annotation of contigs and reconstruction of microbial genomes (MAGs). All metagenomic quality-controlled reads were co-assembled using MEGAHIT [34] software with default settings. The tool "EukRep" was performed to remove eukaryotic DNA from contigs prior to functional profiling and reconstruction of genome [35].

Fecal bacterial taxa and gene annotation were identified using the HUMAnN v2.0 pipeline [36] using the default setting. Metaphlan2 was used for bacterial taxonomical identification [37]. DIAMOND was used to identify genes in our co-assembled dataset [38]. Output was normalized from reads per kilobase to relative abundance for downstream analyses.

Co-assembled contigs were imported on Anvi'o v5 [39]. Contigs less than 1000 bp were removed. Open reading frames were predicted using Prodigal [40]. Protein-coding genes were predicted using Anvi'o custom Hidden Markov model with NCBI COG annotations. Gene annotation (PFAM [41], TIGRFAM [42], GO [43], PIRSF [44] and KEGG [45]) and pathways (Metacyc [46] and KEGG) were predicted using Interproscan [47]. Taxonomical inference of the contig database was classified using Kaiju [48]. Sequence coverage information was mapped for each sample to the assembled contig database using Bowtie2 [49] using the default settings. SAM output files were converted to BAM using samtools (http://github.com/samtools/) and each BAM files were imported onto the Anvi'o platform. BAM mapping files and contigs databased were used to generate sample profiles with a minimum contig length of 2500 bp. Initial automated binning was performed using CONCOCT [50] and later confirmed using DasTool [51]. DasTool output was imported into Anvi'o where summary statistics for abundance and coverage were generated. Bins were manually refined using Anvi'o refine option. Only high and medium quality genome were retained meeting the MIMAG standard developed by the Genomic Standards Consortium [52]. Quality of microbial genome recovered using a broader set of marker genes was performed using CheckM's "lineage wf" function [53].

3.3.7 Phylogenetic placement of assembled genome

Alignment and phylogenetic tree placement were performed using the phylogenomic function on the Anvi'o platform. A total of 137 isolated bacterial genomes from healthy individuals (Accession: PRJEB10915 [54]) was used to perform our phylogenetic placement along with our 18 MAG from PMC6785715. A total of 94 marker genes were used to align the isolated bacterial genome with our MAGs and generated a phylogenetic tree using FastTree [55]. The phylogenetic tree was visualized using iTOL v5 [56].

3.3.8 Statistical analyses

Inhibition assay was tested for significance using a t-test. Normality and equal variance were tested. Ordination plots were performed using principal coordinate analysis using output from the HUMAnN2 [57] pipeline. Protein profile for *merA* was performed using HMMER3 [58] against the MerA database [59]. Enrichment map analysis is based on hypergeometric distribution followed by False Discovery Rate (FDR) adjusted p-value ($\alpha = 0.05$) performed using ShinyGO v0.61 [60].

3.4 Results

Known MeHg degraders in freshwater and marine systems were present or involved in the gut environment using inhibition assays. None of the inhibitor-amended media affected the degradation of MeHg (Figure 3.1, $p < 0.001$). We did not observe MeHg degradation in abiotic treatments (without fecal slurry and autoclaved fecal slurry). Thus, comparing the metagenome of both individuals could gain insights into the genetic determinants associated with *in vitro* MeHg degradation by the human gut microbiota.

Contigs were annotated using the HUMAnN2 pipeline to identify taxonomic differences between both individuals in the protein-amended treatment. A total of 25 taxa were identified, and when comparing individuals in the peptone-amended treatment, we found *Escherichia sps.* (21.2%), *Enterobacter aerogenes* (16.8%), *Streptococcus salivarius* (2.8%) and *Klebsiella pneumoniae* (2.2%) as being more abundant ($p < 0.05$) in Individual A than in Individual B (Figure 3.2A). Subsequently, we explored variations in the microbiota community structure and functional difference between individuals and treatments using a principal coordinate analysis (PCoA) on taxa, genes and pathways using Bray-Curtis dissimilarity. The PCoA showed that both individuals' microbiota were similar in balanced (no excess protein) treatment (Figure 3.2B-D). However, we

observed that upon the addition of peptone, the microbial community (Figure 3.2B), functional gene (Figure 3.2C) and pathway structures (Figure 3.2D) diverged between Individuals A and B post-incubation.

Both individuals' gut metagenome was reconstructed using a binning approach to identify each individual's genetic determinants. In our genome-resolved approach to our metagenomic dataset, a total of 18 draft MAGs (eight high-quality, 10 medium-quality) were phylogenetically assigned to Firmicutes, Proteobacteria, and Bacteroidetes, phyla typically found in the human gut environment (Figure 3.3A). We taxonomically classified each MAG using CheckM and found that Lactobacillales and Selenomonadales were found in higher relative abundance in Individual A gut microbiota (Figure 3.3B, $p < 0.05$). We performed a protein profile search using Hidden Markov Models and did not find *merA* signatures suggesting that the *mer* operon and the organomercury lyase MerB are unlikely to be involved in the phenotype observed. A total of 45 genes were uniquely present in Individual A (Figure 3.4). Pathway analysis using gene ontology enrichment analysis on the 45 genes showed that menaquinone (Enrichment FDR, $p = 8.54 \times 10^{-5}$) and phylloquinone (Enrichment FDR, $p = 1.22 \times 10^{-3}$) biosynthetic and metabolic pathways, and cofactor metabolic processes were over-represented in Individual A protein treatment (Enrichment FDR, $p = 7.44 \times 10^{-4}$).

3.5 Discussion

The inhibition assay results on known demethylators (SRB, methanogens and methanotrophs) showed that none of the microbial guilds tested were involved in the degradation of MeHg in the simulated gut environment. Moreover, neither PCR targeting the *merA* gene nor genome analyses

revealed *mer* determinants in our samples. Therefore, we propose that the MeHg degradation phenotype observed in Individual A samples is likely associated with a novel pathway.

Data were analyzed using both contig annotations and metagenome-assembled genomes (MAGs) approaches. Individual A and B taxonomical and functional structures were similar in the balanced medium but significantly changed in response to peptone-amendment (Figure 3.2B-D). These results suggested that Individual A fecal microbiome may contain genetic elements, absent in Individual B, that could be important in the degradation of MeHg. Alternatively, peptone amendments may have stimulated low abundance microbes present in Individual A samples, providing needed metabolic capabilities for MeHg degradation. Fecal samples are representative of the colonic region [61,62], which is also the primary site for fermentation of exogenous and endogenous substrate, which benefit the host [63]. Microbial fermentation of protein produces numerous essential metabolites (e.g., short-chain fatty acids and amino acids) [64] and involves numerous microbes members of genera in the Firmicutes, Bacteroides, and Actinobacteria phyla[65].

By comparing the microbiome of both individuals, we discovered potential genetic determinants possibly involved in MeHg degradation. First, we employed genome-resolved metagenomics and reconstructed 18 MAGs, for which we performed an enrichment map analysis. We identified the menaquinone biosynthesis pathway as significantly overrepresented among the gene list in Individual A in the peptone-amended treatment. Menaquinone (or Vitamin K_2) plays a vital role in bacterial respiration as part of the electron transport chain [52]. This vitamin is present in the cytoplasmic membrane, where it transports electron between NADH dehydrogenase, succinate dehydrogenase, and cytochrome bc_1 complex. We reviewed the menaquinone biosynthesis pathway on the KEGG database (http://www.genome.jp/kegg/) and found that

demethylmenaquinone methyltransferase (*menG*) could potentially be involved in MeHg degradation. Indeed, the methyltransferase, *menG,* catalyze prenylation of demethylmenaquinol to menaquinol via the transfer of the methyl group on *S*-adenosyl-*L*-methionine (SAM). The link between SAM and methylation of mercury has been proposed in earlier studies [66–68], but none has studied the possible link between SAM and MeHg degradation. The possible link between the menaquinone biosynthesis pathway and MeHg demethylation requires further investigations.

3.6 Conclusions

Here, we reported a possibly novel process for MeHg demethylation by members of the human gut microbiota. Inhibition assays ruled out the possibility of known demethylators as responsible for the degradation of MeHg in our fecal slurry incubation experiments. Moreover, using comparative shotgun metagenomics, menaquinone biosynthesis could be linked to microbially-mediated MeHg degradation in the human gut environment.

This study highlighted the importance of combining culture- and non-culture-based approach in addressing complex microbial mechanistic questions. Additional experimental work will be required to test our findings and identify the essential gene(s) involved in the degradation of MeHg in the human gut environment. Moreover, this study did not address how the protein amendment can enhance MeHg degradation and remains elusive. This study is an important step in identifying a MeHg-degrading biomarker and enhance our ability to monitor MeHg risks.

Author contribution statement: GG, HMC and AJP conceived and planned the experiments. GG carried out the experiment and data analysis. GG wrote the manuscript. All authors edited and provided comments to the final version of the manuscript

3.7 Litterature cited

1. Wu, P. *et al.* The importance of bioconcentration into the pelagic food web base for methylmercury biomagnification: A meta-analysis. *Science of the Total Environment* **646**, 357–367 (2019).

2. Schartup, A. T. *et al.* Climate change and overfishing increase neurotoxicant in marine predators. *Nature* **572**, 648–650 (2019).

3. Li, M. *et al.* Insights from mercury stable isotopes into factors affecting the internal body burden of methylmercury in frequent fish consumers. *Elem. Sci. Anthr.* **4**, 000103 (2016).

4. Bradley, M., Barst, B. & Basu, N. A Review of Mercury Bioavailability in Humans and Fish. *Int. J. Environ. Res. Public Health* **14**, 169 (2017).

5. Caito, S. W. *et al.* Editor's Highlight: Variation in Methylmercury Metabolism and Elimination Status in Humans Following Fish Consumption. *Toxicol. Sci.* **161**, 443–453 (2018).

6. Laird, B., Van De Wiele, T., Corriveau, M., Jamieson, H. & Siciliano, S. Evaluation of the Bioaccessibility of Metals and Metalloids in Eastern Canadian Mine Tailings Using an in Vitro Gastrointestinal Model, the Simulator of the Human Intestinal Microbial Ecology (Shime). *Epidemiology* **17**, (2006).

7. Rowland, I. R., Robinson, R. D. & Doherty, R. A. Effects of diet on mercury metabolism and excretion in mice given methylmercury: role of gut flora. *Arch. Environ. Heal. An Int. J.* **39**, 401–8 (1984).

8. Rowland, I. R., Davies, M. J. & Evans, J. G. Tissue Content of Mercury in Rats Given Methylmercuric Chloride Orally: Influence of Intestinal Flora. *Arch. Environ. Heal. An Int. J.* **35**, 155–160 (1980).

9. Bisanz, J. E. *et al.* Randomized open-label pilot study of the influence of probiotics and the gut microbiome on toxic metal levels in Tanzanian pregnant women and school children. *MBio* **5**, e01580-14 (2014).

10. Seko, Y., Takahashi, M., Hasegawa, T. & Miura, T. Intestinal Absorption of Mercury in Vitro from Intestinal Contents of Methylmercury Administered Mice. *J. Heal. Sci.* **47**, 508–511 (2001).

11. Norseth, T. Biliary excretion and intestinal reabsorption of mercury in the rat after injection of methyl mercuric chloride. *Acta Pharmacol. Toxicol. (Copenh).* **33**, 280–288 (1973).

12. Shimada, H. *et al.* Further study of effects of chelating agents on excretion of inorganic mercury in rats. *Toxicology* **77**, 157–169 (1993).

13. Urano, T., Iwasaki, A., Himeno, S., Naganuma, A. & Imura, N. Absorption of methylmercury compounds from rat intestine. *Toxicol. Lett.* **50**, 159–64 (1990).

14. Oremland, R., Miller, L., Dowdle, P., Connell, T. & Barkay, T. Methylmercury Oxidative

Degradation Potentials in Contaminated and Pristine Sediments of the Carson River, Nevada. *Appl. Envir. Microbiol.* **61**, 2745–2753 (1995).

15. Oremland, R. S., Culbertson, C. W. & Winfrey, M. R. Methylmercury decomposition in sediments and bacterial cultures: involvement of methanogens and sulfate reducers in oxidative demethylation. *Appl. Environ. Microbiol.* **57**, 130–7 (1991).

16. Baldi, F., Pepi, M. & Filippelli, M. Methylmercury Resistance in Desulfovibrio desulfuricans Strains in Relation to Methylmercury Degradation. *Appl. Environ. Microbiol.* **59**, 2479–85 (1993).

17. Barkay, T., Miller, S. M. & Summers, A. O. Bacterial mercury resistance from atoms to ecosystems. *FEMS Microbiol. Rev.* **27**, 355–84 (2003).

18. Liebert, C., Wireman, J., Smith, T. & Summers, A. Phylogeny of mercury resistance (mer) operons of gram-negative bacteria isolated from the fecal flora of primates. *Appl. Envir. Microbiol.* **63**, 1066–1076 (1997).

19. Guo, G., Yumvihoze, E., Poulain, A. J. & Man Chan, H. Monomethylmercury degradation by the human gut microbiota is stimulated by protein amendments. *J. Toxicol. Sci.* **43**, 717–725 (2018).

20. Rothenberg, S. E. *et al.* The role of gut microbiota in fetal methylmercury exposure: insights from a pilot study. *Toxicol. Lett.* **242**, 60–67 (2016).

21. Lu, X. *et al.* Methylmercury uptake and degradation by methanotrophs. *Sci. Adv.* **3**, e1700041 (2017).

22. Dridi, B., Fardeau, M. L., Ollivier, B., Raoult, D. & Drancourt, M. Methanomassiliicoccus luminyensis gen. nov., sp. nov., a methanogenic archaeon isolated from human faeces. *Int. J. Syst. Evol. Microbiol.* **62**, 1902–1907 (2012).

23. Rey, F. E. *et al.* Metabolic niche of a prominent sulfate-reducing human gut bacterium. *Proc. Natl. Acad. Sci. U. S. A.* **110**, 13582–13587 (2013).

24. Muegge, B. D. *et al.* Diet drives convergence in gut microbiome functions across mammalian phylogeny and within humans. *Science (80-.).* **332**, 970–974 (2011).

25. Chaudhary, P. P., Gaci, N., Borrel, G., O'Toole, P. W. & Brugère, J. F. Molecular methods for studying methanogens of the human gastrointestinal tract: current status and future directions. *Applied Microbiology and Biotechnology* **99**, 5801–5815 (2015).

26. Wilkins, D., Lu, X. Y., Shen, Z., Chen, J. & Lee, P. K. H. Pyrosequencing of mcrA and archaeal 16s rRNA genes reveals diversity and substrate preferences of methanogen communities in anaerobic digesters. *Appl. Environ. Microbiol.* **81**, 604–613 (2015).

27. Langille, M. G. I. *et al.* Predictive functional profiling of microbial communities using 16S rRNA marker gene sequences. *Nat. Biotechnol.* **31**, 814–821 (2013).

28. Louca, S., Parfrey, L. W. & Doebeli, M. Decoupling function and taxonomy in the global ocean microbiome. *Science (80-.).* **353**, 1272–1277 (2016).

29. Alivisatos, A. P. *et al.* A unified initiative to harness Earth's microbiomes: Transition from description to causality and engineering. *Science* **350**, 507–508 (2015).

30. Konstantinidis, K. T., Braff, J., Karl, D. M. & DeLong, E. F. Comparative metagenomic analysis of a microbial community residing at a depth of 4,000 meters at station ALOHA in the North Pacific Subtropical Gyre. *Appl. Environ. Microbiol.* **75**, 5345–5355 (2009).

31. Zhang, T. & Hsu-Kim, H. Photolytic degradation of methylmercury enhanced by binding to natural organic ligands. *Nat. Geosci.* **3**, 473–476 (2010).

32. Seller, P., Kelly, C. A., Rudd, J. W. M. & MacHutchon, A. R. Photodegradation of methylmercury in lakes. *Nature* **380**, 694–697 (1996).

33. Bolger, A. M., Lohse, M. & Usadel, B. Trimmomatic: A flexible trimmer for Illumina sequence data. *Bioinformatics* **30**, 2114–2120 (2014).

34. Li, D., Liu, C. M., Luo, R., Sadakane, K. & Lam, T. W. MEGAHIT: An ultra-fast single-node solution for large and complex metagenomics assembly via succinct de Bruijn graph. *Bioinformatics* **31**, 1674–1676 (2015).

35. West, P. T., Probst, A. J., Grigoriev, I. V., Thomas, B. C. & Banfield, J. F. Genome-reconstruction for eukaryotes from complex natural microbial communities. *Genome Res.* **28**, 569–580 (2018).

36. Franzosa, E. A. *et al.* Species-level functional profiling of metagenomes and metatranscriptomes. *Nat. Methods* **15**, 962–968 (2018).

37. Truong, D. T. *et al.* MetaPhlAn2 for enhanced metagenomic taxonomic profiling. *Nature Methods* **12**, 902–903 (2015).

38. Buchfink, B., Xie, C. & Huson, D. H. Fast and sensitive protein alignment using DIAMOND. *Nature Methods* **12**, 59–60 (2014).

39. Eren, A. M. *et al.* Anvi'o: An advanced analysis and visualization platformfor 'omics data. *PeerJ* **2015**, e1319 (2015).

40. Hyatt, D. *et al.* Prodigal: Prokaryotic gene recognition and translation initiation site identification. *BMC Bioinformatics* **11**, 119 (2010).

41. El-Gebali, S. *et al.* The Pfam protein families database in 2019. *Nucleic Acids Res.* **47**, D427–D432 (2019).

42. Haft, D. H. *et al.* TIGRFAMs and genome properties in 2013. *Nucleic Acids Res.* **41**, (2013).

43. Ashburner, M. *et al.* Gene ontology: Tool for the unification of biology. *Nature Genetics* **25**, 25–29 (2000).

44. Nikolskaya, A. N., Arighi, C. N., Huang, H., Barker, W. C. & Wu, C. H. PIRSF family classification system for protein functional and evolutionary analysis. *Evol. Bioinform. Online* **2**, 197–209 (2007).

45. Kanehisa, M. & Goto, S. KEGG: Kyoto Encyclopedia of Genes and Genomes. *Nucleic*

Acids Research **28**, 27–30 (2000).

46. Karp, P. D., Riley, M., Paley, S. M. & Pellegrini-Toole, A. The MetaCyc database. *Nucleic Acids Res.* **30**, 59–61 (2002).

47. Jones, P. *et al.* InterProScan 5: Genome-scale protein function classification. *Bioinformatics* **30**, 1236–1240 (2014).

48. Menzel, P., Ng, K. L. & Krogh, A. Fast and sensitive taxonomic classification for metagenomics with Kaiju. *Nat. Commun.* **7**, 1–9 (2016).

49. Langmead, B. & Salzberg, S. L. Fast gapped-read alignment with Bowtie 2. *Nat. Methods* **9**, 357–359 (2012).

50. Alneberg, J. *et al.* Binning metagenomic contigs by coverage and composition. *Nat. Methods* **11**, 1144–1146 (2014).

51. Sieber, C. M. K. *et al.* Recovery of genomes from metagenomes via a dereplication, aggregation and scoring strategy. *Nat. Microbiol.* **3**, 836–843 (2018).

52. Bowers, R. M. *et al.* Minimum information about a single amplified genome (MISAG) and a metagenome-assembled genome (MIMAG) of bacteria and archaea. *Nature Biotechnology* **35**, 725–731 (2017).

53. Parks, D. H., Imelfort, M., Skennerton, C. T., Hugenholtz, P. & Tyson, G. W. CheckM: Assessing the quality of microbial genomes recovered from isolates, single cells, and metagenomes. *Genome Res.* **25**, 1043–1055 (2015).

54. Browne, H. P. *et al.* Culturing of 'unculturable' human microbiota reveals novel taxa and extensive sporulation. *Nature* **533**, 543–546 (2016).

55. Price, M. N., Dehal, P. S. & Arkin, A. P. FastTree 2 - Approximately maximum-likelihood trees for large alignments. *PLoS One* **5**, e9490 (2010).

56. Letunic, I. & Bork, P. Interactive Tree of Life (iTOL) v4: Recent updates and new developments. *Nucleic Acids Res.* **47**, W256–W259 (2019).

57. Franzosa, E. A. *et al.* Species-level functional profiling of metagenomes and metatranscriptomes. *Nat. Methods* **15**, 962–968 (2018).

58. Eddy, S. R. Accelerated profile HMM searches. *PLoS Comput. Biol.* **7**, e1002195 (2011).

59. Ruuskanen, M. O., Aris-Brosou, S. & Poulain, A. J. Swift evolutionary response of microbes to a rise in anthropogenic mercury in the Northern Hemisphere. *ISME J.* **14**, 788–800 (2020).

60. Ge, S. X., Jung, D. & Yao, R. ShinyGO: a graphical enrichment tool for animals and plants. *Bioinformatics* (2019). doi:10.1093/bioinformatics/btz931

61. Gill, S. R. *et al.* Metagenomic analysis of the human distal gut microbiome. *Science (80-.).* **312**, 1355–1359 (2006).

62. Eckburg, P. B. *et al.* Microbiology: Diversity of the human intestinal microbial flora. *Science (80-.).* **308**, 1635–1638 (2005).

63. Hillman, E. T., Lu, H., Yao, T. & Nakatsu, C. H. Microbial ecology along the gastrointestinal tract. *Microbes and Environments* **32**, 300–313 (2017).

64. Macfarlane, G. T., Gibson, G. R., Beatty, E. & Cummings, J. H. Estimation of short-chain fatty acid production from protein by human intestinal bacteria based on branched-chain fatty acid measurements. *FEMS Microbiol. Ecol.* **10**, 81–88 (1992).

65. Diether, N. E. & Willing, B. P. Microbial fermentation of dietary protein: An important factor in diet–microbe–host interaction. *Microorganisms* **7**, (2019).

66. Reisinger, K., Stoeppler, M. & Nürnberg, H. W. Methylcarbenium ion transfer from S-adenosylmethionine to inorganic mercury-one of the possible biological pathways to methylmercury? *Toxicol. Environ. Chem.* **8**, 45–54 (1984).

67. Ekstrom, E. B. & Morel, F. M. M. Cobalt limitation of growth and mercury methylation in sulfate-reducing bacteria. *Environ. Sci. Technol.* **42**, 93–99 (2008).

68. Landner, L. Biochemical model for the biological methylation of mercury suggested from methylation studies in vivo with neurospora crassa. *Nature* **230**, 452–454 (1971).

3.8 Tables and Figures

Table 3.1 – Summary of MAGs recovered using Anvi'o 6.1. High quality MAGs are highlighted in bold. Medium quality MAGs are italized. Bins with > 50% completion and <10% redundancy were not retained. The guideline are based on the MIMAG standard. Taxa identified using CheckM (v1.1.2)

MAGs	Taxa ID	Total length (Mbp)	GC ratio	Contigs (#)	Mean Contig length (bp)	Max Contig length (bp)	N50	# of Predicted genes	Completeness (%)	Redundancy (%)
MAG_76	**o__Selenomonadales**	**2.24**	**0.44**	**117**	**19,112**	**159,789**	**44,138**	**2,174**	**99.3**	**1.4**
MAG_80	**k__Bacteria**	**3.58**	**0.30**	**133**	**26,922**	**239,088**	**70,301**	**3,354**	**99.3**	**2.9**
MAG_61	**o__Clostridiales**	**2.47**	**0.37**	**61**	**40,514**	**215,711**	**49,692**	**2,335**	**96.4**	**2.9**
MAG_43	**o__Burkholderiales**	**2.35**	**0.50**	**145**	**16,230**	**81,771**	**23,848**	**2,244**	**96.4**	**3.6**
MAG_77	**o__Selenomonadales**	**2.29**	**0.50**	**58**	**39,413**	**225,577**	**84,794**	**2,111**	**96.4**	**5.0**
MAG_36	**o__Clostridiales**	**2.44**	**0.56**	**571**	**4,273**	**29,811**	**5,916**	**2,819**	**95.0**	**3.6**
MAG_72	**g__Streptococcus**	**2.14**	**0.40**	**234**	**9,131**	**89,264**	**18,688**	**2,169**	**92.1**	**2.2**
MAG_41	**o__Clostridiales**	**1.81**	**0.62**	**271**	**6,663**	**41,216**	**10,289**	**1,899**	**92.1**	**5.8**
MAG_66	*o__Clostridiales*	*2.60*	*0.54*	*687*	*3,791*	*55,053*	*5,082*	*2,908*	*86.3*	*8.6*
MAG_54	*o__Clostridiales*	*2.05*	*0.27*	*772*	*2,653*	*23,164*	*3,060*	*2,472*	*84.2*	*6.5*
MAG_65	*g__Streptococcus*	*1.63*	*0.42*	*735*	*2,219*	*13,308*	*2,444*	*2,119*	*84.2*	*7.9*
MAG_7	*g__Burkholderia*	*7.48*	*0.67*	*2,390*	*3,130*	*17,209*	*3,812*	*8,598*	*83.5*	*4.3*
MAG_58	*o__Clostridiales*	*2.20*	*0.49*	*532*	*4,143*	*32,011*	*6,010*	*2,249*	*82.0*	*5.8*
MAG_71	*o__Clostridiales*	*5.91*	*0.48*	*432*	*13,680*	*96,372*	*21,027*	*5,511*	*82.0*	*7.2*
MAG_39	*k__Bacteria*	*2.49*	*0.43*	*1,193*	*2,088*	*10,903*	*2,264*	*3,029*	*75.5*	*1.4*
MAG_30	*o__Bacteroidales*	*2.56*	*0.43*	*1,076*	*2,378*	*12,321*	*2,739*	*2,971*	*71.9*	*2.9*
MAG_37	*k__Bacteria*	*1.89*	*0.43*	*1,215*	*1,554*	*5,969*	*1,550*	*2,628*	*68.3*	*7.2*
MAG_59	*o__Clostridiales*	*1.68*	*0.41*	*815*	*2,061*	*12,641*	*2,245*	*2,085*	*66.9*	*0.7*

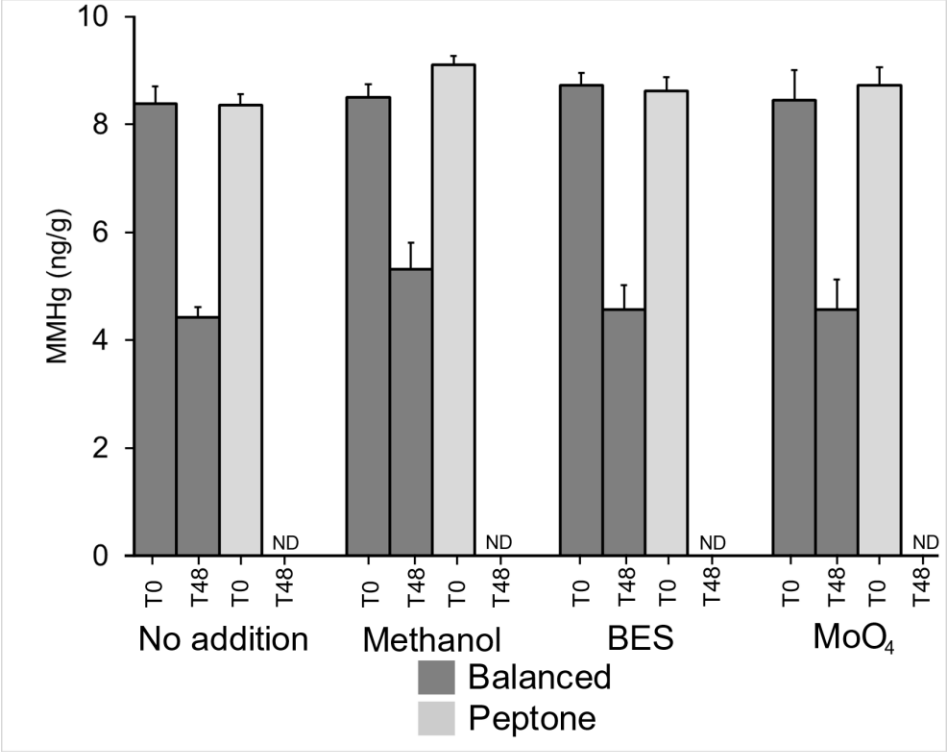

Medium	Treatment	Time	Average	SD
Balanced	*No addition*	0	8.38	0.32
		48	4.42	0.19
	Methanol	0	8.50	0.25
		48	5.31	0.50
	BES	0	8.72	0.22
		48	4.57	0.45
	Molybdate	0	8.45	0.56
		48	4.57	0.56
Protein	*No addition*	0	8.36	0.20
		48	ND	ND
	Methanol	0	9.10	0.16
		48	ND	ND
	BES	0	8.62	0.25
		48	ND	ND
	Molybdate	0	8.73	0.32
		48	ND	ND

Figure 3.1 – Inhibition assay for MeHg demethylation from known microbial guilds.

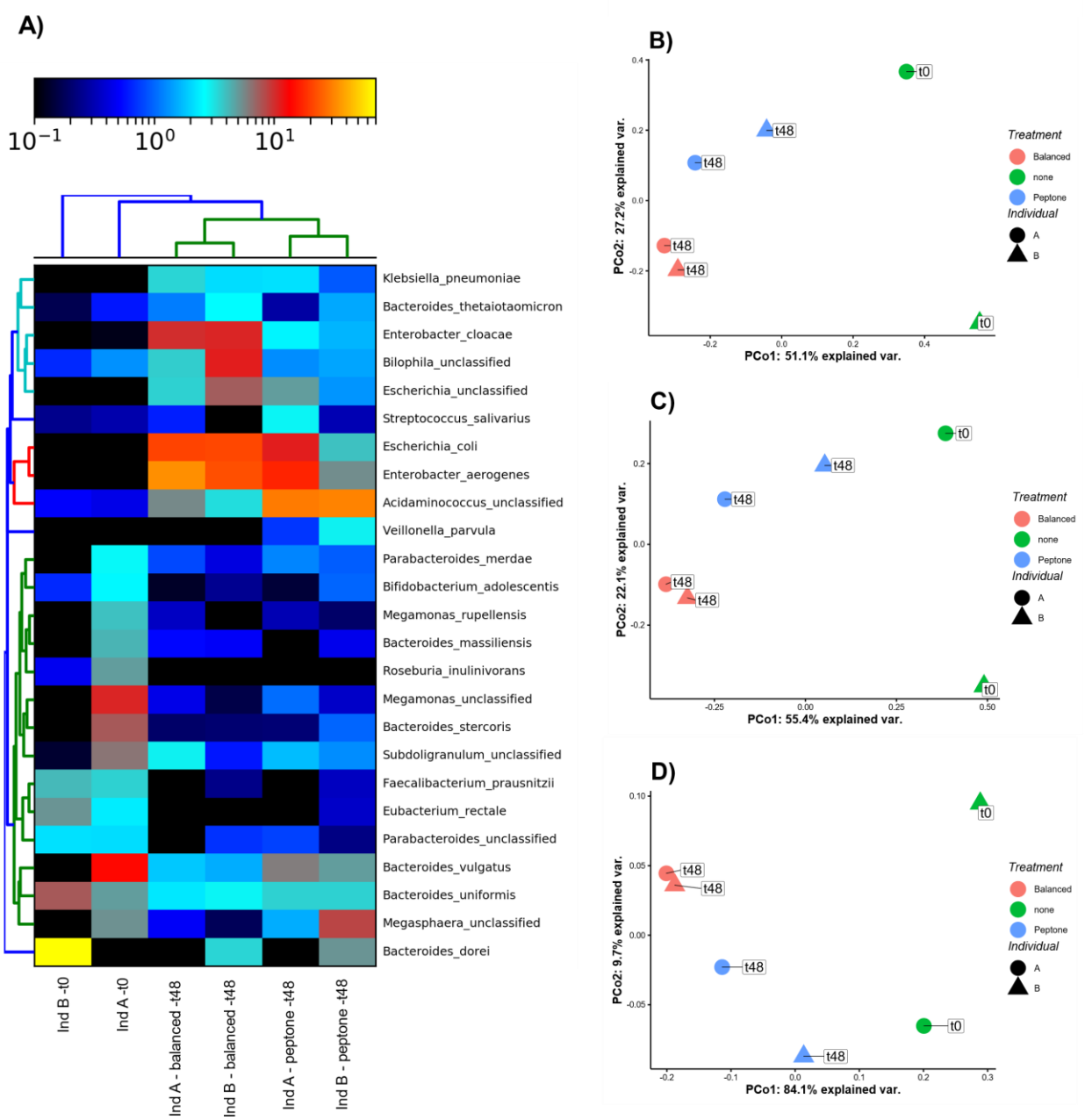

Figure 3.2 – A) Heatmap showing the distribution of taxa among the different treatment. Hierachical clustered gut microbiota by treatment and time. B-D) Principle coordinate analysis using Bray-Curtis dissimilarity distance of taxonomic (B), gene (C) and pathway (D) dataset. Individual A and B respond to nutrient similarly in balanced media. In peptone-amended medium, they respond differently.

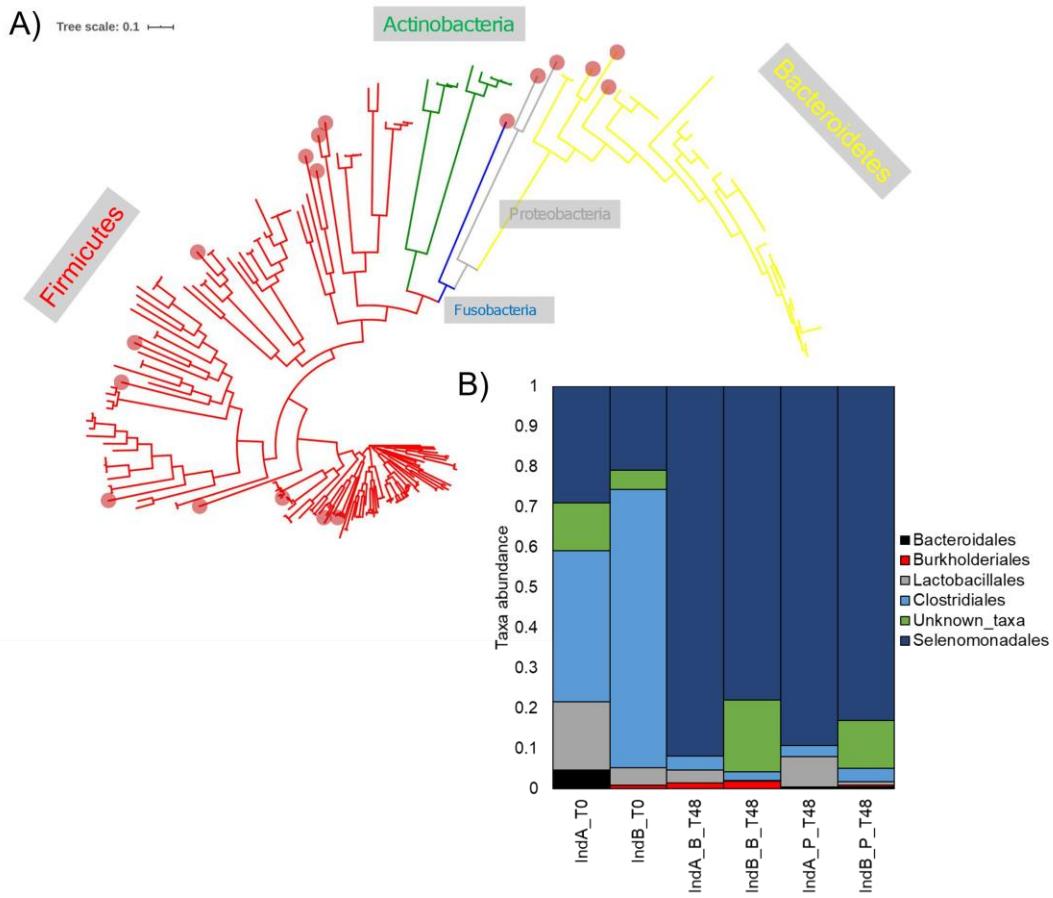

Figure 3.3 – Microbial tree reconstructed from genome representing taxa reported in Browne et al [41] with complete genomes available on NCBI. Incorporation of MAGs (red shaded dots) in their phylogenetic context using anvi'o's anvi-gen-phylogenomic-tree function and fasttree. Taxonomy of the MAGs was refined via their phylogenetic position among other bacterial genome found in healthy human gut microbiota. Relative abundance of MAGs found in all the different treatments.

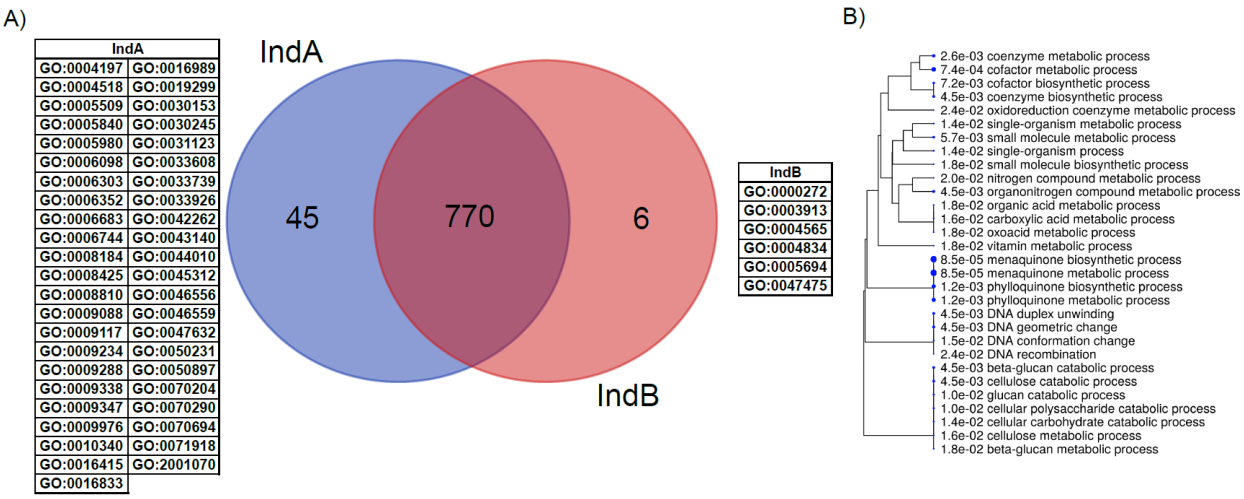

IndA	
GO:0004197	GO:0016989
GO:0004518	GO:0019299
GO:0005509	GO:0030153
GO:0005840	GO:0030245
GO:0005980	GO:0031123
GO:0006098	GO:0033608
GO:0006303	GO:0033739
GO:0006352	GO:0033926
GO:0006683	GO:0042262
GO:0006744	GO:0043140
GO:0008184	GO:0044010
GO:0008425	GO:0045312
GO:0008810	GO:0046556
GO:0009088	GO:0046559
GO:0009117	GO:0047632
GO:0009234	GO:0050231
GO:0009288	GO:0050897
GO:0009338	GO:0070204
GO:0009347	GO:0070290
GO:0009976	GO:0070694
GO:0010340	GO:0071918
GO:0016415	GO:2001070
GO:0016833	

IndB
GO:0000272
GO:0003913
GO:0004565
GO:0004834
GO:0005694
GO:0047475

Figure 3.4 – A total of 45 gene ontology annotated genes were uniquely found Individual A in protein amended post-incubation samples. Enrichment map analysis shows genes to be mostly correlated with vitamin K metabolisms. A) Venn diagram comparing genes from the gut microbiome of both individuals. B) A hierarchical tree of the most significant KEGG pathways identified by the enrichment analysis. Pathways are clustered based on the number of genes shared. Size of circles indicate higher significant P-values. Enrichment analysis based on hypergeometric distribution and FDR adjusted.

3.9 Supplemental tables and figures

Table B1- Summary table of enrichment map analysis

Enrichment FDR	Genes in list	Functional Category
8.54E-05	2	menaquinone metabolic process
8.54E-05	2	menaquinone biosynthetic process
7.44E-04	5	cofactor metabolic process
1.22E-03	2	phylloquinone biosynthetic process
1.22E-03	2	phylloquinone metabolic process
2.58E-03	4	coenzyme metabolic process
4.55E-03	3	coenzyme biosynthetic process
4.55E-03	2	cellulose catabolic process
4.55E-03	2	DNA geometric change
4.55E-03	2	DNA duplex unwinding
4.55E-03	2	beta-glucan catabolic process
4.55E-03	7	organonitrogen compound metabolic process
5.70E-03	7	small molecule metabolic process
7.22E-03	3	cofactor biosynthetic process
1.03E-02	2	glucan catabolic process
1.03E-02	2	cellular polysaccharide catabolic process
1.43E-02	2	cellular carbohydrate catabolic process
1.43E-02	15	single-organism process
1.43E-02	10	single-organism metabolic process
1.55E-02	2	DNA conformation change
1.64E-02	5	carboxylic acid metabolic process
1.64E-02	2	cellulose metabolic process
1.85E-02	5	organic acid metabolic process
1.85E-02	2	vitamin metabolic process
1.85E-02	5	oxoacid metabolic process
1.85E-02	4	small molecule biosynthetic process
1.85E-02	2	beta-glucan metabolic process
2.01E-02	10	nitrogen compound metabolic process
2.43E-02	2	DNA recombination
2.43E-02	2	oxidoreduction coenzyme metabolic process

Chapter 4: The gut microbial community structure of the North American river otter (*Lontra canadensis*) in the Alberta Oil Sands Region in Canada: relationship with local environmental variables and metal body burden

Authors: Galen Guo[1], Kristin M Eccles[1], Morgan McMillan[1], Philippe J. Thomas[1, 2], Hing Man Chan[1], Alexandre J. Poulain[1]

Affiliations:

[1]Department of Biology, University of Ottawa, ON, Canada

[2] Science and Technology Branch, Environment and Climate Change Canada, National Wildlife Research Center, Ottawa, ON, Canada

This chapter has been published as

Guo, G., Eccles, K.M., McMillan, M., Thomas, P.J., Chan, H.M., and Poulain, A.J., **(2020)** The gut microbial community structure of the North American river Otter (*Lontra canadensis*) in the Alberta Oil Sands Region of Canada: relationship with local environmental variables and metal body burden. *Environmental Toxicology & Chemistry.* published on *18 September 2020.* *https://doi.org/10.1002/etc.4876*

4.1 Abstract

The Alberta Oil Sands Region in Canada is home to one of the largest oil bitumen deposits in the world. The North American river otter (*Lontra canadensis*) is a top predator with a small home range and is sensitive to disturbances; it has been designated as a sentinel species for the potential impacts of the natural resource exploitation on freshwater ecosystems in the Alberta Oil Sands Region. With an increasing interest in noninvasive biomarkers, recent studies suggest that gut microbiota can be used as a potential biomarker of early biological effects on aquatic wildlife. The goal of the present study was to determine the river otter gut microbial structure related to environmental variables characterizing mining activities and metal body burden. We obtained 18 trapped animals from and surrounding the surface mineable area of the Alberta Oil Sands Region. The gut microbial community structure was characterized using high-throughput sequencing of 16S rRNA gene amplicon analyses. Trace metal concentrations in the liver were measured by inductively coupled plasma–mass spectrometry. Our study revealed that the gut bacteria of river otters in the Alberta Oil Sands Region clustered in 4 groups dominated by Peptostreptococcaceae, Carnobacteriaceae, Enterobacteriaceae, Clostridiaceae, and Nostocaceae. We show that arsenic, barium, rubidium, liver-body weight ratio, and δ15N were associated with each cluster. When comparing affected versus less affected sites, we show that river otter gut bacterial community and structure are significantly related to trophic level of the river otter but not to Alberta Oil Sands Region mining activities. Our study reveals that the gut bacterial dynamics can provide insights into the diet and habitat use of river otters but that more work is needed to use it as a pollution biomarker

Keyword: biomarker, river otter, gut microbiota, high-throughput sequencing, AOSR

4.2 Introduction

The Alberta Oil Sands in Canada are petroleum deposits where the soil contains a mixture of sand, clay, water, and bitumen. Crude oil is recovered through in situ steam injection or excavation through open-pit mines (Natural Resources Canada 2017). In 2019, the Alberta Energy Regulator (AER) reported that Alberta's total crude bitumen production is estimated at 3.1 million barrels/d (Alberta Energy Regulator 2019). Exploitation of the oil sands is an integral part of the Canadian economy, but it carries an environmental cost. Current monitoring efforts have shown that open-pit or surface mining significantly contributes to atmospheric contaminant releases such as heavy metals into the surrounding environment, with potential impacts on neighboring ecosystems (Kelly et al. 2010; Kirk et al. 2014; Huang et al. 2016). The use of sentinel species such as the North American river otter (*Lontra canadensis*) could aid in evaluating the health of the ecosystem. Sentinel species are organisms, usually animals, sensitive to environmental changes that are chosen to reveal and monitor the bioavailability of contaminants and to detect risks to humans by providing early warning of danger (Bossard 2006). River otters are semi-aquatic mustelids that live primarily in freshwater ecosystems and are usually top predators. River otters are also highly sensitive to natural (Lariviere and Walton 1998) and anthropogenic disturbances (Bowyer et al. 1994, 2003; Guertin et al. 2010), and to metal pollution (Harding et al. 1998; Basu et al. 2005). Moreover, river otter populations in North America have suffered dramatic declines as a result of habitat degradation (Lariviere and Walton 1998). Due to its sensitivity to disturbances, small home range, and nonmigratory and fish consumption behavior (apex predator), the river otter is considered a sentinel species of freshwater ecosystems (Basu 2012).

Current biomonitoring approaches relying on river otters involve census estimates via indirect counts and scat surveys to determine population dynamics (Mowry et al. 2011). However, due to the elusive nature of the animals, monitoring the population demographics of this species is challenging. Furthermore, this approach is unreliable due to its inability to identify individuals repeatedly. Certain DNA-based techniques such as polymorphic microsatellite loci in mustelid scats were used to evaluate river otter demography, to determine contaminant presence (Guertin et al. 2010), and to understand population genetic structure (Klütsch and Thomas 2018). In addition, river otter and mink fur were determined to be a good biomarker for determining mercury body burden (Eccles et al. 2020). Recent studies suggest that the gut microbiota could be a potential biomarker for aquatic toxicology and chemical risk assessment (Adamovsky et al. 2018), but no data have been available on freshwater mammals such as river otters.

The mammalian gut microbiota plays a significant role in its host's digestion, immune system, and detoxification (Fraune and Bosch 2010; McFall-Ngai et al. 2013; Kohl and Carey 2016; Guo et al. 2018). Environmental exposure significantly shapes the collective genomic potential of the gut microbiota (the gut microbiome; Rothschild et al. 2018), especially through diet (Ley et al. 2008). The mammalian gut microbiome can change in response to the metabolic demands of its host's diet, as shown in desert woodrats harboring creosote toxins that degrade microbes (Kohl et al. 2014), or in baleen whales, whose microbiome contains chitin-fermentative bacteria (Sanders et al. 2015). The environment can also alter the gut microbiota community structure. For instance, Coolon et al. (2010) found that deer mice living in formerly contaminated sites that underwent remediation have different gut microbial community structure than animals at reference sites, a difference that was attributed to the toxicity of remnant heavy metals. Similarly,

in vitro experiments in which zebrafish were chronically exposed to titanium dioxide nanoparticles and bisphenol A showed an altered gut microbiota composition and decreased abundance of commensal bacteria (Chen et al. 2018). Currently, there is no baseline study on the gut microbial community of river otters. However, based on the lifestyle of river otters, we expect that their gut microbiota would be similar to that of other semiaquatic mammals such as the American mink (*Neovison vison*) or the Eurasian otter (*Lutra lutra*; An et al. 2017; Bahl et al. 2017; Zhao et al. 2017). These species are also top predators in their respective ecosystems.

The present study aimed to explore the relationship between local environmental metal body burden and the gut microbial community structure of river otters at the time of capture and to further evaluate whether the data could be used to develop biomarkers for ecosystem health. First, we hypothesized that multistressor environments including habitat degradation and increased contaminant releases in the Alberta Oil Sands Region would be significantly associated with the gut microbiota of river otters, as shown in other mammalian gut environments (McKenzie et al. 2017). Second, we used geospatial analyses to identify environmental drivers that can potentially affect the river otter gut microbiota structure and to explore the use of gut microbiota as a biomarker of early biological effect in wildlife impacted by oil sands extraction activities.

4.3 Materials and Methods

4.3.1 Ethics

All animals were trapped following the Alberta Code for Responsible Trapping and the Agreement on International Humane Trapping Standards.

4.3.2 Site of river otter and environmental data collection

River otter carcasses (n = 18) already trapped under permit for the commercial fur trade were collected from willing trappers in the Alberta Oil Sands Region (Figure 4.1). Carcasses were stored at –20 °C until wildlife postmortem evaluations, and dissections were conducted at the National Wildlife Research Centre (Ottawa, ON, Canada). Environmental variables relevant to the habitat of each river otter were extracted using a geographic information system (GIS; Supplemental Data, Table C1). All environmental variables were calculated using a 9-km-radius circle around the trapline centroid. This value was chosen to simulate a realistic home range area for each river otter and would be representative of the environment it lives in. This metric was based on previous radiotelemetry data of river otters (Reid et al. 1994; Eccles et al. 2020).

4.3.3 Sample collection and preparation

Biological data, including body weight, organ weight, and sex, were collected during the gross necropsy of each animal. Metal contaminant burdens were generated in liver tissue. Liver samples were homogenized following an National Wildlife Research Centre operating protocol (#SOP-TP-PROC-07F). An aliquot of approximately 3.0 g was submitted for trace element and heavy metal analysis at National Wildlife Research Centre. The aliquot sample destined for trace element analysis was stored in preweighed, acid-washed, polypropylene vials and an exact wet weight was recorded. Samples were placed on a Labconco FreeZone, 6-L, –50 °C Console Freeze Dryer for at least 48 h. After removal, samples were weighed immediately to record dry weight and subsequently stored in a desiccator at room temperature until analysis. Percentage of moisture was calculated.

After drying, 100 mg (exact weight recorded) of dried sample was aliquoted into digestion tubes (15-mL DigiTUBEs; SCP Science). Nitric acid (1.5 mL) was added to each sample, including blank and quality control samples. Samples were capped loosely and left to sit overnight at ambient temperature. Samples were then heated to 70 °C for 100 min in a DigiPrep block (DigiPREP MS Graphite Digestion system; SCP Science) followed by 100 °C for 330 min. Samples were shaken by hand periodically throughout this incubation period to ensure homogeneous digestion. Following digestion, samples were left to cool overnight in the block at ambient temperature. Once cooled, the sample digest volume was adjusted to 5 mL with ultrapure water. Digests were finally stored at room temperature until further analysis.

Gastrointestinal tracts were surgically removed from the carcasses, kept in Ziploc bags, and stored at –20 °C until further processing. Gastrointestinal tracts were thawed at 4 °C. Scat samples were surgically removed from the gastrointestinal tract in a biosafety cabinet using ethanol-flamed sterilized scalpel and forceps to minimize cross-contamination and airborne microbial contamination. Scat was placed in 50-mL sterile canonical tubes and stored at –20 °C until DNA extraction.

4.3.4 Scat sampling and microbial community analysis

The DNA was extracted using the DNeasy PowerSoil DNA extraction kit (Qiagen) as per the manufacturer's protocol. The forward primer 341F (5′-CCTACGGGNGGCWGCAG-3′) and reverse primer 805R (5′-GACTACHVGGGTATCTAATCC- 3′) were used (Takahashi et al. 2014). Library preparation, amplicon sequencing, and demultiplexing were performed by Integrated Microbiome Resource (Dalhousie University, Halifax, NS, Canada) on the Illumina MiSeq PE 2 × 300 platform (Comeau et al. 2017). Preprocessing and processing of raw data were performed

using the Microbiome Helper processing pipeline (Comeau et al. 2017), which is based on QIIME2 (Bolyen et al. 2019). Adapter and primers were cut, and amplicons were trimmed using the Cutadapt tool (Martin 2011). Trimmed amplicons were processed (at 270 and 218 bp for forward and reverse reads, respectively), chimera-checked, and assigned taxonomy using DADA2 (Callahan et al. 2016). We performed our taxonomical assignments of our amplicon sequence variant (ASV) using the Naive Bayes approach (QIIME2 plugin) built for our primers using the SILVA 132 database (Quast et al. 2013). The phylogenetic tree was built using the SEPP QIIME2 plugin and generated using the R phyloseq package (McMurdie and Holmes 2013).

4.3.5 Trace metal analysis

Trace metal analyses were undertaken at the National Wildlife Research Centre, a CALA-accredited and ISO 17025 certified facility using a standardized operating protocol (#SOP-MTH-MET-TE-01C). Digests were analyzed using a PerkinElmer NexION 300d inductively coupled plasma–mass spectrometer (ICP-MS). The method was developed following the general principles of the US Environmental Protection Agency methods 6020 (2014) and 200.8 (1994), with modifications for wildlife tissues. The ICP–MS was run by the Syngistix Ver 1.1 and ESI SC Ver 2.8.0.3 software equipped with an ESI SC-2 DX FAST Basic autosampler. All samples (calibration blanks and standards, quality control samples and standards, and analytical samples) were analyzed with an internal standard (germanium, lutetium, rhodium, and scandium mixed in-house purchased from Delta Scientific). Quality assurance and control methods included the use of certified reference material (NIST CRM Oyster Tissue 1566b and CRM Lobster Hepatopancreas TORT-2). Data were corrected for % recovery of each internal standard. Blanks of HNO3 (1%) were injected at the beginning and end of each set of samples and before and after the calibration

standards to monitor cross-contamination. In addition, we made use of sample blanks analyzed with each set of 9 samples, and duplicate/triplicate extractions of one random sample/set of 9 livers. Results were expressed in μg g^{-1} dry weight.

4.3.6 Fur Data

Fur samples were analyzed for δ15N (‰) and δ13C (‰) using an elemental analyzer (Vario EL Cube; Elementar) interfaced (Conflo III; Thermo) to an isotope ratio mass spectrometer (Delta Advantage; Thermo). The internal standards used included C-51 nicotinamide (0.07, −22.95), C-52 mix of ammonium sulfate + sucrose (16.58, −11.94), C-54 caffeine (−16.61, −34.46), and blind standard C-55: glutamic acid (−3.98, −28.53), which represent a natural range of C and N values. The δ15N (‰) and δ13C (‰) values were calculated based on Equation 1, where d is the δ15N or δ13C values, R is the ratio of the abundance of the heavy to the light isotope, x is the sample, and std is an abbreviation for standard.

$$\mathrm{d} = R\,\frac{(x-std)}{std} * 1000 \qquad (1)$$

Total mercury (THg) was measured in the fur samples using a direct thermal decomposition Hg analyzer (Mercury Analyzer 3000; Nippon Instruments). Approximately 10 mg of fur was subsampled for analysis. Both DORM-4 and DOLT-5 were used as standard reference material, and 10% of samples were run in duplicate for quality assurance and quality control.

The cortisol was extracted from the fur samples using the protocol developed by Macbeth et al. (2010) and analyzed using an enzyme-linked immunosorbent assay (ELISA; Oxford EA-65 Cortisol EIA kit; Oxford Biomedical; Macbeth et al. 2010). The fur was washed 3 times in methanol and then ground using a ball mixer mill. The cortisol was extracted from the ground fur

using the extraction buffer from the ELISA kit. Once extracted, the absorbance of the samples was analyzed with the 96-well ELISA plate using a 650-nm filter. All samples and 8 known concentrations were run in duplicate. A standard curve developed from the known concentration, and this was used to convert the measured absorbance into concentrations.

4.3.7 Statistical analysis

All statistical analysis was performed in R (Ver 3.5.0) unless stated otherwise. The river otter gut bacterial structures were clustered employing a t-distributed stochastic neighbor embedding (t-SNE) method with a perplexity of 5, performed for dimension reduction (van der Maaten and Hinton 2008; van der Maaten 2014), and a hierarchical density-based spatial clustering of applications with noise (H-DBSCAN) with minPts of 3 was performed for density-based clustering (Mcinnes et al. 2017). The Rtsne package was used for dimension reduction, and the dbscan package was used for density-based clustering, both on the R platform (Hahsler et al. 2019). The output of these steps will indicate potential clustering of similar gut bacteria community. The biological relevance of the output from these steps was visually confirmed using principal component analysis on weight UniFrac distance.

The alpha diversity indices Chao1, Shannon, Faith's phylogenetic diversity, and ASV observed were calculated to evaluate between and within experimental groups. The Chao1 index is an estimation of taxa in a sample obtained by extrapolating rare species to overcome undersampling, whereas the Shannon diversity index measures abundance and evenness. Faith's phylogenetic diversity is a measure of the number of taxa built on the phylogenetic information generated based on the number of distinct sequence variants identified. Observed sequence variants are a measure of inferred sequences of taxa observed in a sample. A nonparametric

Kruskal–Wallis test was performed to determine significant effects between the different clusters generated, and multiple comparisons for significant differences were performed using Dunn's pairwise test, with the p value adjusted with Bonferroni correction. The Mann–Whitney rank sum test and equal variance test were performed to determine the significant difference in alpha diversity. Analysis of similarities (ANOSIM) was performed to determine the significant difference in beta diversity between river otter bacterial community structure from individuals living within the surface mining and outside the surface mining area.

Weighted UniFrac measurements were used to assess differences in gut bacterial communities between individuals and the different environmental variables measures, and accounts for taxa abundances (Lopuzone et al. 2006). We performed a multiple regression of environmental variables using EnvFit (vegan package; Oksanen et al. 2009), and the significance of fitted vectors and factors was assessed using random permutations (999). Linear discriminant analysis of effect size (LEFse) was used to determine taxa explaining the most difference between clusters (Segata et al. 2011). This analysis was set at an alpha value of 0.05 for Wilcoxon tests and a logarithmic linear discriminant analysis (LDA) score threshold set at 4.5. The ASVs with a relative abundance $<10^{-5}$, not seen more than 3 times in at least 20% of the samples, were eliminated. An alpha level of 0.05 was used as a guide for statistical significance, and an alpha level of 0.20 was used to determine environmental variables deemed important for further investigation.

4.4 Results

4.4.1 Characterizing the river otter gut bacterial community structure

To evaluate multistressor effects on the river otter gut bacterial community structure, we first characterized the transient gut bacterial assemblage, for which no data currently exist. We analyzed a total of 18 fecal samples extracted from river otter carcasses (10 males and 8 females). We generated a total of 371 181 filtered-quality reads with 20 621 average reads/sample. After de-noising and filtering steps, we were left with an average of 10 052.5 reads/sample. A total of 967 ASVs were obtained, for which firmicutes (74.7%), proteobacteria (14.5%), and actinobacteria (4.9%) accounted for more than 94%.

We identified similar gut bacterial community structures using density-based clustering. Using this approach, we identified 4 different gut bacterial clusters and identified representative taxa for each cluster. Our analysis identified the families Peptostreptococcaceae, Carnobacteriaceae, Enterobacteriaceae, and Nostocaceae as dominant in clusters 1, 2, 3, and 4, respectively (Figure 4.2; $p < 0.05$). Alpha diversity indices indicated significant differences between cluster 2 versus cluster 4 in all indices measured (Figure 4.3; $p < 0.05$).

4.4.2 Relationship with local environmental factors

We explored the relationship between chemical environmental exposure and the gut bacterial community structure. Our multiple comparisons (EnvFit) analysis revealed that the sex of the river otter had no impact on the gut bacterial composition and structure ($r^2 = 0.11$; $p = 0.36$). Environmental fitting analysis suggested that liver arsenic (As) concentrations were significantly correlated with the bacterial community structures of cluster 1 and 3 (Figure 4.4; $r^2 = 0.54$; $p =$

0.04). Liver zinc (Zn; Figure 4.4; $r^2 = 0.47$; $p = 0.07$) and δ15N (Figure 4.4; $r^2 = 0.62$; $p = 0.11$) were weakly related to the bacterial structure of cluster 1. We measured isotopic fur δ15N as a proxy for trophic level (Post 2002). Liver barium (Ba) was weakly related to cluster 2 (Figure 4.4; $r^2 = 0.36$; $p = 0.14$). Lastly, liver rubidium (Rb; Figure 4.4; $r^2 = 0.38$; $p = 0.15$) and liver to body weight ratio (liver_body wt_ratio; Figure 4.4; $r^2 = 0.34$; $p = 0.20$) were also weakly related to cluster 4.

4.4.3 Relationships with landscape

We assessed the relationship between surface mining and other anthropogenic activities in terms of the structure of the gut bacteria. We measured alpha diversity indices between river otter carcasses found in traplines within the mineable oil sands area and river otter carcasses found in traplines outside the mineable area (Figure 4.5). Results from the nonparametric t test indicated that there were no differences in the structure of river otter gut bacteria within and outside the mineable surface area for both alpha and beta diversity (Figure 4.5; Mann–Whitney rank sum test, Chao 1: $t = 50.0$, $p = 0.84$; Faith's phylogenetic diversity: $t = 50.0$, $p = 0.55$; and equal variance test, Shannon: $t = 0.88$, $p = 0.39$, ANOSIM: $p = 0.32$). Lastly, the median human impact score is based on a ranked metric related to the degree of anthropogenic land disturbance (i.e., concrete, house, roads, agricultural fields); this was calculated for each trapline and applied as a custom GIS layer. The median human impact score also showed no significant relationship with the gut bacterial community structure (Figure 4; $r^2 = 0.05$; $p = 0.98$).

4.5 Discussion

4.5.1 The bacterial community of the river otter gut was structured in 4 clusters

We have shown that the transient river otter gut microbiome is composed mainly of Firmicutes, Proteobacteria, and Actinobacteria. This gut bacterial structure is similar to that of the American mink and Eurasian river otter gut microbiota. Our analyses revealed 4 river otter gut bacterial clusters. We also identified representative taxa and potential environmental stressors correlating with each cluster. First, our analysis of cluster 1 revealed that it could reflect the gut microbiota of a predatory carnivore. Our analysis identified Peptostreptococcaceae as a potential biomarker for cluster 1 (Figure 4.2), which is typical of the microbial community structure of predatory carnivores (Nishida and Ochman 2018) as well as that of the Eurasian otter (An et al. 2017). Moreover, this cluster contains river otter with higher biomarker isotope δ15N, indicating that otters in cluster 1 consume higher trophic position organisms compared with the other river otters tested. River otter diet is varied, and prey selection depends on its habitat type (Day et al. 2015). Previous studies have indicated the importance of diet in shaping the gut microbiota structure of animals (Kohl and Dearing 2016; Ley et al. 2008; Nelson et al. 2013; Nishida and Ochman 2018; Youngblut et al. 2019). Additional information on river otter's prey items could help determine if Peptostreptococcaceae is a reliable biomarker for a predatory carnivore.

Second, we identified Carnobacteriaceae as a biomarker for cluster 2 (Figure 4.2). Carnobacterium, found within the Carnobacteriaceae family, is a psychrotrophic lactic acid bacterium that grows on a variety of foods and that may contribute to the rapid spoilage of meat during storage (Leisner et al. 2007; Casaburi et al. 2011). The role of this nonpathogenic bacterium in mammalian gut microbiota is unknown. However, we do know that this genus is associated with

marine and freshwater animals and may reflect the fish- based diet of river otters (Gilbert and Nancekivell 1982; Reid et al. 1994). Carnobacterium was also found in mink gut microbiota (Zhao et al. 2017), and minks and river otters share a similar diet (Eccles et al. 2020).

Third, our analysis identified Enterobacteriaceae and Clostridiaceae as core members for cluster 3 (Figure 4.4). Enterobacteriaceae and Clostridiaceae are large families that include not only pathogens but also commensal microorganisms of the gut environment (Octavia and Lan 2014; Youngblut et al. 2019). This cluster could potentially indicate river otters suffering from gastrointestinal disease, because a high abundance of Enterobacteriaceae (Janeczko et al. 2008; Linninge et al. 2018) and Clostridiaceae, more specifically Clostridium perfringens, is involved in mammalian gastrointestinal diseases. Furthermore, C. perfringens was observed to cause myositis and enterotoxemia in hooded seals (Aschfalk and Müller 2001) and significant tissue damage in long-beaked common dolphins (Danil et al. 2014). Interestingly, a study looking at anthropogenic fecal contamination of coastal marine habitat in California showed that dead sea otters were more likely to test positive for C. perfringens, Campylobacter, and Vibrio parahaemolyticus (Miller et al. 2010). Our results suggest that freshwater runoff, sewage, or a more urbanized center can represent significant risk factors for river otter health, which need to be further assessed. However, we are not able to link the presence of Enterobacteriaceae and Clostridiaceae with river otter gastrointestinal disease because we do not have any health-related information. Further studies linking the gut microbiota to health and disease could establish the correlation of these bacterial groups to river otter gastrointestinal disease.

Finally, we identified Nostocaceae (Cyanobacteria) and Actinobacteria as core members of cluster 4 (Figure 4.3). The family Nostocaceae contains nitrogen-fixing cyanobacteria typically

found in freshwaters (Dodds et al. 1995). Actinobacteria are widespread in terrestrial environments (Lawson 2018) and are known to be a core member of most mammalian microbiota (Nishida and Ochman 2018). This cluster likely reflects the amphibious behavior of river otters.

4.5.2 Correlation between local environmental variables and river otter clusters

Arsenic is of concern in the Alberta Oil Sands Region watersheds (Kelly et al. 2010; Moncur et al. 2015). High concentrations. of As in the Athabasca region are attributed to legacy atmospheric deposition from anthropogenic sources (Donner et al. 2019). In the Athabasca River, As concentrations were measured averaging 0.37 ± 0.01 and 0.34 ± 0.01 μg g−1 in 2014 and 2015, respectively (Donner et al. 2017). In our study, river otter liver As concentrations ranged from 0.07 to 0.42 μg g−1 (Supplemental Data, Table C2). Our environmentally driven patterns analysis showed a correlation between δ15N and As (Figure 4.4), which is in agreement with the bioaccumulative nature of As. It is unclear whether exposure to As alters the gut microbiome of river otter or vice versa. However, the bacterial composition of cluster 1 attributed to a carnivorous diet could be associated with metal(loid)s bioaccumulation at higher trophic levels. Additional work is required to further establish a correlation between As exposure and the gut microbial structure of river otters.

4.5.3 Surface mining does not appear to affect the river otters' gut bacterial community structure

Using geospatial analyses, we did not observe a direct relationship between the proximity to the surface mineable area or human activities, and the structure of river otter gut bacterial communities. Alberta has substantial oil extraction projects surrounding the mineable surface area (Figure 4.6). Other studies have shown that oil pumps and pipelines occasionally leak and increase contaminant levels locally (Timoney and Lee 2009; Schindler 2014; Korosi et al. 2016). These more elusive

sources of contamination could confound the effect that surface mining directly has on river otter gut bacterial community structure. One weakness of our study is the lack of data collected from a control population of river otters from an area that experiences no direct or indirect effects of oil sand activities. Our results suggest that oil pumps and pipeline leaks may affect river otter gut bacterial community structure similarly to effects directly associated with Alberta Oil Sands Region extraction activities. Establishing such a relationship warrants a broader and more extensive sampling effort and associated analyses than what was afforded by this exploratory study.

4.6 Conclusions

This is the first attempt to establish the use of gut bacterial community structure in river otter as biomarkers for anthropogenic disturbances and metal pollution. We identified 4 gut bacterial clusters, and we were able to identify the plausible taxonomical environmental exposure biomarkers attributed to each cluster. However, we were not able to positively identify the Alberta Oil Sands Region as uniquely responsible for variations in the river otter gut bacteria. More importantly, we realize that most of our samples could be influenced by factors that were initially outside the scope of our study, such as presence and location of oil pumps and pipelines, and would require further attention. Further studies obtaining health and clinical indices and environmental exposure data are needed to meaningfully use gut microbiota as biomarkers.

4.7 Acknowledgments

First, we would like to acknowledge the Alberta Trappers' Association, Treaty 8 Indigenous communities, and Métis Nations, whose traditional lands contributed river otter carcasses used for our study. Thanks are extended to the Oil Sands Monitoring program, Environment and Climate Change Canada, and the Province of Alberta. We want to thank the Ján Veizer Stable Isotope

Laboratory at the University of Ottawa for their isotopic analysis expertise. We also thank the numerous summer students who processed the river otter carcasses as well as the National Wildlife Specimen Bank (Ottawa, ON, Canada) technicians from the National Wildlife Research Centre. Special thanks go to E. Littlewood for processing the river otter fur samples. We would also like to thank laboratory members for insightful and constructive discussions and help throughout our study. Funding (# 296243 PBL5 A-001103.072 2903) was provided by Oil Sands Monitoring to P.J. Thomas, by Natural Sciences and Engineering Research Council of Canada (NSERC) Discovery Grants to A.J. Poulain and H.M. Chan, by the Canada Foundation for Innovation to A.J. Poulain, by a Canada Research Chair to H.M. Chan, and by an NSERC CREATE-REACT scholarship to G. Guo.

4.8 Data Accessibility statement

Raw sequence files that support the findings of this study are openly available in NCBI SRA (http://www.ncbi.nlm.nih.gov/bioproject/632926) BioProject ID: PRJNA632926.

Author contribution statement: GG, HMC, AJP conceived and planned the experiments. GG and MM carried out the experiment and data analysis. KME performed the geospatial analysis and fur isotope analysis. PJT obtained the samples and performed metal analysis. GG wrote the manuscript. All authors edited and provided comments to the final version of the manuscript

4.9 References

1. Adamovsky O, Buerger AN, Wormington AM, Ector N, Griffitt RJ, Bisesi JH, Martyniuk CJ. 2018. The gut microbiome and aquatic toxicology: An emerging concept for environmental health. Environ Toxicol Chem. 37(11):2758–2775. doi:10.1002/etc.4249. [accessed 2019 Aug 8]. http://doi.wiley.com/10.1002/etc.4249.
2. An C, Okamoto Y, Xu S, Eo KY, Kimura J, Yamamoto N. 2017. Comparison of fecal microbiota of three captive carnivore species inhabiting Korea. J Vet Med Sci. 79(3):542–546. doi:10.1292/jvms.16-0472. [accessed 2019 Jul 16]. http://www.ncbi.nlm.nih.gov/pubmed/28049922.
3. Aschfalk A, Müller W. 2001. Clostridium perfringens toxin types in hooded seals in the Greenland Sea, determined by PCR and ELISA. J Vet Med Ser B. 48(10):765–769. doi:10.1046/j.1439-0450.2001.00507.x.
4. Bahl MI, Hammer AS, Clausen T, Jakobsen A, Skov S, Andresen L. 2017. The gastrointestinal tract of farmed mink (Neovison vison) maintains a diverse mucosa-associated microbiota following a 3-day fasting period. Microbiologyopen. 6(3). doi:10.1002/mbo3.434. [accessed 2018 Dec 6]. http://www.ncbi.nlm.nih.gov/pubmed/28093882.
5. Basu N. 2012. Piscivorous Mammalian Wildlife as Sentinels of Methylmercury Exposure and Neurotoxicity in Humans. In: Methylmercury and Neurotoxicity. Boston, MA: Springer US. p. 357–370. [accessed 2019 Jul 16]. http://link.springer.com/10.1007/978-1-4614-2383-6_20.
6. Basu N, Scheuhammer A, Grochowina N, Klenavic K, Evans D, And MO, Chan HM. 2005. Effects of Mercury on Neurochemical Receptors in Wild River Otters (Lontra

canadensis). Environ Sci Technol. 39(10):3585–3591. doi:10.1021/ES0483746. [accessed 2019 Jul 16]. https://pubs.acs.org/doi/abs/10.1021/es0483746.

7. Bolyen E, Rideout JR, Dillon MR, Bokulich NA, Abnet CC, Al-Ghalith GA, Alexander H, Alm EJ, Arumugam M, Asnicar F, et al. 2019. Reproducible, interactive, scalable and extensible microbiome data science using QIIME 2. Nat Biotechnol. 37(8):852–857. doi:10.1038/s41587-019-0209-9. [accessed 2019 Nov 1]. http://www.nature.com/articles/s41587-019-0209-9.
8. Bossard G. 2006. Marine Mammals as Sentinel Species for Oceans and Human Health. Oceanography. 19(2):134–137. doi:10.5670/oceanog.2006.77. [accessed 2020 Mar 19]. https://tos.org/oceanography/article/marine-mammals-as-sentinel-species-for-oceans-and-human-health.
9. Bowyer RT, Blundell GM, Ben-David M, Jewett SC, Dean TA, Duffy LK. 2003. Effects of the Exxon Valdez Oil Spill on River Otters: Injury and Recovery of a Sentinel Species. Wildl Monogr. 153:1–53. doi:10.2307/3830746. [accessed 2017 Jul 3]. https://www.jstor.org/stable/3830746.
10. Bowyer RT, Testa JW, Faro JB, Schwartz CC, Browning JB. 1994. Changes in diets of river otters in Prince William Sound, Alaska: effects of the Exxon Valdez oil spill. Can J Zool. 72(6):970–976. doi:10.1139/z94-133. [accessed 2019 Jul 16]. http://www.nrcresearchpress.com/doi/10.1139/z94-133.
11. Callahan BJ, McMurdie PJ, Rosen MJ, Han AW, Johnson AJA, Holmes SP. 2016. DADA2: High-resolution sample inference from Illumina amplicon data. Nat Methods. 13(7):581–583. doi:10.1038/nmeth.3869. [accessed 2019 Mar 8]. http://www.nature.com/articles/nmeth.3869.

12. Casaburi A, Nasi A, Ferrocino I, Di Monaco R, Mauriello G, Villani F, Ercolini D. 2011. Spoilage-related activity of Carnobacterium maltaromaticum strains in air-stored and vacuum-packed meat. Appl Environ Microbiol. 77(20):7382–93. doi:10.1128/AEM.05304-11. [accessed 2019 Feb 20]. http://www.ncbi.nlm.nih.gov/pubmed/21784913.
13. Chen L, Guo Y, Hu C, Lam PKS, Lam JCW, Zhou B. 2018. Dysbiosis of gut microbiota by chronic coexposure to titanium dioxide nanoparticles and bisphenol A: Implications for host health in zebrafish. Environ Pollut. 234:307–317. doi:10.1016/J.ENVPOL.2017.11.074. [accessed 2018 Mar 13]. https://www-sciencedirect-com.proxy.bib.uottawa.ca/science/article/pii/S0269749117338046.
14. Comeau AM, Douglas GM, Langille MGI. 2017. Microbiome Helper: a Custom and Streamlined Workflow for Microbiome Research. mSystems. 2(1):e00127-16. doi:10.1128/mSystems.00127-16. [accessed 2019 Mar 7]. http://www.ncbi.nlm.nih.gov/pubmed/28066818.
15. Coolon JD, Jones KL, Narayanan S, Wisely SM. 2010. Microbial ecological response of the intestinal flora of Peromyscus maniculatus and P. leucopus to heavy metal contamination. Mol Ecol. 19(s1):67–80. doi:10.1111/j.1365-294X.2009.04485.x. [accessed 2018 Mar 13]. http://doi.wiley.com/10.1111/j.1365-294X.2009.04485.x.
16. Danil K, St. Leger JA, Dennison S, De Quirós YB, Scadeng M, Nilson E, Beaulieu N. 2014. Clostridium perfringens septicemia in a long-beaked common dolphin Delphinus capensis: An etiology of gas bubble accumulation in cetaceans. Dis Aquat Organ. 111(3):183–190. doi:10.3354/dao02783.
17. Day CC, Westover MD, McMillan BR. 2015. Seasonal diet of the northern river otter

(Lontra canadensis): what drives prey selection? Can J Zool. 93(3):197–205. doi:10.1139/cjz-2014-0218. [accessed 2019 Aug 2]. http://www.nrcresearchpress.com/doi/10.1139/cjz-2014-0218.

18. Dodds WK, Gudder DA, Mollenhauer D. 1995. The Ecology of Nostoc. J Phycol. 31(1):2–18. doi:10.1111/j.0022-3646.1995.00002.x. [accessed 2020 Jan 21]. http://doi.wiley.com/10.1111/j.0022-3646.1995.00002.x.
19. Eccles KM, Thomas PJ, Chan HM. 2019 Nov. Relationships between mercury concentrations in fur and stomach contents of river otter (Lontra canadensis) and mink (Neovison vison) in Northern Alberta Canada and their applications as proxies for environmental factors determining mercury bioavailability. Environ Res.:108961. doi:10.1016/j.envres.2019.108961. [accessed 2019 Dec 11]. https://linkinghub.elsevier.com/retrieve/pii/S0013935119307583.
20. Eccles KM, Thomas PJ, Chan HM. 2020. Relationships between mercury concentrations in fur and stomach contents of river otter (Lontra canadensis) and mink (Neovison vison) in Northern Alberta Canada and their applications as proxies for environmental factors determining mercury bioavailability. Environ Res. 181. doi:10.1016/j.envres.2019.108961.
21. Fraune S, Bosch TCG. 2010. Why bacteria matter in animal development and evolution. BioEssays. 32(7):571–580. doi:10.1002/bies.200900192. [accessed 2019 Jul 17]. http://doi.wiley.com/10.1002/bies.200900192.
22. Gilbert FF, Nancekivell EG. 1982. Food Habits of Mink (Mustela Vison) and Otter (Lutra Canadensis) in Northeastern Alberta. Can J Zool. 60(6):1282–1288.
23. Guertin DA, Harestad AS, Ben-David M, Drouillard KG, Elliott JE. 2010. Fecal

genotyping and contaminant analyses reveal variation in individual river otter exposure to localized persistent contaminants. Environ Toxicol Chem. 29(2):275–84. doi:10.1002/etc.53. [accessed 2016 Nov 21]. http://www.ncbi.nlm.nih.gov/pubmed/20821445.

24. Guo G, Yumvihoze E, Poulain AJ, Man Chan H. 2018. Monomethylmercury degradation by the human gut microbiota is stimulated by protein amendments. J Toxicol Sci. 43(12):717–725. doi:10.2131/jts.43.717. https://www.jstage.jst.go.jp/article/jts/43/12/43_717/_article.
25. Harding LE, Harris ML, Elliott JE. 1998. Heavy and Trace Metals in Wild Mink (Mustela vison) and River Otter (Lontra canadensis) Captured on Rivers Receiving Metals Discharges. Bull Environ Contam Toxicol. 61(5):600–607. doi:10.1007/s001289900803. [accessed 2017 Apr 5]. http://link.springer.com/10.1007/s001289900803.
26. Huang R, McPhedran KN, Yang L, Gamal El-Din M. 2016. Characterization and distribution of metal and nonmetal elements in the Alberta oil sands region of Canada. Chemosphere. 147:218–229. doi:10.1016/J.CHEMOSPHERE.2015.12.099. [accessed 2018 Dec 10]. https://www.sciencedirect.com/science/article/pii/S0045653515305543?via%3Dihub#fig1.
27. Janeczko S, Atwater D, Bogel E, Greiter-Wilke A, Gerold A, Baumgart M, Bender H, McDonough PL, McDonough SP, Goldstein RE, et al. 2008. The relationship of mucosal bacteria to duodenal histopathology, cytokine mRNA, and clinical disease activity in cats with inflammatory bowel disease. Vet Microbiol. 128(1–2):178–193.

doi:10.1016/j.vetmic.2007.10.014.

28. Kelly EN, Schindler DW, Hodson P V, Short JW, Radmanovich R, Nielsen CC. 2010. Oil sands development contributes elements toxic at low concentrations to the Athabasca River and its tributaries. Proc Natl Acad Sci U S A. 107(37):16178–83. doi:10.1073/pnas.1008754107. [accessed 2017 Nov 22]. http://www.ncbi.nlm.nih.gov/pubmed/20805486.
29. Kirk JL, Muir DCG, Gleason A, Wang X, Lawson G, Frank RA, Lehnherr I, Wrona F. 2014. Atmospheric deposition of mercury and methylmercury to landscapes and waterbodies of the Athabasca oil sands region. Environ Sci Technol. 48(13):7374–83. doi:10.1021/es500986r. [accessed 2015 Oct 29]. http://pubs.acs.org/doi/10.1021/es500986r.
30. Klütsch CFC, Thomas PJ. 2018. Improved genotyping and sequencing success rates for North American river otter (Lontra canadensis). Eur J Wildl Res. 64(2):16. doi:10.1007/s10344-018-1177-y. [accessed 2019 Jul 15]. http://link.springer.com/10.1007/s10344-018-1177-y.
31. Kohl KD, Carey H V. 2016. A place for host-microbe symbiosis in the comparative physiologist's toolbox. J Exp Biol. 219(Pt 22):3496–3504. doi:10.1242/jeb.136325. [accessed 2019 Jul 17]. http://www.ncbi.nlm.nih.gov/pubmed/27852759.
32. Kohl KD, Dearing MD. 2016. The Woodrat Gut Microbiota as an Experimental System for Understanding Microbial Metabolism of Dietary Toxins. Front Microbiol. 7:1165. doi:10.3389/fmicb.2016.01165. [accessed 2017 Nov 8]. http://journal.frontiersin.org/Article/10.3389/fmicb.2016.01165/abstract.
33. Kohl KD, Weiss RB, Cox J, Dale C, Denise Dearing M. 2014. Gut microbes of

mammalian herbivores facilitate intake of plant toxins. van Dam N, editor. Ecol Lett. 17(10):1238–1246. doi:10.1111/ele.12329. [accessed 2017 Nov 8]. http://doi.wiley.com/10.1111/ele.12329.

34. Korosi JB, Cooke CA, Eickmeyer DC, Kimpe LE, Blais JM. 2016. In-situ bitumen extraction associated with increased petrogenic polycyclic aromatic compounds in lake sediments from the Cold Lake heavy oil fields (Alberta, Canada). Environ Pollut. 218:915–922. doi:10.1016/j.envpol.2016.08.032. [accessed 2020 Mar 23]. http://www.ncbi.nlm.nih.gov/pubmed/27554977.
35. Lariviere S, Walton LR. 1998. Lontra canadensis. Mamm Species.(587):1. doi:10.2307/3504417. [accessed 2017 Apr 5]. https://academic.oup.com/mspecies/article-lookup/doi/10.2307/3504417.
36. Lawson PA. 2018. The Phylum Actinobacteria. In: The Bifidobacteria and Related Organisms. Elsevier. p. 1–8.
37. Leisner JJ, Laursen BG, Prévost H, Drider D, Dalgaard P. 2007. Carnobacterium: positive and negative effects in the environment and in foods. FEMS Microbiol Rev. 31(5):592–613. doi:10.1111/j.1574-6976.2007.00080.x. [accessed 2019 Feb 20]. http://www.ncbi.nlm.nih.gov/pubmed/17696886.
38. Ley RE, Hamady M, Lozupone C, Turnbaugh PJ, Ramey RR, Bircher JS, Schlegel ML, Tucker TA, Schrenzel MD, Knight R, et al. 2008. Evolution of mammals and their gut microbes. Science (80-). 320(5883):1647–1651. doi:10.1126/science.1155725. [accessed 2014 Jul 22]. http://www.sciencemag.org/content/320/5883/1647.abstract.
39. Licht TR, Bahl MI. 2018 Oct 3. Impact of the gut microbiota on chemical risk assessment. Curr Opin Toxicol. doi:10.1016/J.COTOX.2018.09.004. [accessed 2019 Aug

8]. https://www.sciencedirect.com/science/article/pii/S2468202018300172.

40. Linninge C, Roth B, Erlanson-Albertsson C, Molin G, Toth E, Ohlsson B. 2018. Abundance of Enterobacteriaceae in the colon mucosa in diverticular disease . World J Gastrointest Pathophysiol. 9(1):18–27. doi:10.4291/wjgp.v9.i1.18.
41. Lopuzone, C., Hamadi, M., Knight. R. UniFrac – An online tool for comparing microbial community diversity in a phylogenetic context BMC Bioinformatics 7, 371 (2006)
42. van der Maaten L, Hinton G. 2008. Visualizing Data using t-SNE. J Mach Learn Res. 9(Nov):2579–2605.
43. Macbeth BJ, Cattet MRL, Stenhouse GB, Gibeau ML, Janz DM. 2010. Hair cortisol concentration as a noninvasive measure of long-term stress in free-ranging grizzly bears (Ursus arctos): considerations with implications for other wildlife. Can J Zool. 88(10):935–949. doi:10.1139/Z10-057. [accessed 2019 Jul 16]. http://www.nrcresearchpress.com/doi/10.1139/Z10-057.
44. Martin M. 2011. Cutadapt removes adapter sequences from high-throughput sequencing reads. EMBnet.journal. 17(1):10. doi:10.14806/ej.17.1.200.
45. McFall-Ngai M, Hadfield MG, Bosch TCG, Carey H V, Domazet-Lošo T, Douglas AE, Dubilier N, Eberl G, Fukami T, Gilbert SF, et al. 2013. Animals in a bacterial world, a new imperative for the life sciences. Proc Natl Acad Sci U S A. 110(9):3229–36. doi:10.1073/pnas.1218525110. [accessed 2019 Jul 17]. http://www.ncbi.nlm.nih.gov/pubmed/23391737.
46. Mcinnes L, Healy J, Astels S. 2017. hdbscan: Hierarchical density based clustering. J Open Source Softw. doi:10.21105/joss.00205.
47. McKenzie VJ, Song SJ, Delsuc F, Prest TL, Oliverio AM, Korpita TM, Alexiev A,

Amato KR, Metcalf JL, Kowalewski M, et al. 2017. The effects of captivity on the mammalian gut microbiome. In: Integrative and Comparative Biology. Vol. 57. Oxford University Press. p. 690–704.

48. McMurdie PJ, Holmes S. 2013. phyloseq: An R Package for Reproducible Interactive Analysis and Graphics of Microbiome Census Data. Watson M, editor. PLoS One. 8(4):e61217. doi:10.1371/journal.pone.0061217. [accessed 2020 Jan 10]. https://dx.plos.org/10.1371/journal.pone.0061217.
49. Miller MA, Byrne BA, Jang SS, Dodd EM, Dorfmeier E, Harris MD, Ames J, Paradies D, Worcester K, Jessup DA, et al. 2010. Enteric bacterial pathogen detection in southern sea otters (*Enhydra lutris nereis*) is associated with coastal urbanization and freshwater runoff. Vet Res. 41(1):01. doi:10.1051/vetres/2009049. [accessed 2019 Dec 5]. http://www.vetres.org/10.1051/vetres/2009049.
50. Mowry RA, Gompper ME, Beringer J, Eggert LS. 2011. River otter population size estimation using noninvasive latrine surveys. J Wildl Manage. 75(7):1625–1636. doi:10.1002/jwmg.193. [accessed 2020 Feb 2]. http://doi.wiley.com/10.1002/jwmg.193.
51. Nelson TM, Rogers TL, Carlini AR, Brown M V. 2013. Diet and phylogeny shape the gut microbiota of Antarctic seals: a comparison of wild and captive animals. Environ Microbiol. 15(4):1132–1145. doi:10.1111/1462-2920.12022. [accessed 2019 Dec 11]. http://doi.wiley.com/10.1111/1462-2920.12022.
52. Nishida AH, Ochman H. 2018. Rates of gut microbiome divergence in mammals. Mol Ecol. 27(8):1884–1897. doi:10.1111/mec.14473. [accessed 2019 Dec 5]. http://www.ncbi.nlm.nih.gov/pubmed/29290090.
53. Octavia S, Lan R. 2014. The Family Enterobacteriaceae. In: The Prokaryotes. Berlin,

Heidelberg: Springer Berlin Heidelberg. p. 225–286. [accessed 2019 Dec 5]. http://link.springer.com/10.1007/978-3-642-38922-1_167.

54. Oksanen J, Kindt R, Legendre P, O'Hara B, Simpson GL, Solymos P, Stevens MHH, Wagner H. 2009. The vegan Package. [accessed 2020 Jan 10]. http://vegan.r-forge.r-project.org/.
55. Parajuli A, Grönroos M, Kauppi S, Płociniczak T, Roslund MI, Galitskaya P, Laitinen OH, Hyöty H, Jumpponen A, Strömmer R, et al. 2017. The abundance of health-associated bacteria is altered in PAH polluted soils—Implications for health in urban areas? Virolle M-J, editor. PLoS One. 12(11):e0187852. doi:10.1371/journal.pone.0187852. [accessed 2019 Dec 7]. https://dx.plos.org/10.1371/journal.pone.0187852.
56. Post DM. 2002. Using stable isotopes to estimate trophic position: Models, methods, and assumptions. Ecology. 83(3):703–718. doi:10.1890/0012-9658(2002)083[0703:USITET]2.0.CO;2.
57. Quast C, Pruesse E, Yilmaz P, Gerken J, Schweer T, Yarza P, Peplies J, Glöckner FO. 2013. The SILVA ribosomal RNA gene database project: Improved data processing and web-based tools. Nucleic Acids Res. 41(D1). doi:10.1093/nar/gks1219.
58. Reid DG, Code TE, Reid ACH, Herrero SM. 1994. Food habits of the river otter in a boreal ecosystem. Can J Zool. 72(7):1306–1313. doi:10.1139/z94-174. [accessed 2019 Jul 16]. http://www.nrcresearchpress.com/doi/10.1139/z94-174.
59. Rothschild D, Weissbrod O, Barkan E, Kurilshikov A, Korem T, Zeevi D, Costea PI, Godneva A, Kalka IN, Bar N, et al. 2018. Environment dominates over host genetics in shaping human gut microbiota. Nature. doi:10.1038/nature25973. [accessed 2018 Mar 6].

http://www.nature.com/doifinder/10.1038/nature25973.

60. Sanders JG, Beichman AC, Roman J, Scott JJ, Emerson D, McCarthy JJ, Girguis PR. 2015. Baleen whales host a unique gut microbiome with similarities to both carnivores and herbivores. Nat Commun. 6(1):8285. doi:10.1038/ncomms9285. [accessed 2019 Aug 2]. http://www.nature.com/articles/ncomms9285.
61. Schindler DW. 2014. Unravelling the complexity of pollution by the oil sands industry. Proc Natl Acad Sci. 111(9):3209–3210. doi:10.1073/pnas.1400511111. [accessed 2019 Jul 16]. www.pnas.org/cgi/doi/10.1073/pnas.1400511111.
62. Segata N, Izard J, Waldron L, Gevers D, Miropolsky L, Garrett WS, Huttenhower C. 2011. Metagenomic biomarker discovery and explanation. Genome Biol. 12(6):R60. doi:10.1186/gb-2011-12-6-r60. [accessed 2019 Mar 7]. http://www.ncbi.nlm.nih.gov/pubmed/21702898.
63. Takahashi S, Tomita J, Nishioka K, Hisada T, Nishijima M. 2014. Development of a Prokaryotic Universal Primer for Simultaneous Analysis of Bacteria and Archaea Using Next-Generation Sequencing. Bourtzis K, editor. PLoS One. 9(8):e105592. doi:10.1371/journal.pone.0105592. [accessed 2019 Aug 9]. http://www.ncbi.nlm.nih.gov/pubmed/25144201.
64. Timoney KP, Lee P. 2009. Does the Alberta Tar Sands Industry Pollute? The Scientific Evidence. [accessed 2019 Jul 16]. https://benthamopen.com/contents/pdf/TOCONSBJ/TOCONSBJ-3-65.pdf.
65. Youngblut ND, Reischer GH, Walters W, Schuster N, Walzer C, Stalder G, Ley RE, Farnleitner AH. 2019. Host diet and evolutionary history explain different aspects of gut microbiome diversity among vertebrate clades. Nat Commun. 10(1). doi:10.1038/s41467-

019-10191-3.

66. Zhao H, Sun W, Wang Z, Zhang T, Fan Y, Gu H, Li G. 2017. Mink (Mustela vison) Gut Microbial Communities from Northeast China and Its Internal Relationship with Gender and Food Additives. Curr Microbiol. 74(10):1169–1177. doi:10.1007/s00284-017-1301-3. [accessed 2017 Nov 22]. http://link.springer.com/10.1007/s00284-017-1301-3.

4.10 Tables and Figures

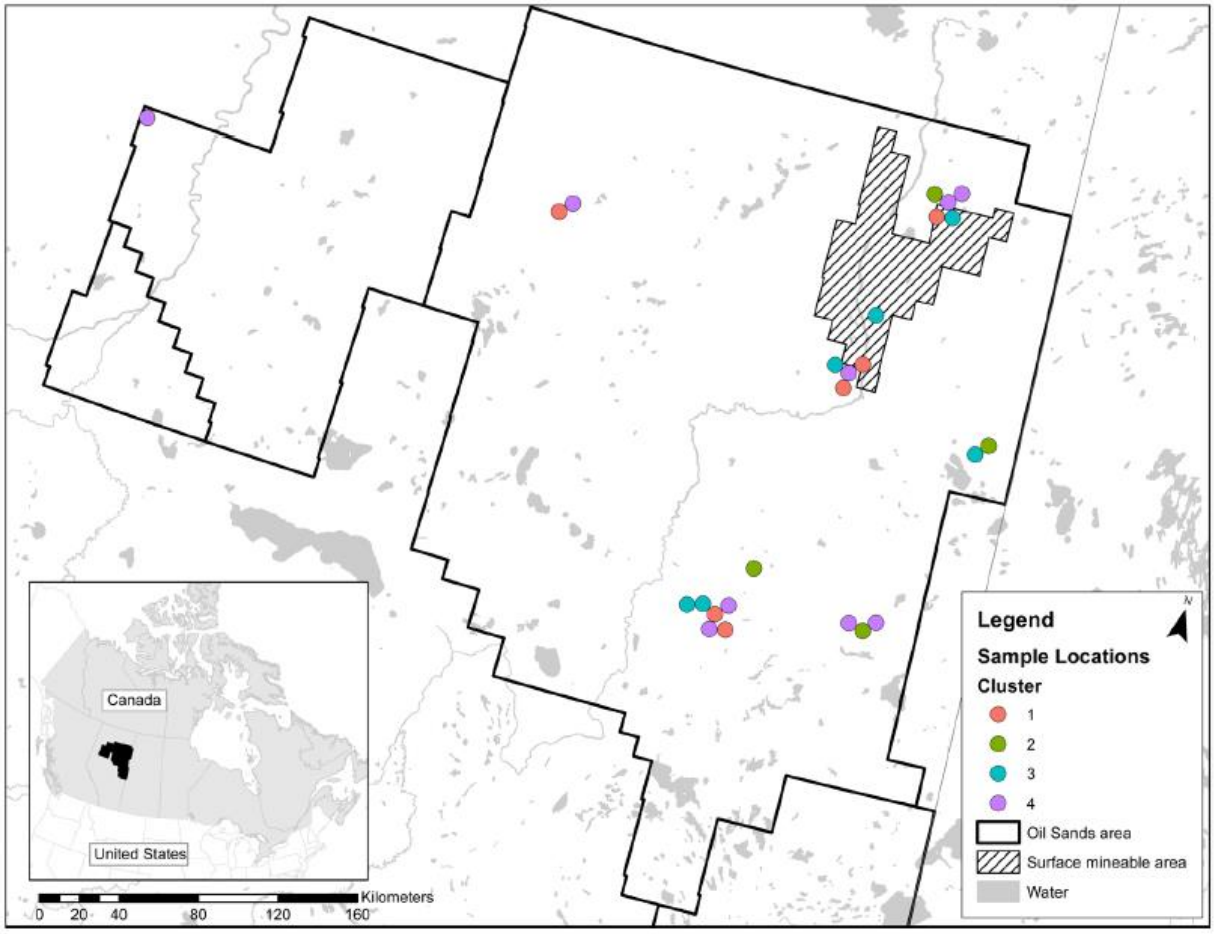

Figure 4.1 – Map of the Alberta Oil Sand Region with markers on the geographical location of the river otter samples.

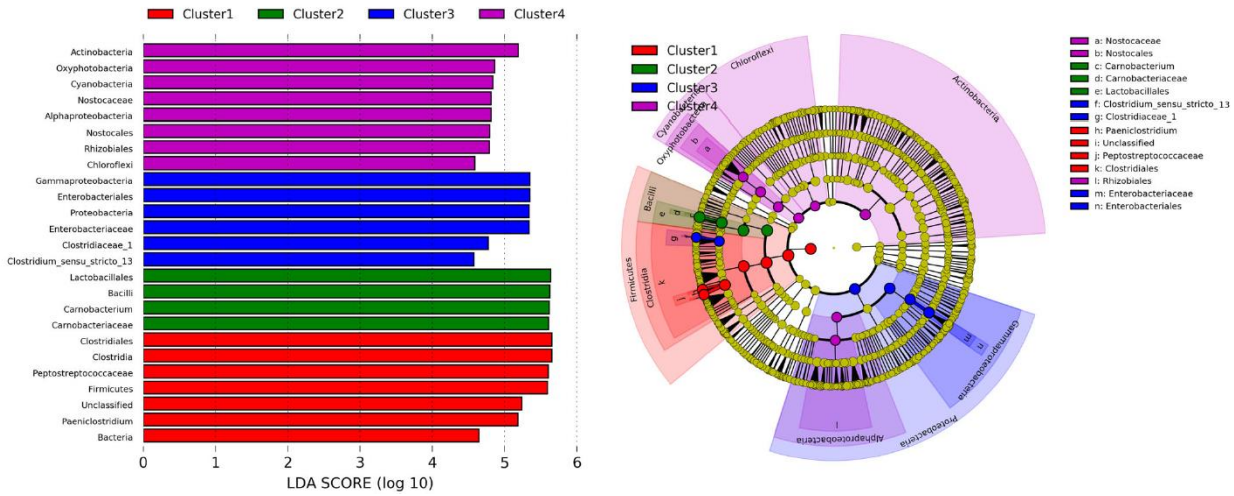

Figure 4.2 - Linear discriminant analysis (LDA) of effect size (LEfse) to determine taxa most representative each cluster. The LEfse was performed with an alpha value of 0.05 for Wilcoxon tests and a logarithmic LDA score threshold set at 4.5. This analysis has identified Peptostreptococcaceae, Carnobacteriaceae, Clostridiaceae_1, and Nostocaceae representing clusters 1, 2, 3, and 4, respectively.

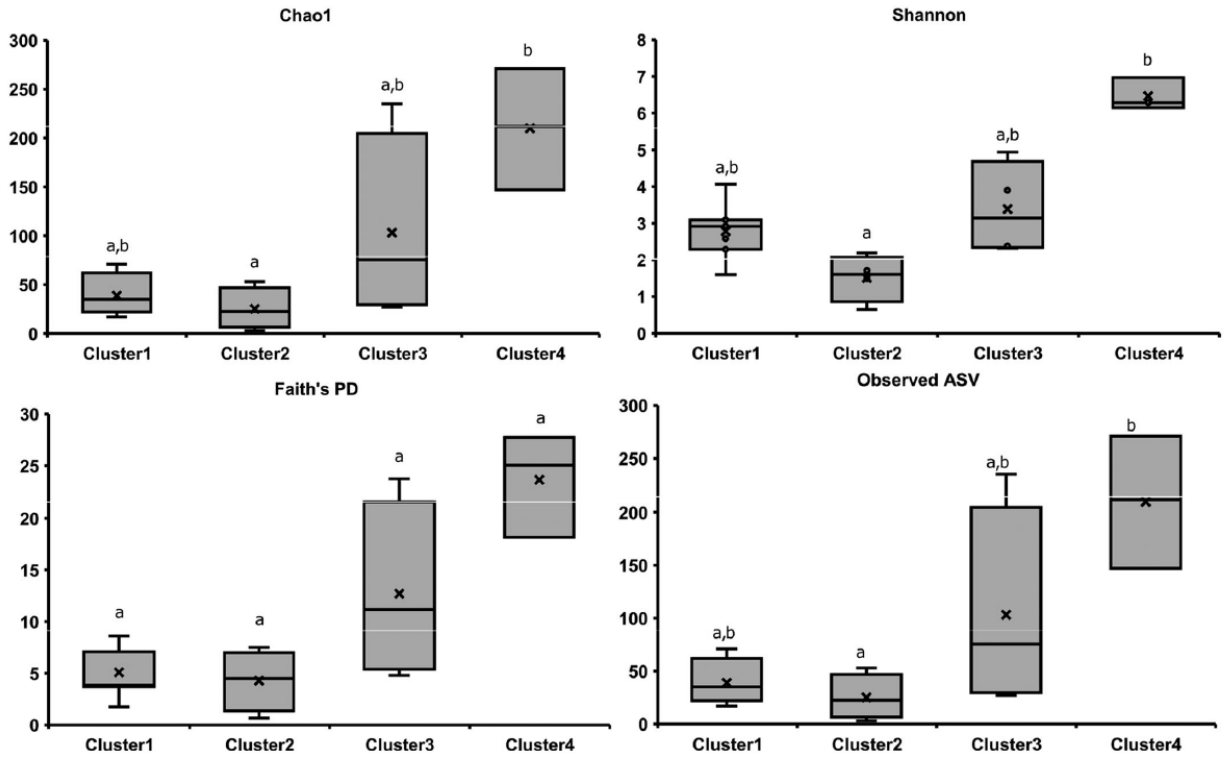

Figure 4.3 – Whisker plot of alpha diversity (Chao1, Shannon, and Faith's phylogenetic diversity [PD]) and total observed amplicon sequence variant (ASV) of each cluster. Letters represent significant differences between each cluster.

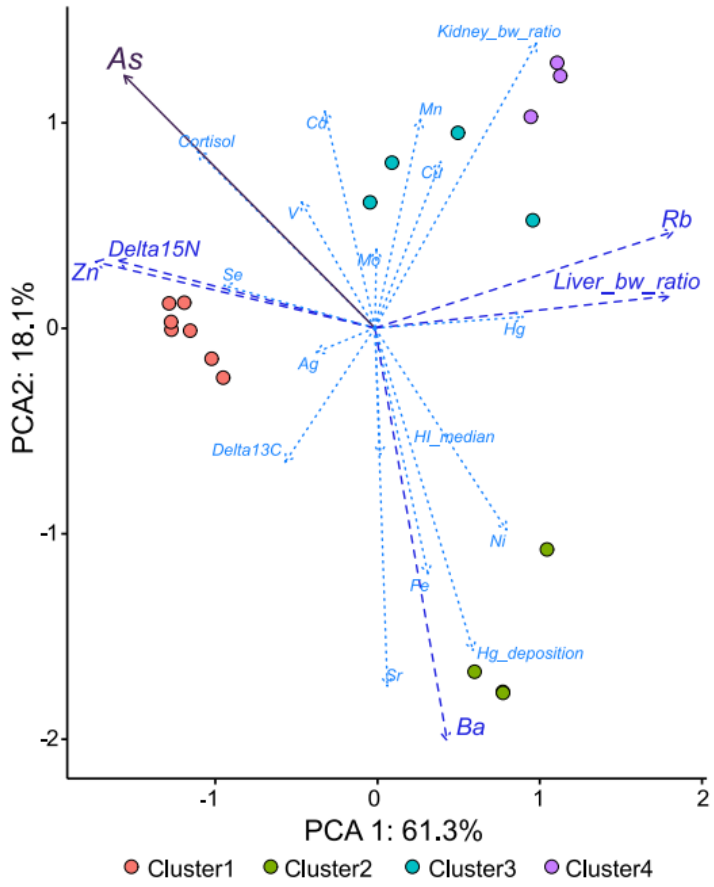

Vectors	R^2	p <0.05 *; p < 0.20 +
As	**0.54**	**0.04 ***
Zn	0.47	0.07 +
$\delta^{15}N$	0.41	0.12 +
Ba	0.36	0.14 +
Rb	0.38	0.15 +
Liver_bw_ratio	0.34	0.20 +
Kidney_bw_ratio	*0.30*	*0.24* .
Cortisol	*0.29*	*0.28* .
Sr	*0.27*	*0.29* .
Hg_deposition	*0.23*	*0.35* .
Sex	*0.11*	*0.36* .
Se	*0.16*	*0.48* .
Cd	*0.16*	*0.52* .
Fe	*0.12*	*0.59* .
Mn	*0.12*	*0.61* .
$\delta^{13}C$	*0.10*	*0.66* .
Ni	*0.13*	*0.66* .
V	*0.10*	*0.66* .
Cu	*0.08*	*0.71* .
Hg	*0.07*	*0.73* .
Surface mineable area	*0.03*	*0.79* .
Ag	*0.04*	*0.88* .
Hl_median	*0.03*	*0.89* .
Mo	*0.03*	*0.93* .

Figure 4.4 – Principal component analysis (PCA) of river otter gut microbiota using weighted UniFrac distance. Environmental vectors were fitted and represent the influence of each environmental variable on the river otter gut microbiota. Strontium (Sr) statistically influenced cluster 2 and is represented with a solid line ($p < 0.05$); barium (Ba), copper (Cu), and δ15N have some influence on clusters 2, 3, 4, and 1 and are presented with a dashed line ($p < 0.20$). All other environmental factors are represented with a dotted line. Each circle represents a river otter gut microbiota and is color-coded for the cluster identified using t-distributed stochastic neighbor embedding (t-SNE) to reduce the dimensionality of our dataset and hierarchical density-based spatial clustering of applications with noise (H-DBSCAN) for clustering. bw = body weight; As = arsenic; Zn = zinc; Rb = rubidium; Se = selenium; Cd = cadmium; Fe = iron; Mn = manganese; Ni = nickel; V = vanadium; Hg = mercury; Ag = silver; Mo = molybdenum.

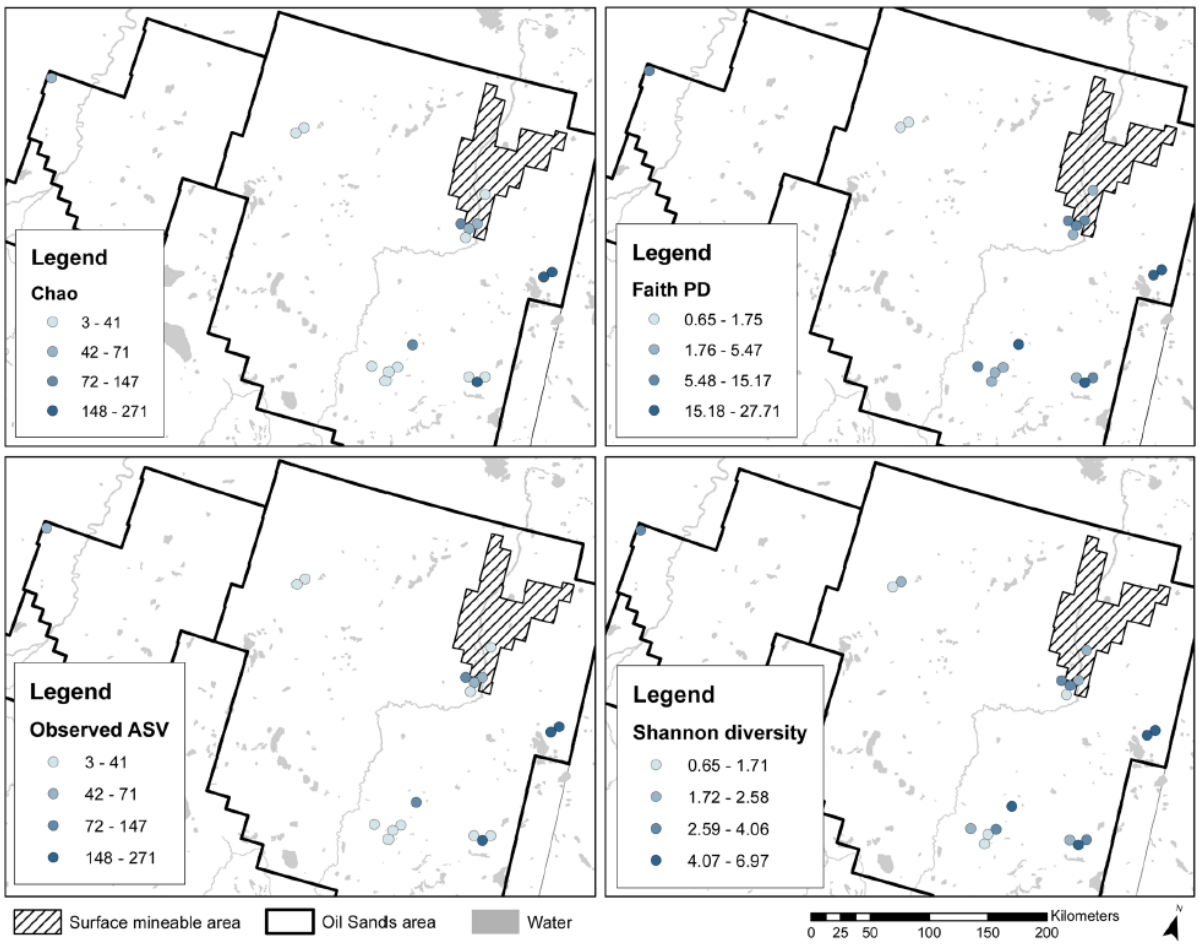

Figure 4.5 - Spatial distribution of each river otter sampled with its respective alpha diversity of gut microbiota. PD = phylogenetic diversity; ASV = amplicon sequence variant.

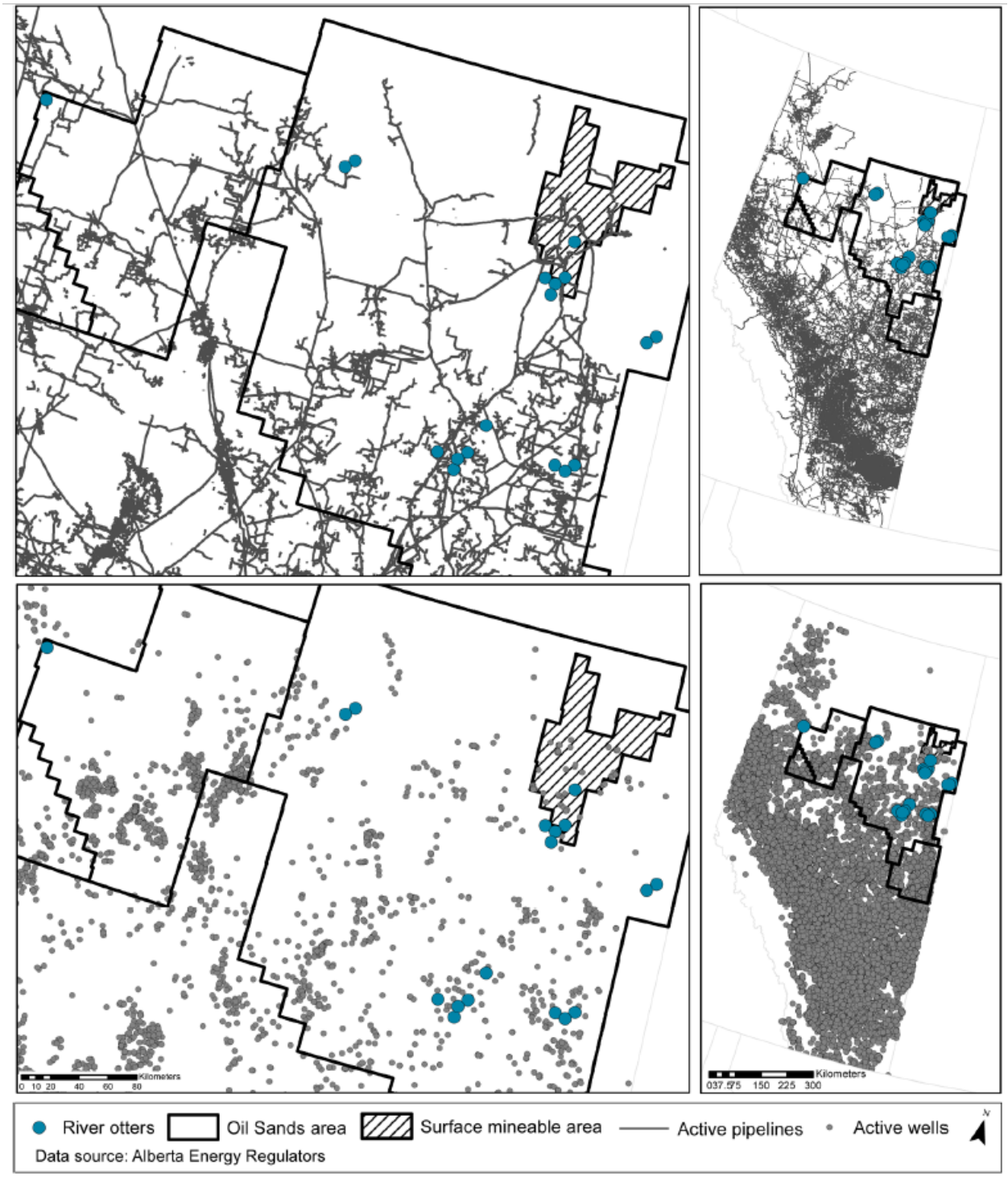

Figure 4.6 – Map indicating site where active pipelines and wells are found in the Alberta Oil Sands Region. The position of our river otters coincides with heavy oil extraction activity

4.11 Supplemental tables and figures

Table C1. Summary of environmental variables used for analysis.

Predictor	**Metric**	**Source**
Hg Deposition	Home range average 2012-2015	Environment and Climate Change Canada, Air Quality Research Division
Human Influence	Median value and each home range	Environment and Climate Change Canada, Canadian Wildlife Services (*Anthropogenic Influence Layer Model 1.0*. 2016)

Factors	Median	Range		Mean	SD
		min	max		
liver_bw_ratio	50.27	33.55	81.94	53.33	12.50
kidney_bw_ratio	12.36	9.03	14.28	12.49	1.32
Delta13C	-25.93	-31.45	-19.98	-26.07	3.13
Delta15N	10.68	8.71	15.25	10.90	1.49
Cortisol	5.89	1.056	17.39	8.33	6.59
Gut_Hg	229.59	22.16	540.48	244.14	145.90
Hg	3.14	1.15	6.63	3.29	1.62
MeHg	1.84	0.611	3.32	1.77	0.94
V	0.08	0.036	0.15	0.09	0.03
Mn	10.85	5.36	27.6	12.12	4.90
Fe	1244	661	2259	1375.00	493.69
Co	0.06	<0.04	0.1	0.05	0.03
Ni	0.06	<0.15	1.33	0.16	0.33
Cu	20.95	13.7	76	24.52	14.54
Zn	77.6	57.5	228	86.82	37.51
Ga	0.005	<0.005	0.01	0.01	0.002
As	0.18	0.077	0.42	0.20	0.09
Se	2.79	2.01	4.44	2.99	0.61
Rb	13.9	5.14	40.1	16.82	8.12
Sr	0.1	0.01	1.08	0.21	0.26
Mo	1.84	1.29	3.66	2.03	0.64
Ag	0.06	0.01	0.91	0.12	0.20
Cd	0.04	0.003	0.18	0.06	0.05
Ba	0.04	<0.030	0.33	0.06	0.07
HI_median	63	47	95	68.33	18.20
Hg_Deposition	15.94	12.99	17.22	15.67	1.12

Table C2 – Metadata gathered for all 18 river otters. Liver body weight and kidney body weight ratios were calculated by dividing the weight of each organ against total body weight. Liver metals ($\mu g.g^{-1}$) are dry weight measurements. Fur cortisol Hg deposition and gut Hg are measured at $\mu g.g^{-1}$. Human impact median (HI median) the median value of environmental variables extracted from GIS that is related to anthropogenic activity (i.e.: farming, house, roads)

Table C3 – Top 10 phylum and genus classified for each clusters

Phylum	Cluster1
Bacteria;Firmicutes	99.1%
Bacteria;Actinobacteria	0.4%
Bacteria;Proteobacteria	0.4%
Bacteria;Chloroflexi	0.0%
Bacteria;Fusobacteria	0.0%
Bacteria;Cyanobacteria	0.0%
Bacteria;Bacteroidetes	0.0%
Bacteria;Planctomycetes	0.0%
Bacteria;Tenericutes	0.0%
Bacteria;Patescibacteria	0.0%

	Cluster2
Bacteria;Firmicutes	93.5%
Bacteria;Proteobacteria	6.3%
Bacteria;Actinobacteria	0.1%
Bacteria;Cyanobacteria	0.0%
Bacteria;Tenericutes	0.0%
Bacteria;Verrucomicrobia	0.0%
Bacteria;Chloroflexi	0.0%
Archaea;Euryarchaeota	0.0%
Bacteria;Fusobacteria	0.0%
Bacteria;Bacteroidetes	0.0%

	Cluster3
Bacteria;Firmicutes	56.5%
Bacteria;Proteobacteria	35.2%
Bacteria;Actinobacteria	4.5%
Bacteria;Chloroflexi	2.1%
Bacteria;Cyanobacteria	0.9%
Bacteria;Planctomycetes	0.2%
Archaea;Euryarchaeota	0.2%
Bacteria;Patescibacteria	0.1%
Bacteria;Fusobacteria	0.1%
Bacteria;Dependentiae	0.1%

	Cluster4
Bacteria;Proteobacteria	26.7%
Bacteria;Actinobacteria	25.8%
Bacteria;Firmicutes	19.0%
Bacteria;Cyanobacteria	13.0%
Bacteria;Chloroflexi	9.2%
Bacteria;Planctomycetes	2.2%
Bacteria;Patescibacteria	1.1%
Bacteria;Dependentiae	0.7%
Bacteria;Verrucomicrobia	0.7%
Archaea;Euryarchaeota	0.6%

	Cluster1
Bacteria ; Firmicutes ; Clostridia ; Clostridiales ; Clostridiaceae 1 ; Clostridium sensu stricto 1 ; Clostridium perfringens	26.5%
Bacteria ; Firmicutes ; Clostridia ; Clostridiales ; Peptostreptococcaceae ; Paeniclostridium ; unclassified	22.8%
Bacteria ; Firmicutes ; Clostridia ; Clostridiales ; Peptostreptococcaceae ; unclassified ; unclassified	22.1%
Bacteria ; Firmicutes ; Clostridia ; Clostridiales ; Peptostreptococcaceae ; Romboutsia ; unclassified	5.2%
Bacteria ; Firmicutes ; Clostridia ; Clostridiales ; Clostridiaceae 1 ; Clostridium sensu stricto 1 ; unclassified	3.6%
Bacteria ; Firmicutes ; Clostridia ; Clostridiales ; Peptostreptococcaceae ; Paeniclostridium ; uncultured bacterium	3.3%
Bacteria ; Firmicutes ; Clostridia ; Clostridiales ; Clostridiaceae 1 ; Clostridium sensu stricto 1 ; Clostridium sp. Marseille-P2434	2.5%
Bacteria ; Firmicutes ; Clostridia ; Clostridiales ; Peptostreptococcaceae ; Terrisporobacter ; unclassified	2.0%
Bacteria ; Firmicutes ; Bacilli ; Lactobacillales ; Carnobacteriaceae ; Carnobacterium ; unclassified	1.9%
Bacteria ; Firmicutes ; Clostridia ; Clostridiales ; Clostridiaceae 1 ; Clostridium sensu stricto 13 ; unclassified	1.5%

	Cluster2
Bacteria ; Firmicutes ; Bacilli ; Lactobacillales ; Carnobacteriaceae ; Carnobacterium ; unclassified	48.4%
Bacteria ; Firmicutes ; Bacilli ; Lactobacillales ; Carnobacteriaceae ; Carnobacterium ; Ambiguous_taxa	34.1%
Bacteria ; Proteobacteria ; Gammaproteobacteria ; Enterobacteriales ; Enterobacteriaceae ; Hafnia-Obesumbacterium ; unclassified	5.8%
Bacteria ; Firmicutes ; Bacilli ; Lactobacillales ; Enterococcaceae ; Enterococcus ; unclassified	4.3%
Bacteria ; Firmicutes ; Bacilli ; Lactobacillales ; Lactobacillaceae ; Lactobacillus ; Lactobacillus sakei	2.7%
Bacteria ; Firmicutes ; Clostridia ; Clostridiales ; Peptostreptococcaceae ; unclassified ; unclassified	0.8%
Bacteria ; Firmicutes ; Clostridia ; Clostridiales ; Peptostreptococcaceae ; Romboutsia ; unclassified	0.7%
Bacteria ; Firmicutes ; Clostridia ; Clostridiales ; Peptostreptococcaceae ; Paeniclostridium ; uncultured bacterium	0.6%
Bacteria ; Firmicutes ; Clostridia ; Clostridiales ; Peptostreptococcaceae ; Paeniclostridium ; unclassified	0.6%
Bacteria ; Firmicutes ; Clostridia ; Clostridiales ; Ruminococcaceae ; uncultured ; uncultured Firmicutes bacterium	0.4%

	Cluster3
Bacteria ; Firmicutes ; Clostridia ; Clostridiales ; Clostridiaceae 1 ; Clostridium sensu stricto 1 ; Clostridium perfringens	22.4%
Bacteria ; Proteobacteria ; Gammaproteobacteria ; Enterobacteriales ; Enterobacteriaceae ; Hafnia-Obesumbacterium ; unclassified	16.4%
Bacteria ; Proteobacteria ; Gammaproteobacteria ; Enterobacteriales ; Enterobacteriaceae ; Plesiomonas ; unclassified	11.8%
Bacteria ; Firmicutes ; Clostridia ; Clostridiales ; Clostridiaceae 1 ; Clostridium sensu stricto 13 ; unclassified	11.8%
Bacteria ; Firmicutes ; Clostridia ; Clostridiales ; Enterococcaceae ; Enterococcus ; unclassified	5.8%
Bacteria ; Firmicutes ; Bacilli ; Lactobacillales ; Carnobacteriaceae ; Carnobacterium ; unclassified	3.4%
Bacteria ; Proteobacteria ; Gammaproteobacteria ; Enterobacteriales ; Enterobacteriaceae ; Escherichia-Shigella ; unclassified	2.9%
Bacteria ; Firmicutes ; Clostridia ; Clostridiales ; Peptostreptococcaceae ; Paraclostridium ; unclassified	2.0%
Bacteria ; Firmicutes ; Clostridia ; Clostridiales ; Peptostreptococcaceae ; unclassified ; unclassified	1.7%
Bacteria ; Proteobacteria ; Gammaproteobacteria ; Aeromonadales ; Aeromonadaceae ; Aeromonas ; unclassified	1.6%

	Cluster4
Bacteria ; Actinobacteria ; Actinobacteria ; Corynebacteriales ; Mycobacteriaceae ; Mycobacterium ; unclassified	10.0%
Bacteria ; Proteobacteria ; Alphaproteobacteria ; Rhizobiales ; Rhizobiales Incertae Sedis ; uncultured ; Ambiguous_taxa	3.6%
Bacteria ; Firmicutes ; Bacilli ; Lactobacillales ; Streptococcaceae ; Streptococcus ; unclassified	3.5%
Bacteria ; Proteobacteria ; Gammaproteobacteria ; Diplorickettsiales ; Diplorickettsiaceae ; Rickettsiella ; Ambiguous_taxa	3.3%
Bacteria ; Firmicutes ; Clostridia ; Clostridiales ; Clostridiaceae 1 ; Clostridium sensu stricto 13 ; unclassified	3.2%
Bacteria ; Cyanobacteria ; Oxyphotobacteria ; Nostocales ; Nostocaceae ; Anabaena BECID22 ; Ambiguous_taxa	2.3%
Bacteria ; Chloroflexi ; Anaerolineae ; Caldilineales ; Caldilineaceae ; uncultured ; metagenome	2.2%
Bacteria ; Firmicutes ; Clostridia ; Clostridiales ; Peptostreptococcaceae ; unclassified ; unclassified	2.1%
Bacteria ; Proteobacteria ; Alphaproteobacteria ; Rhizobiales ; Hyphomicrobiaceae ; Hyphomicrobium ; unclassified	2.0%
Bacteria ; Cyanobacteria ; Oxyphotobacteria ; Nostocales ; Nostocaceae ; Nostoc PCC-7524 ; Ambiguous_taxa	2.0%

Figure C1 – Bargraph of relative abundance ordered by cluster group

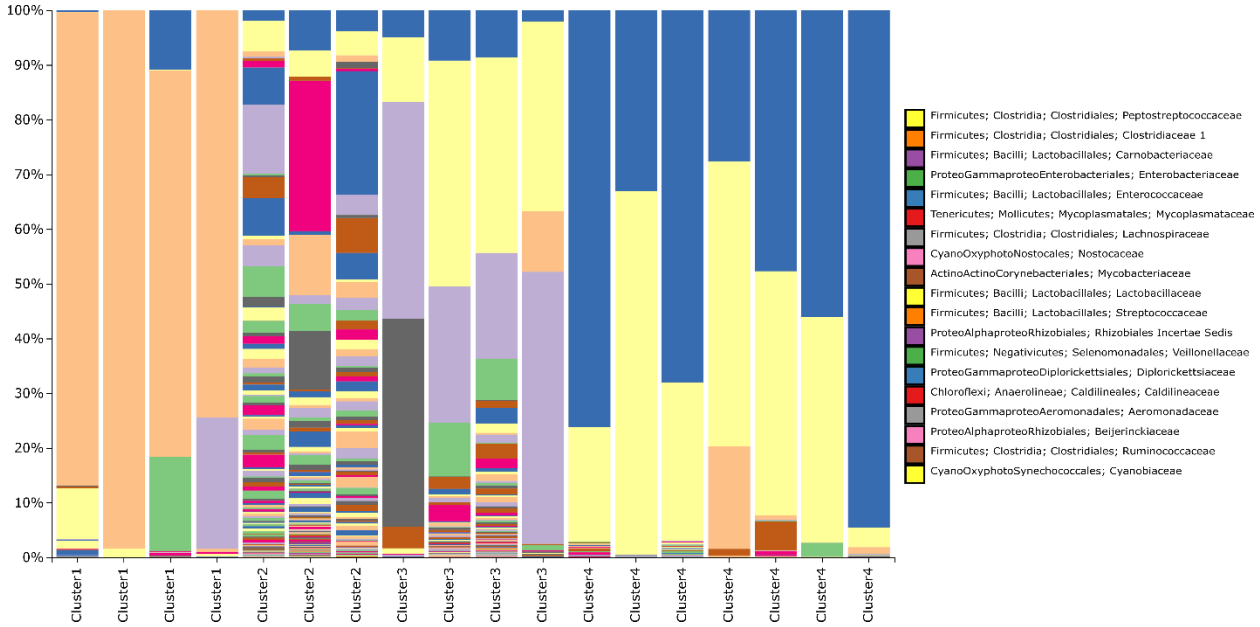

Figure C2 – phylogenetic tree representing species that appear in more than 3 river otters in more than 20% of relative abundance.

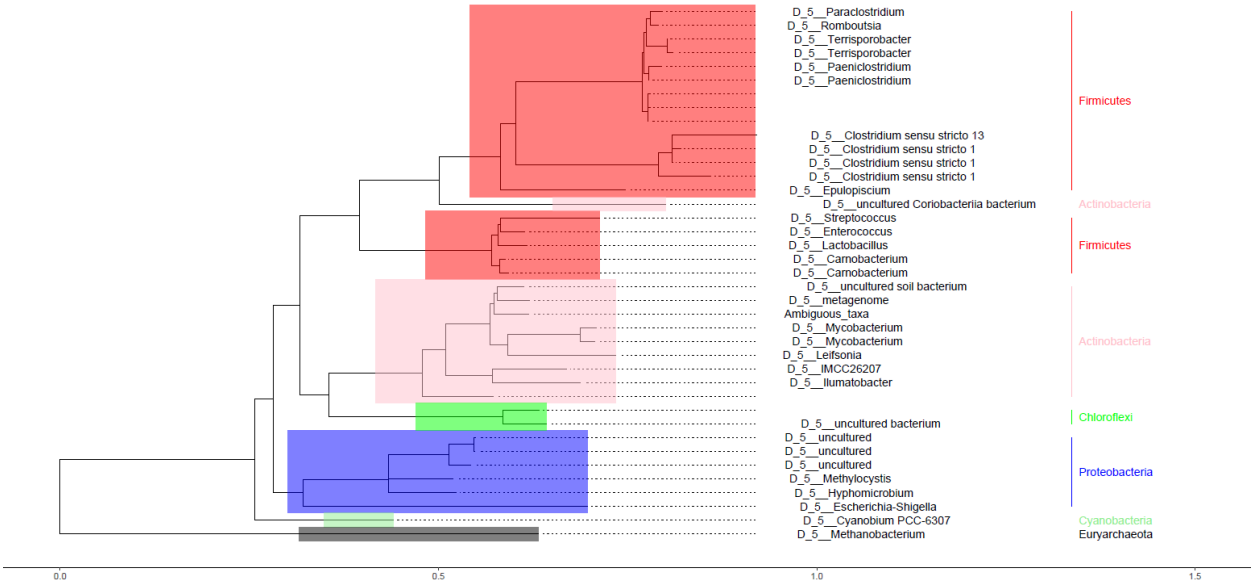

Chapter 5: Prey selection correlates with different gut microbial structure of seabirds in Sheet Harbour, Nova Scotia, Canada

Galen Guo[1], Rui Zhang[1], Mark L Mallory[2], Hing Man Chan[1], Alexandre J Poulain[1]

Affiliations:

[1]Department of Biology, University of Ottawa, Ottawa, ON, K1N 6N5, Canada

[2]Biology Department, Acadia University, Wolfville, NS, B4P 2R6, Canada

This chapter is being prepared for submission to Environmental Science & Technology

5.1 Abstract

Seabirds have adapted different foraging techniques and feed at various ocean zones (nearshore vs offshore, surface feeding vs plunge-diving). However, environmental degradation and habitat loss in coastal areas are causing a substantial population decline. The gut microbiome of seabirds can be used as bioindicators for their health but remains unexplored. This study explored the use of gut microbiome of seabirds as bioindicators of environmental health by determining the relationship between the gut microbiome of seabirds, their prey selections, and body burden of mercury and selenium. We obtained a total of 25 seabirds spanning five different species of seabirds (Arctic Tern [*Sterna paradisaea*], Black Guillemot [*Cepphus grylle*], Common Eider [*Somateria mollissima*], Double-crested Cormorant [*Phalacrocorax auritus*], Leach's Storm-Petrel [*Oceanodroma leucorhoa*]). We studied the gut microbiota using high-throughput sequencing of 16S rRNA gene amplicons and measured trophic index (isotopic tracer $\delta^{13}C$ and $\delta^{15}N$), liver mercury, and selenium. Our findings revealed the seabird gut microbiome clustered in four groups based primarily on prey selections. Cluster 1 included seabirds that consumed at a higher trophic position and showed the highest mercury body burden. Cluster 2 is comprised of seabirds that preyed on littoral benthic consumers. Cluster 3 and 4 included seabirds consumed mostly in the pelagic zone and had higher selenium liver concentration. Interestingly, seabirds with higher liver selenium concentration were correlated with lower liver mercury concentration. This study showed a correlation between the gut microbiome, contaminant body burden and prey selection in Atlantic seabirds. This study is an important first step in developing a seabird gut microbiome as a non-invasive biomarker for marine ecosystem health.

5.2 Introduction

Seabirds have been widely used as bioindicators for chemical pollution in the marine ecosystem changes such as heavy metals (1, 2). Seabirds are abundant and widespread, which allows for sustainable and ethical sampling. These seabirds' collection and sacrifice allowed extensive studies on the mercury (Hg) distribution across trophic levels and food webs (3). However, environmental factors such as habitat degradation or marine pollution threaten the livelihood of the seabirds (4). Some species are facing an important population decline. Therefore, non-invasive biomonitoring methods such as collecting eggs from breeding colonies are becoming preferred methods (5). Hg concentrations in seabird eggs showed a wide variation between species and appeared to be driven primarily on their diet (5). Moreover, a comparison of egg Hg concentrations across different latitudes showed different Hg accumulation patterns within the same bird species (6), suggesting that the geographical distribution and diet of seabirds are the prevalent causes of differential Hg accumulation in seabirds.

Hg enters the marine environment through atmospheric and terrestrial deposition pathways (7). Transformation of Hg to methylmercury (MeHg) occurs in the ocean water column and marine sediments via a microbially-mediated process (8). MeHg enters the marine food web by consuming algae and bacteria by zooplankton and is further biomagnified to higher trophic levels, including seabirds (9). The effects of Hg on seabird populations are not known, but there is evidence showing that elevated Hg concentrations can cause adverse outcomes on seabird fitness. For example, a study observed decreased little auk (*Alle alle*) chick growth rate and body adult condition with increasing Hg exposure (10). Another study has shown an increase in parasitic levels and reduced abdominal fat in common eider from elevated Hg exposure (11).

Selenium (Se) is an essential trace element that is found at high concentrations in seabirds (12) but can lead to deleterious effects at higher doses (13). Hg has a high affinity for Se and together form mercuric selenide complexes in the liver of seabirds (12). It has also been reported that Se can induce the demethylation of MeHg in the intestinal environment in black seabream (*Spondyliosoma cantharus*) (14). In seabirds, a diet rich in Se could compensate for the reduction of blood Se caused by Hg complexation, preserving Se-dependent enzymatic function in the host's central nervous system (15).

Feeding ecology is important in determining the Hg and Se body burden in seabirds. Coupling quantitative trophic tracers such as stable carbon ($\delta^{13}C$) and nitrogen isotopes ($\delta^{15}N$) could highlight important geographical differences in contaminants uptake by seabirds (16, 17). A recent study focusing on Magnificent frigatebirds (*Fregata magnificens*) have shown positive correlations between Hg, $\delta^{15}N$, and $\delta^{13}C$, suggesting that Hg bioaccumulated and biomagnified in these birds. The authors also attributed the variation in Hg concentration to their feeding location (18). Seabirds feeding in warmer waters have also been more prone to higher Hg body burden (19). Therefore, the feeding ecology of seabirds is important in the overall risk assessment of their Hg exposure.

The gut microbiota plays a significant role in its host’s digestion, immune system, and detoxification (20–23). Research on bird gut microbiome generally lacks compared to other organisms, such as mammals. The avian gut microbiota generally has a conserved group of core taxa (Firmicutes, Proteobacteria, Actinobacteria and Bacteroidetes) (24–26) and its structure is mostly influenced by environmental pressure exhibited by the host’s habitat and diet (27–30). Several studies have shown the effects of contaminants such as Hg on the gut microbiome or the

gut microbiome's effects on Hg biotransformation in other species (21, 31–33). None was conducted to evaluate the relationship between contaminant exposure and the avian gut microbiota. Only one study reported that the foregut of the hoatzin (*Opisthocomus hoazin*) contains saponins detoxifying microbes (34). In this study, we investigated the relationship between Hg and Se body burden and the gut microbiota structure of five different species of seabirds (Arctic Tern [*Sterna paradisaea*], Black Guillemot [*Cepphus grylle*], Common Eider [*Somateria mollissima*], Double-crested Cormorant [*Phalacrocorax auritus*], Leach's Storm-Petrel [*Oceanodroma leucorhoa*]). The goal is to explore the use of seabird gut microbiome as an indicator of the seabirds and the marine environment by studying the relationship between the diet, body burden of Hg and Se, and the gut microbiota of seabirds. Seabirds consuming at higher trophic position, such as the Double-Crested Cormorant, would exhibit a higher Hg body burden and result in a relatively diverse microbial structure compare to lower trophic position consuming seabirds.

5.3 Materials and method

5.3.1 Ethics

Collections of birds were conducted under approved animal care permit (ACC 02-15R2) and Canadian Wildlife Service scientific permit (ST2785).

5.3.2 Bird location and sampling

Birds were sampled in the Eastern Shore Islands Wildlife Management Area, east of Sheet Harbour, Nova Scotia, centred approximately 44 53'N, 62 20'W (Figure 5.1). Birds were shot by 12-gauge shotgun with steel #4 shot. Within 1 hr, birds were dissected where liver and muscle samples were placed in 2 mL centrifuge tubes and kept frozen in liquid nitrogen. Samples were then transferred

to a -40ºC freezer until further analysis. Samples were freeze-dried before shipment for tissue analyses.

5.3.3 Bird fecal collection and preparation

In a biosafety cabinet, fecal samples were removed from the gastrointestinal tract. Scalpel and forceps were sterilized by flamed ethanol to minimized microbial contamination. Fecal samples were placed in 15 mL sterile canonical tubes and stored at -20 ºC until use.

5.3.4 Optimization of bacterial DNA extraction in bird fecal sample

DNA extraction of bird fecal samples is notoriously tricky. Indeed, bird fecal samples are enveloped in a biofilm-like substance that prevented the mechanical and chemical disruption of the bacterial cell wall during the DNA extraction process. Fecal samples were soaked in 1.5M NaCl and 10% Tween 80 solution and shaken at 330 rpm for 2 hours in an ice box, to improve the yield of DNA extracted. Fecal samples were centrifuged to concentrate DNA was extracted using the PowerSoil DNA extraction kit (QIAGEN, MD, USA) as per manufacturer's protocol.

5.3.5 16S amplicon sequence analysis

The forward primer 515F (5- GTGYCAGCMGCCGCGGTAA-3) and reverse primer 806R (5-GGACTACNVGGGTWTCTAAT-3) were used (35). Library preparation, amplicon sequencing and demultiplexing were performed by Genome Quebec (Montreal, QC, Canada). Processing of raw sequencing data was performed using *QIIME2* (36). Adapter and primers were cut and amplicons trimmed using *Cutadapt* (37). Sequences were cleaned and taxonomy assigned using *DADA2* (38). We performed our taxonomical assignments of our ASV using the Naive-Bayes approach (*QIIME2* plugin) built for our primers using the *SILVA 132* database (39).

5.3.6 C and N Isotope analyss

Whole muscle samples were freeze-dried, grounded, and sent to the Stable Isotopes in Nature Laboratory (SINLAB, University of New Brunswick, Canada) for analysis of carbon and nitrogen isotopes. Samples were combusted in an elemental analyzer, and gases were sent to the isotope-ratio mass spectrometer using a continuous flow interface. Data are reported as differences in isotopic ratios, for which the units are parts per thousand (or per mil; ‰), compared to Pee Dee Belemnite (PDB), for carbon, and atmospheric nitrogen (AIR), for nitrogen, according to the following equation:

$$\delta X = \left(\frac{R_{sample}}{R_{std}} - 1\right) * 1000$$

δX is the isotope of interest (either $\delta^{15}N$ or $\delta^{13}C$, in ‰). R is the ratio of the abundance of the heavy to the light isotope ($^{15}N/^{14}N$ or $^{13}C/^{12}C$), with R_{sample} being the ratio within the sample, and R_{std} the ratio of heavy to light isotope within the international (40).

5.3.7 Hg and Se analysis

A 2 g liver sample was processed for analysis of trace elements at RPC Science & Engineering, (Fredericton, Canada). Samples were digested overnight by adding 1.0 mL of HNO_3 (70%) to material placed in test tubes. Samples were heated, loosely capped, and stored at 100°C in dry heating blocks for 4 h. Cooled samples were diluted to 4.0 mL in reverse osmosis purified water, and then diluted 20 times for analysis. Trace element concentrations were analyzed according to CALA-accredited standard operating procedures (Environment Canada, 1989), following procedure MET-CHEM-ICP-01A (modified from EPA Method 200.8 for biological samples), and using Inductively Coupled Plasma Mass Spectrometry (ICP-MS, Thermo-Series II). Hg was

analyzed using Cold Vapour Atomic Absorption (using a Teledyne Hydra II; method based on EPA 245.6). Quality assurance/quality control procedures included analysis of two method blanks (purified water), two repeats each of two certified biological reference tissues (bovine liver NIST 1577b, US National Institute of Standards and Technology; DOLT-5, National Research Council, Canada), and three randomly selected duplicate samples. Trace element recovery rates ranged from ±10% for analytes; Hg recovery was 93%. All QA/QC measures were in compliance with standard laboratory operating procedures at the time of analysis.

5.3.8 Statistical analysis

All statistical analyses were performed on R. We performed alpha diversity indices on our microbiota dataset using observed amplicon sequence variant (ASV), Shannon diversity index, Faith's phylogenetic diversity and Pielou's evenness. One-way ANOVA was performed to determine the significant difference between alpha diversity indices. Beta diversity was calculated using weighted UniFrac distance matrix (41). Weighted unifrac accounts for taxa abundances. Multivariate data were visualized using principle coordinate analysis using vegan package on the R platform (http://vegan.r-forge.r-project.org/). Visualization of complex seabird gut microbiota data was performed using t-distributed stochastic neighbor embedding algorithm (t-sNE, perplexity = 5) and clustering was performed using hierarchical density-based spatial clustering of applications with noise (HDBSCAN, MinPts = 3) using Rtsne (https://cran.r-project.org/web/ packages/Rtsne/index.html) and dbscan (https:// cran.r-project.org/ web/ packages/ dbscan/ index.html) package, respectively. Over-representative taxa for each cluster were identified using a linear discriminant analysis of effect size (LEfse) was performed to find microbial biomarkers between the four clusters (42).

5.4 Results and discussion

5.4.1 Characterization of the seabirds' gut microbial community structure

We identified the gut microbial (bacterial and archaeal) assemblages of each seabird at the time of sampling. At the phylum level, reads from all birds gut microbiota were assigned to 18 different phyla, and their microbial composition differed between bird species (Figure 5.2A). Across all seabird species sampled, the gut microbiota was composed mainly of Proteobacteria, Firmicutes and Fusobacteria (31.5%, 26.9% and 24.8%, respectively; Table 5.2). In the Arctic Tern (ARTE), the Black Guillemot (BLGU) and the Leach's Storm Petrel (LHSP), the most abundant phylum was Proteobacteria with a relative abundance of 69.3%, 37.7% and 76.5%, respectively (Table 5.2), while in the Common Eider (COEI) and the Double-Crested Cormorant (DCCO), Firmicutes was the most abundant phylum with 52.2% and 71.0%, respectively.

Our next objective was to compare the gut microbiota structure of seabirds between species and trophic levels. Alpha diversity indices (number of observed ASV, Faith's phylogenetic diversity and Shannon diversity index) revealed significant differences between seabird species (Figure 5.1B). The gut microbiota of the Arctic Tern was the least diverse, and the gut microbiota of the Common Eider was the most diverse of all bird species sampled. The gut microbiota of Black Guillemot, the Double-Crested Cormorant and the Leach's Storm Petrel had similar species richness, and all seabird species have similar ASV evenness.

Next, we aimed to characterize the seabirds' gut microbial signatures using a t-distributed Stochastic Neighbor Embedding (t-SNE) and a density-based clustering (H-DBSCAN). Using this approach, we identified four clusters among the bird species collected (Figure 5.3). Cluster 1 was primarily composed of the gut microbiota of the Double-Crested Cormorant and was over-

represented by the Clostridiales order, more specifically, Clostridiaceae, Lachnospiraceae, and Peptostreptococcaceae family (Figure 5.4). The microbial community structure of cluster 1 shared many similarities to the gut microbiome of dolphins and other land carnivorous mammals and could represent a piscivorous microbial assemblage (43, 44). Cluster 2 is grouped with the Common Eider and the Black Guillemot's gut microbiota with Lactobacilliales detected as a biomarker (Figure 5.4). This cluster contained benthic foragers, such as the Common Eider and Black Guillemot, that fed on intertidal and subtidal fishes, mollusks, and crustaceans (45, 46). Both Clostridiales and Lactobacilliales were commonly found in mammalian and bird gut environment (47, 48). Cluster 3 and 4 included the gut microbiota of the Leach's Storm Petrel and the Arctic Tern, respectively. Both clusters were predominantly represented by the Enterobacteriaceae and Pseudomonales taxa, respectively (Figure 5.4). Enterobacteriaceae is a common resident of animals' gut microbiome, including seabirds, and Pseudomonales is also found in different bird species gut microbiome (49–52). The Arctic Tern and the Leach's Storm are epipelagic and mesopelagic feeders in the open sea. Cluster 4 gut microbiome could be indicative of seabirds that are pelagic feeders.

5.4.2 Relationship between feeding location, contaminant exposure, and seabirds gut microbiota

We explored the relationship between trophic feeding position and gut microbiota of seabirds using environmental fitting analysis. Our analysis suggested that $\delta^{15}N$ is correlated with cluster 1 (Table 5.1*;* $\delta^{15}N$ = 14.53). Double-Crested Cormorants' gut microbial structure formed most of this cluster and fed at a significantly higher trophic position (Table 5.1; $\delta^{15}N$ = 14.98). The Arctic Tern, the Common Eider and the Leach's Storm Petrel had lower $\delta^{15}N$ suggesting that they fed at a lower trophic level. The isotopic marker $\delta^{15}N$ indicates trophic level consumption, and the Double-

Crested Cormorant foraged at a higher trophic position than the other clusters. Cluster 1 gut microbial structure could be an indicator of higher trophic position seabirds.

Our environmental fitting analysis suggested the isotopic marker $\delta^{13}C$ vector is associated with cluster 2 (Table 5.1; $\delta^{13}C$ = -19.7), which is overrepresented by the Lactobacillales order. The Common Eider, most Black Guillemot and some Arctic Tern are grouped within cluster 2 (Figure 5.3; Figure 5.5). We observed the highest $\delta^{13}C$ value in The Common Eider (Table 5.1; $\delta^{13}C$ =-18.74), the Black Guillemot Table 5.1; $\delta^{13}C$ =-19.91) and the Double-Crested Cormorant (Table 5.1; $\delta^{13}C$ =-19.41) and significantly smaller $\delta^{13}C$ value in the Arctic Tern (Table 5.1; $\delta^{13}C$ =-20.88) and the Leach's Storm Petrel (Table 5.1; $\delta^{13}C$ =-21.20). The isotopic $\delta^{13}C$ value is a good spatial tracer, and a higher $\delta^{13}C$ value is typically associated with nearshore seabirds, while a lower $\delta^{13}C$ value is associated with pelagic seabirds (53). The Common Eider, the Black Guillemot, and the Double-Crested Cormorant also feed on nearshore fishes, explaining the correlation with higher $\delta^{13}C$ value and $\delta^{13}C$ vector in our environmental fitting analysis (54) (Table 5.1; Figure 5.5). The opposite is true for most Arctic Terns and Leach's Storm Petrels, who feed in pelagic and mesopelagic fishes and phytoplanktons. Clusters 3 and 4 were inversely correlated with the $\delta^{13}C$ vector in our environmental fitting analysis (Figure 5.5). With supporting observation from our isotopic tracer $\delta^{13}C$, cluster 2 gut microbial structure could represent littoral seabirds' gut microbial structure.

Our data indicated a significant correlation between liver Hg levels and the microbial community structure of the Double-Crested Cormorant, which also exhibited the highest liver Hg concentration (35.94 $\mu g.g^{-1}$ w.w.) when compared to the Arctic Tern (1.93 $\mu g.g^{-1}$ w.w.), the Leach's Storm Petrel (4.71 $\mu g.g^{-1}$ w.w.), the Common Eider (4.06 $\mu g.g^{-1}$ w.w.) and the Black

Guillemot (8.24 µg.g^{-1} w.w.) (Table 5.1). Liver Hg concentrations of these seabirds were similar to those observed in the Common Eider found in Nova Scotia, Canada (55). Environmental fitting analysis indicated a significant correlation between the Hg vector, cluster 1, and δ^{15}N (Figure 5.5). These observations were consistent with literature where feeding at a higher trophic level led to a higher Hg body burden due to Hg's biomagnification in food webs (56). Moreover, this cluster contained gut microbiota of Double-Crested Cormorants and was overrepresented by bacterial species *Clostridium s.s* and *Tyzerella 3* (Figure 5.5, $p < 0.001$). A higher abundance of *Clostridium s.s* has been positively correlated with Hg polluted soils (57), while the high relative abundance of *Tyzerella 3* (within the Clostridiales order) has been associated with long-term metal exposure in human gut microbiota (58). Long term Hg exposure to contaminants through diet could select for both genera.

We observed a correlation between liver Se and the Arctic Tern and Leach's Storm Petrel gut microbiota. Our data indicated the Leach's Storm Petrel having the highest Se concentration (Table 5.1; 74.66 µg.g^{-1} w.w) comparative to the Arctic Tern (Table 5.1; 22.08 µg.g^{-1} w.w), the Common Eider (Table 5.1; 19.79 µg.g^{-1} w.w), the Double-Crested Cormorant (Table 5.1; 15.42 µg.g^{-1} w.w) and the Black Guillemot (Table 5.1; 7.50 µg.g^{-1} w.w). Liver Se is inversely correlated with δ^{13}C. Carbon isotopic signature in different seabirds was driven by nearshore and offshore feeding behaviour (17). Because the ocean is a major source of biogenic Se (59), seabirds feeding offshore are exposed to higher Se. Moreover, liver Se concentration is correlated with cluster 3 and 4, which is overrepresented by Enterobacteriaceae and Pseudomonadales, respectively, and grouped Arctic Tern and most Leach's Storm Petrel gut microbial structure from our dataset Figure 5.4). It has been reported that Pseudomonadales (more specifically, Pseudomonadaceae) can

reduce selenite anaerobically (60), and *Enterobacter* (within the Enterobacteriaceae family) can also reduce selenite, but aerobically (61). However, from our observation, it is unclear if exposure to Se alters the seabirds' gut microbiota to select for *Pseudomonadales* and *Enterobacter*. Further studies controlling for Se exposure could determine the correlation between both taxa and Se exposure.

5.5 Conclusion

The gut microbial community of seabirds are clustered primarily based on the feeding choice of the seabirds. Cluster 1 gut microbial structure represented seabirds fed at a higher trophic position, hence displaying a higher Hg body burden. Cluster 2 gut microbial structure grouped seabirds fed on littoral benthic fishes, invertebrates, and correlated with higher $\delta^{13}C$ value. Cluster 3 and 4 gut microbial assemblage are clustered with seabirds consuming pelagic and mesopelagic fishes, mollusks, and crustaceans in the open sea higher Se concentrations and lower $\delta^{13}C$ value. We had also identified representative microbial taxa for each cluster, which could be a candidate for further investigation as potential biomarkers for seabirds prey selection and contaminant exposure. It is important to note that fecal samples, such as those used in this study, represent the transient influence of diet on the seabird gut microbiome at the time of capture. Moreover, we did not collect information on the functional potential of the microbial community.

We have shown an association between seabirds' prey selection and their gut microbiome, but not with Hg and Se exposure. Future observation of seabirds in a controlled environment could identify the relationship between Hg and Se exposure to the seabirds gut microbiota. Moreover, mining seabirds gut microbiota's metagenomes would provide insights into the mechanisms of absorption and metabolism of contaminants and eventually contribute to developing non-invasive

biomarkers for marine ecosystem health. In a changing environment, providing comprehensive tools for the biomonitoring of sentinel species is crucial for proper policy decisions in safeguarding the marine ecosystem's health.

5.6 Acknowledgment

First, we would like to acknowledge the Wabanaki Confederacy and the Mi'kmaq People, where sampling was conducted. We would also like to thank lab members for insightful and constructive discussions and help throughout this study. A special thanks to Danielle Fife for her assistance with field work. Our work was funded by Nova Scotia Department of Lands and Forestry, NSERC, and Acadia University to MM, NSERC Discovery Grants to AP and HMC, CFI funding to AP, Canada Research Chair to HMC and an NSERC CREATE-REACT scholarship to GG.

Author contribution statement: GG, MLM, HMC and AJP conceived and planned the experiments. GG and RZ carried out the experiment and data analysis. MLM obtained the samples and performed metal analysis. GG wrote the manuscript. All authors edited and provided comments to the final version of the manuscript

5.7 References

1. Thompson DR, Stewart FM, Furness RW. 1990. Using seabirds to monitor mercury in marine environments. The validity of conversion ratios for tissue comparisons. Mar Pollut Bull 21:339–342.

2. Goodale MW, Evers DC, Mierzykowski SE, Bond AL, Burgess NM, Otorowski CI, Welch LJ, Hall CS, Ellis JC, Allen RB, Diamond AW, Kress SW, Taylor RJ. 2008. Marine foraging birds as bioindicators of mercury in the gulf of maine. Ecohealth 5:409–425.

3. Provencher JF, Mallory ML, Braune BM, Forbes MR, Gilchrist HG. 2014. Mercury and marine birds in Arctic Canada: effects, current trends, and why we should be paying closer attention. Environ Rev 22:244–255.

4. Croxall JP, Butchart SHM, Lascelles B, Stattersfield AJ, Sullivan B, Symes A, Taylor P. 2012. Seabird conservation status, threats and priority actions: A global assessment. Bird Conserv Int 22:1–34.

5. Klein R, Bartel-Steinbach M, Koschorreck J, Paulus M, Tarricone K, Teubner D, Wagner G, Weimann T, Veith M. 2012. Standardization of egg collection from aquatic birds for biomonitoring - A critical review. Environ Sci Technol 46:5273–5284.

6. Mallory CD, Gilchrist HG, Robertson GJ, Provencher JF, Braune BM, Forbes MR, Mallory ML. 2017. Hepatic trace element concentrations of breeding female common eiders across a latitudinal gradient in the eastern Canadian Arctic. Mar Pollut Bull 124:252–257.

7. Mason RP, Choi AL, Fitzgerald WF, Hammerschmidt CR, Lamborg CH, Soerensen AL, Sunderland EM. 2012. Mercury biogeochemical cycling in the ocean and policy implications. Environ Res 119:101–117.

8. Braune B, Chételat J, Amyot M, Brown T, Clayden M, Evans M, Fisk A, Gaden A, Girard C, Hare A, Kirk J, Lehnherr I, Letcher R, Loseto L, Macdonald R, Mann E, McMeans B, Muir D, O'Driscoll N, Poulain A, Reimer K, Stern G. 2015. Mercury in the marine

environment of the Canadian Arctic: Review of recent findings. Sci Total Environ. Elsevier.

9. Stern GA, Macdonald RW, Outridge PM, Wilson S, Chételat J, Cole A, Hintelmann H, Loseto LL, Steffen A, Wang F, Zdanowicz C. 2012. How does climate change influence arctic mercury? Sci Total Environ. Elsevier.

10. Amélineau F, Grémillet D, Harding AMA, Walkusz W, Choquet R, Fort J. 2019. Arctic climate change and pollution impact little auk foraging and fitness across a decade. Sci Rep 9:1–15.

11. Wayland M, Gilchrist HG, Dickson DL, Bollinger T, James C, Carreno RA, Keating J. 2001. Trace elements in king eiders and common eiders in the Canadian arctic. Arch Environ Contam Toxicol 41:491–500.

12. Ikemoto T, Kunito T, Tanaka H, Baba N, Miyazaki N, Tanabe S. 2004. Detoxification mechanism of heavy metals in marine mammals and seabirds: Interaction of selenium with mercury, silver, copper, zinc, and cadmium in liver. Arch Environ Contam Toxicol 47:402–413.

13. Fan TWM, Teh SJ, Hinton DE, Higashi RM. 2002. Selenium toxicity: cause and effects in aquatic birds. Aquat Toxicol 57:27–37.

14. Wang X, Wang W-X. 2017. Selenium induces the demethylation of mercury in marine fish. Environ Pollut 231:1543–1551.

15. Spiller HA. 2018. Rethinking mercury: the role of selenium in the pathophysiology of mercury toxicity. Clin Toxicol. Taylor and Francis Ltd.

16. Michelutti N, Blais JM, Mallory ML, Brash J, Thienpont J, Kimpe LE, Douglas MSV, Smol JP. 2010. Trophic position influences the efficacy of seabirds as metal biovectors. Proc Natl Acad Sci U S A 107:10543–10548.

17. Ceia FR, Cherel Y, Paiva VH, Ramos JA. 2018. Stable Isotope Dynamics (δ13C and δ15N) in Neritic and Oceanic Waters of the North Atlantic Inferred From GPS-Tracked Cory's

Shearwaters. Front Mar Sci 5:377.

18. Sebastiano M, Bustamante P, Eulaers I, Malarvannan G, Mendez-Fernandez P, Churlaud C, Blévin P, Hauselmann A, Covaci A, Eens M, Costantini D, Chastel O. 2017. Trophic ecology drives contaminant concentrations within a tropical seabird community. Environ Pollut 227:183–193.

19. Blévin P, Carravieri A, Jaeger A, Chastel O, Bustamante P, Cherel Y. 2013. Wide Range of Mercury Contamination in Chicks of Southern Ocean Seabirds. PLoS One 8:e54508.

20. McFall-Ngai M, Hadfield MG, Bosch TCG, Carey H V, Domazet-Lošo T, Douglas AE, Dubilier N, Eberl G, Fukami T, Gilbert SF, Hentschel U, King N, Kjelleberg S, Knoll AH, Kremer N, Mazmanian SK, Metcalf JL, Nealson K, Pierce NE, Rawls JF, Reid A, Ruby EG, Rumpho M, Sanders JG, Tautz D, Wernegreen JJ. 2013. Animals in a bacterial world, a new imperative for the life sciences. Proc Natl Acad Sci U S A 110:3229–36.

21. Guo G, Yumvihoze E, Poulain AJ, Man Chan H. 2018. Monomethylmercury degradation by the human gut microbiota is stimulated by protein amendments. J Toxicol Sci 43:717–725.

22. Fraune S, Bosch TCG. 2010. Why bacteria matter in animal development and evolution. BioEssays 32:571–580.

23. Kohl KD, Dearing MD. 2016. The Woodrat Gut Microbiota as an Experimental System for Understanding Microbial Metabolism of Dietary Toxins. Front Microbiol 7:1165.

24. Dewar ML, Arnould JPY, Krause L, Dann P, Smith SC. 2014. Interspecific variations in the faecal microbiota of Procellariiform seabirds. FEMS Microbiol Ecol 89:47–55.

25. Waite DW, Taylor MW. 2015. Exploring the avian gut microbiota: Current trends and future directions. Front Microbiol. Frontiers Media S.A.

26. Fuirst M, Veit RR, Hahn M, Dheilly N, Thorne LH. 2018. Effects of urbanization on the foraging ecology and microbiota of the generalist seabird Larus argentatus. PLoS One

13:e0209200.

27. Hird SM, Carstens BC, Cardiff SW, Dittmann DL, Brumfield RT. 2014. Sampling locality is more detectable than taxonomy or ecology in the gut microbiota of the brood-parasitic Brown-headed Cowbird (Molothrus ater). PeerJ 2014:e321.

28. Grond K, Santo Domingo JW, Lanctot RB, Jumpponen A, Bentzen RL, Boldenow ML, Brown SC, Casler B, Cunningham JA, Doll AC, Freeman S, Hill BL, Kendall SJ, Kwon E, Liebezeit JR, Pirie-Dominix L, Rausch J, Sandercock BK. 2019. Composition and Drivers of Gut Microbial Communities in Arctic-Breeding Shorebirds. Front Microbiol 10:2258.

29. Lucas FS, Heeb P. 2005. Environmental factors shape cloacal bacterial assemblages in great tit *Parus major* and blue tit *P. caeruleus* nestlings. J Avian Biol 36:510–516.

30. Wu Y, Yang Y, Cao L, Yin H, Xu M, Wang Z, Liu Y, Wang X, Deng Y. 2018. Habitat environments impacted the gut microbiome of long-distance migratory swan geese but central species conserved. Sci Rep 8:1–11.

31. Wang X, Wu F, Wang W-X. 2017. In Vivo Mercury Demethylation in a Marine Fish (*Acanthopagrus schlegeli*). Environ Sci Technol 51:6441–6451.

32. Rowland IR, Davies MJ, Grasso P. 1975. The methylation of mercury by the gastro intestinal contents of the rat. Biochem Soc Trans 3:502–504.

33. Rieder SR, Brunner I, Daniel O, Liu B, Frey B. 2013. Methylation of Mercury in Earthworms and the Effect of Mercury on the Associated Bacterial Communities. PLoS One 8:e61215.

34. García-Amado MA, Michelangeli F, Gueneau P, Perez ME, Domínguez-Bello MG. 2007. Bacterial detoxification of saponins in the crop ofthe avian foregut fermenter Opisthocomus hoazin. J Anim Feed Sci 16:82–85.

35. Walters W, Hyde ER, Berg-Lyons D, Ackermann G, Humphrey G, Parada A, Gilbert JA, Jansson JK, Caporaso JG, Fuhrman JA, Apprill A, Knight R. 2016. Improved Bacterial 16S

rRNA Gene (V4 and V4-5) and Fungal Internal Transcribed Spacer Marker Gene Primers for Microbial Community Surveys. mSystems 1:9–15.

36. Bolyen E, Rideout JR, Dillon MR, Bokulich NA, Abnet CC, Al-Ghalith GA, Alexander H, Alm EJ, Arumugam M, Asnicar F, Bai Y, Bisanz JE, Bittinger K, Brejnrod A, Brislawn CJ, Brown CT, Callahan BJ, Caraballo-Rodríguez AM, Chase J, Cope EK, Da Silva R, Diener C, Dorrestein PC, Douglas GM, Durall DM, Duvallet C, Edwardson CF, Ernst M, Estaki M, Fouquier J, Gauglitz JM, Gibbons SM, Gibson DL, Gonzalez A, Gorlick K, Guo J, Hillmann B, Holmes S, Holste H, Huttenhower C, Huttley GA, Janssen S, Jarmusch AK, Jiang L, Kaehler BD, Kang K Bin, Keefe CR, Keim P, Kelley ST, Knights D, Koester I, Kosciolek T, Kreps J, Langille MGI, Lee J, Ley R, Liu Y-X, Loftfield E, Lozupone C, Maher M, Marotz C, Martin BD, McDonald D, McIver LJ, Melnik A V., Metcalf JL, Morgan SC, Morton JT, Naimey AT, Navas-Molina JA, Nothias LF, Orchanian SB, Pearson T, Peoples SL, Petras D, Preuss ML, Pruesse E, Rasmussen LB, Rivers A, Robeson MS, Rosenthal P, Segata N, Shaffer M, Shiffer A, Sinha R, Song SJ, Spear JR, Swafford AD, Thompson LR, Torres PJ, Trinh P, Tripathi A, Turnbaugh PJ, Ul-Hasan S, van der Hooft JJJ, Vargas F, Vázquez-Baeza Y, Vogtmann E, von Hippel M, Walters W, Wan Y, Wang M, Warren J, Weber KC, Williamson CHD, Willis AD, Xu ZZ, Zaneveld JR, Zhang Y, Zhu Q, Knight R, Caporaso JG. 2019. Reproducible, interactive, scalable and extensible microbiome data science using QIIME 2. Nat Biotechnol 37:852–857.

37. Martin M. 2011. Cutadapt removes adapter sequences from high-throughput sequencing reads. EMBnet.journal 17:10.

38. Callahan BJ, McMurdie PJ, Rosen MJ, Han AW, Johnson AJA, Holmes SP. 2016. DADA2: High-resolution sample inference from Illumina amplicon data. Nat Methods 13:581–583.

39. Quast C, Pruesse E, Yilmaz P, Gerken J, Schweer T, Yarza P, Peplies J, Glöckner FO. 2013. The SILVA ribosomal RNA gene database project: Improved data processing and web-based tools. Nucleic Acids Res 41.

40. Hobson KA, Clark RG. 1992. Assessing Avian Diets Using Stable Isotopes I: Turnover of

^{13} C in Tissues. Condor 94:181–188.

41. Lozupone C, Lladser ME, Knights D, Stombaugh J, Knight R. 2011. UniFrac: an effective distance metric for microbial community comparison. ISME J 5:169–72.

42. Segata N, Izard J, Waldron L, Gevers D, Miropolsky L, Garrett WS, Huttenhower C. 2011. Metagenomic biomarker discovery and explanation. Genome Biol 12:R60.

43. TM N, TL R, MV B. The gut bacterial community of mammals from marine and terrestrial habitats. PLoS One 8:e83655.

44. Dolan JR, Forster D, Dunthorn M, Bass D, Bittner L, Boutte C, Christen R, Claverie J, Decelle J, Edvardsen B, Egge E, Eikrem W, Kooistra WHCF, Logares R, Massana R, Montresor M, Not F, Ogata H, Pawlowski J, Pernice MC, Romac S, Shalchian-tabrizi K, Sarno D, Simon N, Richards TA, Siano R, Vaulot D, Wincker P, Zingone A, Vargas C De, Stoeck T, Csic M, Mar P. 2016. Fiv046.Full. FEMS Microbiol Ecol 92:1–11.

45. Goudie RI, Robertson GJ, Reed A. 2020. Common Eider (Somateria mollissima)Birds of the World. Cornell Lab of Ornithology.

46. Butler RG, Buckley DE, Nettleship DN, Boesman PFD, Garcia E. 2020. Black Guillemot (Cepphus grylle)Birds of the World. Cornell Lab of Ornithology.

47. Meehan CJ, Beiko RG. 2014. A Phylogenomic View of Ecological Specialization in the Lachnospiraceae, a Family of Digestive Tract-Associated Bacteria. Genome Biol Evol 6:703–713.

48. García-Amado MA, Shin H, Sanz V, Lentino M, Martínez LM, Contreras M, Michelangeli F, Domínguez-Bello MG. 2018. Comparison of gizzard and intestinal microbiota of wild neotropical birds. PLoS One 13:e0194857.

49. Bowman TA, Jacobson ER. 1980. Cloacal Flora of Clinically Normal Captive Psittacine Birds. J Zoo Anim Med 11:81.

50. Kenzaka T, Kataoka K, Fujimitsu T, Tani K. 2018. Intestinal Microbiota in Migrating Barn Swallows around Osaka. YAKUGAKU ZASSHI 138:117–122.

51. Ben Yahia H, Chairat S, Gharsa H, Alonso CA, Ben Sallem R, Porres-Osante N, Hamdi N, Torres C, Ben Slama K. 2020. First Report of KPC-2 and KPC-3-Producing Enterobacteriaceae in Wild Birds in Africa. Microb Ecol 79:30–37.

52. Lobato E, Geraldes M, Melo M, Doutrelant C, Covas R. 2017. Diversity and composition of cultivable gut bacteria in an endemic island bird and its mainland sister species. Symbiosis 71:155–164.

53. Ceia FR, Cherel Y, Paiva VH, Ramos JA. 2018. Stable Isotope Dynamics (δ13C and δ15N) in Neritic and Oceanic Waters of the North Atlantic Inferred From GPS-Tracked Cory's Shearwaters. Front Mar Sci 5:377.

54. Billerman SM, Keeney BK, Rodewald PG, Schulenberg TS. 2020. Birds of the World. Cornell Lab Ornithol Ithaca, NY, USA.

55. Pratte I, Tomlik MD, Betsch TA, Braune BM, Milton GR, Mallory ML. 2015. Trace elements in eggs of common eiders (Somateria mollissima) breeding in Nova Scotia, Canada. Mar Pollut Bull 100:586–591.

56. Lavoie RA, Jardine TD, Chumchal MM, Kidd KA, Campbell LM. 2013. Biomagnification of mercury in aquatic food webs: A worldwide meta-analysis. Environ Sci Technol 47:13385–13394.

57. Liu YR, Delgado-Baquerizo M, Bi L, Zhu J, He JZ. 2018. Consistent responses of soil microbial taxonomic and functional attributes to mercury pollution across China. Microbiome 6:183.

58. Shao M, Zhu Y. 2020. Long-term metal exposure changes gut microbiota of residents surrounding a mining and smelting area. Sci Rep 10:1–9.

59. Amouroux D, Liss PS, Tessier E, Hamren-Larsson M, Donard OFX. 2001. Role of ocens

as biogenic sources of selenium. Earth Planet Sci Lett 189:277–283.

60. Gonzalez-Gil G, Lens PNL, Saikaly PE. 2016. Selenite Reduction by Anaerobic Microbial Aggregates: Microbial Community Structure, and Proteins Associated to the Produced Selenium Spheres. Front Microbiol 7:571.

61. Song D, Li X, Cheng Y, Xiao X, Lu Z, Wang Y, Wang F. 2017. Aerobic biogenesis of selenium nanoparticles by Enterobacter cloacae Z0206 as a consequence of fumarate reductase mediated selenite reduction. Sci Rep 7:1–10.

5.8 Tables and Figures

Table 5.1 – Summary table of environmental variables measured in this study by birds and clusters. All value are in $g.kg^{-1}$ wet weight, except for Se:Hg which is calculated as molar ratios. Standard deviation are in brackets. Letters denote significant differences between each bird species based on each environmental factor (TukeyHSD). No significant difference were detected among the different clusters.

Bird	$\delta^{13}C$	$\delta^{15}N$	Hg	Se	Se:Hg molar ratio
ARTE	-20.88 (0.53) a	11.7 (0.21) a	1.93 (0.33) a	22.08 (4.95) a	29.74 (8.75) a
BLGU	-19.91 (0.56) abc	14.24 (0.45) b	8.24 (2.05) a	7.5 (0.44) a	2.42 (0.59) b
COEI	-18.74 (0.39) c	11.28 (0.65) a	4.06 (0.69) a	19.79 (14.51) a	13.37 (11.49) ab
DCCO	-19.41 (1.57) c	14.98 (0.65) b	35.94 (23.74) b	15.42 (3.11) a	1.64 (1.21) b
LHSP	-21.2 (0.17) ab	12.2 (0.08) a	4.71 (0.33) a	74.64 (35.22) c	39.91 (17.28) a

Cluster	$\delta^{13}C$	$\delta^{15}N$	Hg	Se	Se:Hg molar ratio
Cluster1	-19.25 (1.54)	14.53 (1.41)	19.68 (16.1)	14.62 (2.55)	2.81 (1.21)
Cluster2	-19.7 (1.15)	12.63 (1.67)	13.81 (22.51)	15.54 (11.22)	5.76 (5.22)
Cluster3	-20.94 (0.5)	12.05 (0.28)	3.59 (1.4)	42.1 (17.19)	8.43 (2.94)
Cluster4	-20.71 (0.54)	12.51 (1.09)	4.97 (3.47)	51.31 (51.98)	7.43 (3.37)

Table 5.2 - Top 5 phyla of each species and all species.

Phylum	ARTE
Proteobacteria	69.3%
Deinococcus-Thermus	14.0%
Tenericutes	12.4%
Chlamydiae	2.8%
Firmicutes	1.4%

Phylum	BLGU
Proteobacteria	37.7%
Firmicutes	31.9%
Tenericutes	24.9%
Epsilonbacteraeota	4.9%
Actinobacteria	0.6%

Phylum	LHSP
Proteobacteria	76.5%
Cyanobacteria	7.0%
Actinobacteria	6.7%
Firmicutes	4.9%
Planctomycetes	2.2%
Other phyla	2.8%

Phylum	COEI
Firmicutes	51.2%
Fusobacteria	22.7%
Actinobacteria	11.5%
Tenericutes	7.0%
Proteobacteria	3.9%
other phyla	3.6%

Phylum	DCCO
Firmicutes	71.1%
Fusobacteria	21.6%
Actinobacteria	4.5%
Epsilonbacteraeota	2.1%
Proteobacteria	0.8%

Phylum	All species
Proteobacteria	31.5%
Firmicutes	26.9%
Fusobacteria	23.8%
Tenericutes	7.4%
Actinobacteria	3.9%
Deinococcus-Thermus	2.3%
Epsilonbacteraeota	1.5%
Cyanobacteria	1.2%
other phyla	1.7%

Table 5.3 - Top taxa identified for each cluster.

Cluster1	Family	Genus
0.36	Lachnospiraceae	Tyzzerella_3
0.15	Clostridiaceae_1	Clostridium_sensu_stricto_1
0.15	Peptostreptococcaceae	Peptostreptococcus
0.07	Peptostreptococcaceae	Peptoclostridium
0.05	Clostridiales Family_XIII	Unclassified
0.02	Lachnospiraceae	Unclassified
0.02	Actinomycetaceae	Varibaculum
0.02	Fusobacteriaceae	Fusobacterium
0.01	Clostridiaceae_1	uncultured_bacterium
0.01	Coriobacteriaceae	Collinsella

Cluster2	Family	Genus
0.25	Enterococcaceae	Catellicoccus
0.12	Fusobacteriaceae	Fusobacterium
0.10	Enterobacteriaceae	Escherichia-Shigella
0.09	Mycoplasmataceae	Mycoplasma
0.07	Fusobacteriaceae	Cetobacterium
0.06	Deinococcaceae	Deinococcus
0.04	Mycoplasmataceae	Candidatus_Lumbricincola
0.03	Mycoplasmataceae	Candidatus_Bacilloplasma
0.03	Lactobacillaceae	Lactobacillus

Cluster3	Family	Genus
0.28	Pseudomonadaceae	Pseudomonas
0.08	Chroococcidiopsaceae	uncultured
0.08	Acetobacteraceae	Acidiphilium
0.05	Xanthomonadaceae	Pseudoxanthomonas
0.05	Micrococcaceae	Unclassified
0.04	Parachlamydiaceae	Candidatus_Protochlamydia
0.03	Beijerinckiaceae	Unclassified
0.03	Pasteurellaceae	Nicoletella

Cluster4	Family	Genus
0.78	Enterobacteriaceae	Escherichia-Shigella
0.20	Enterobacteriaceae	Unclassified
0.01	Erysipelotrichaceae	Breznakia
0.01	Mycoplasmataceae	Candidatus_Lumbricincola

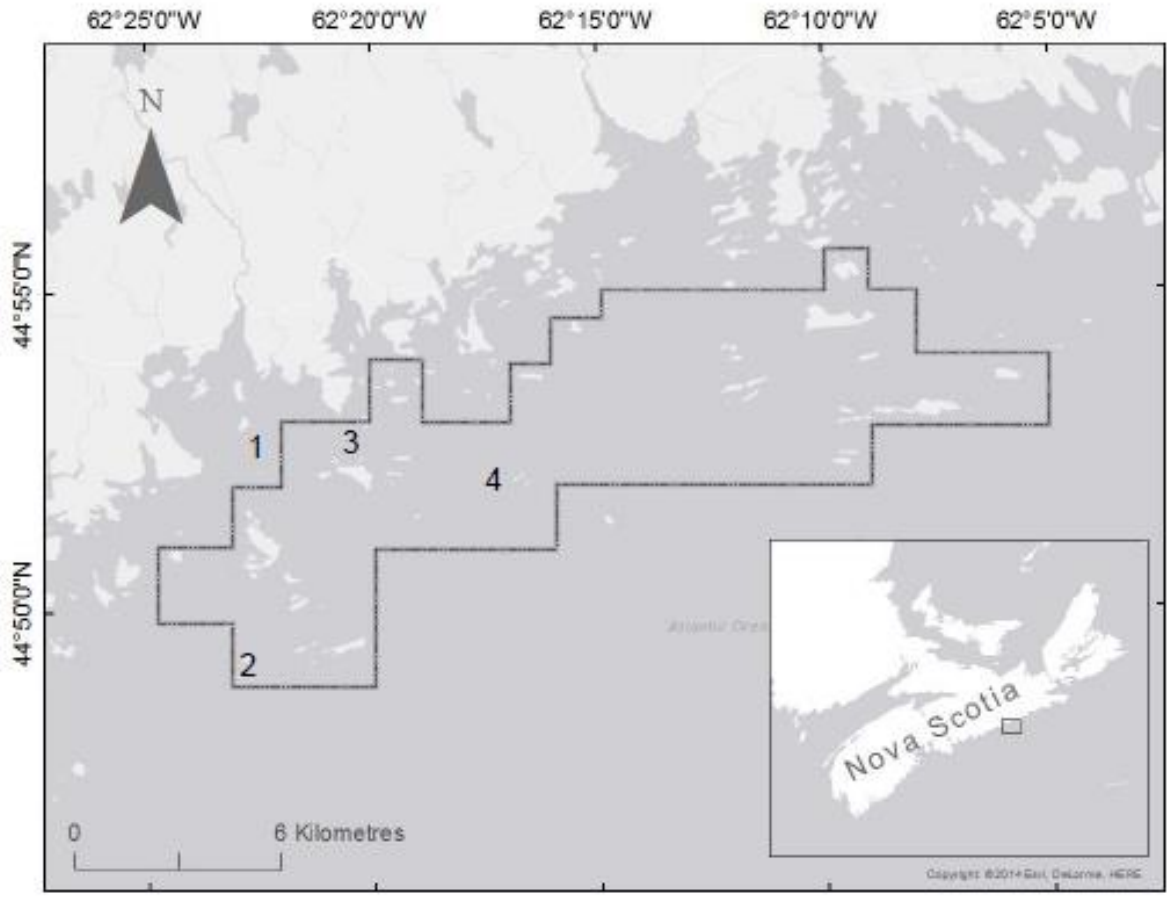

Figure 5.1 – Map of Eastern Shore Islands Wildlife Management Area, east of Sheet Harbour (NS, Canada). Seabirds were sampled on islands 1,2,3 and 4

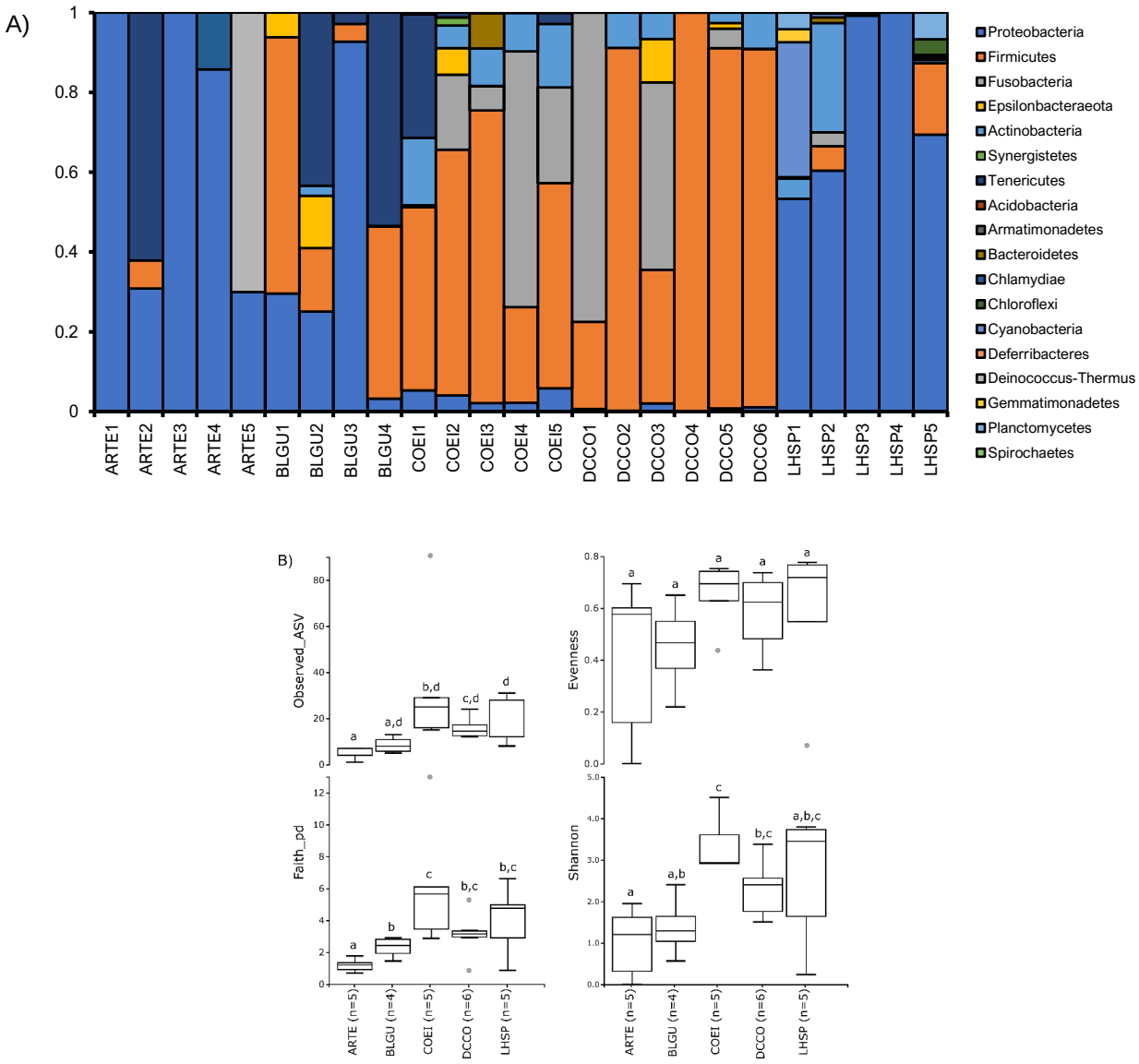

Figure 5.2 – Bird species had different gut microbiota diversity that could reflect the range in diet. (A) Relative abundance of phyla observed in each arctic seabird. Seabird represented with standardized four-letter codes. **ARTE** = Arctic Tern; **BLGU** = Black Guillemot; **COEI** = Common Eider; **DCCO** = Double-crested Cormorant; **LHSP** = Leach's Storm-Petrel. (B) Whisker plot of observed OTUs, Faith's phylogenetic diversity, Pielou's Evenness index and Shannon index. Significant differences (Kruskal-Wallis test) indicated with letters shown above each box (α = 0.05).

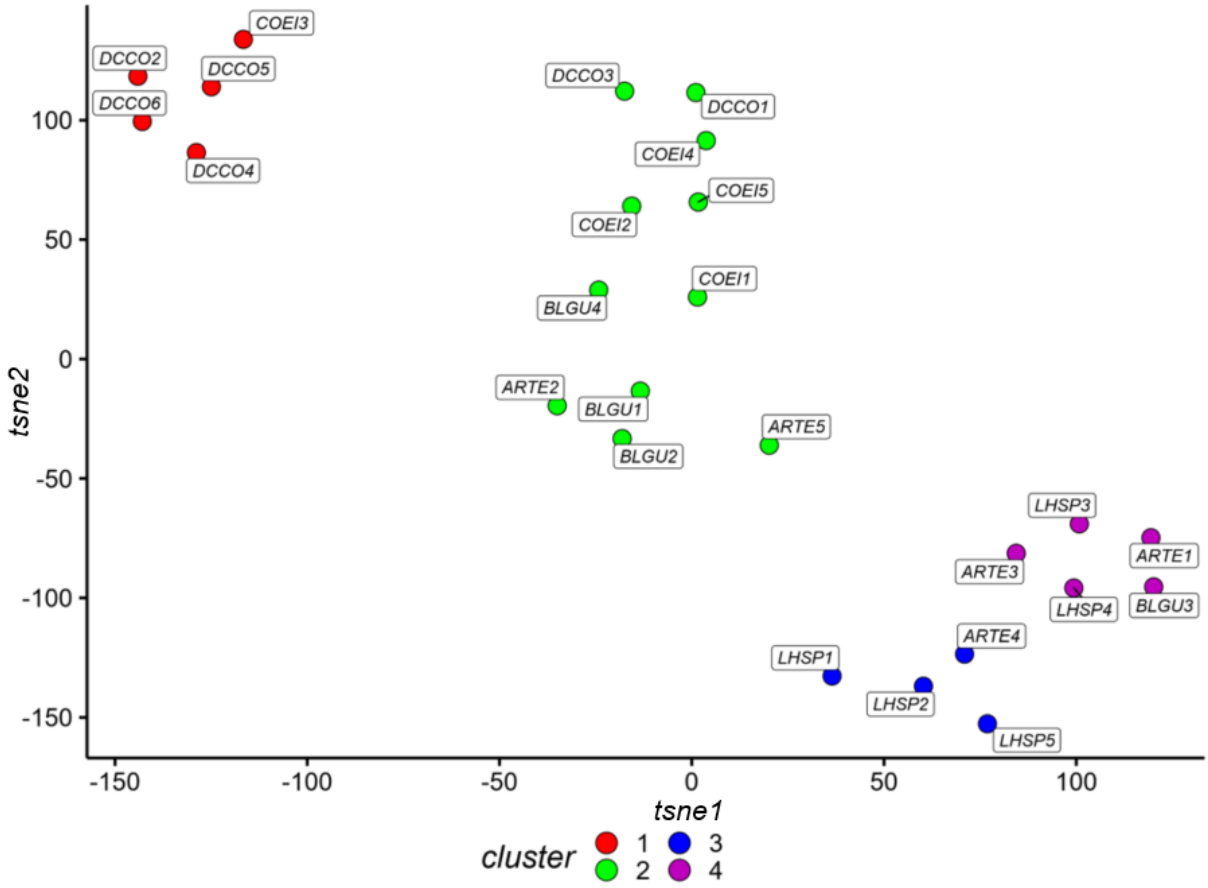

Figure 5.3 – Bird gut microbiota structure clustered based on bird species and sizes. Dimension reduction was performed using t-SNE analysis (perplexity = 5). t-SNE is a non-linear dimension reduction technique that constructs a probability distribution where it accentuates similarity and accentuates dissimilarity between pairs while minimizing the pairs probability distribution (Kullback-Leiber divergence). Clustering was performed using H-DBSCAN (Minpts = 3) on bird gut microbial samples.

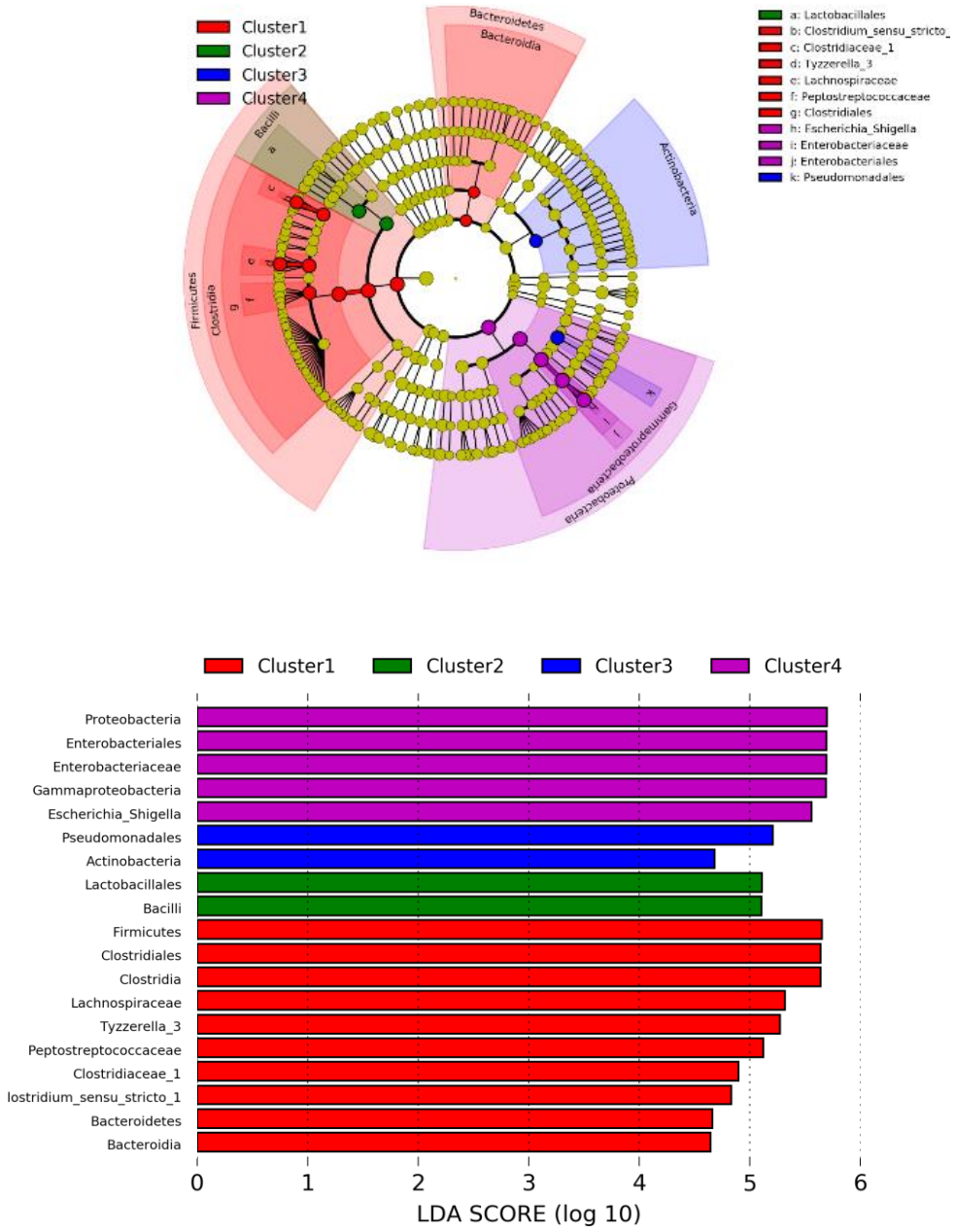

Figure 5.4 – Cladogram of the taxa represented in LDA analysis colour-coded for each cluster. LDA analysis showing indicator bacterial species for each clusters (LDA score > 4.0).

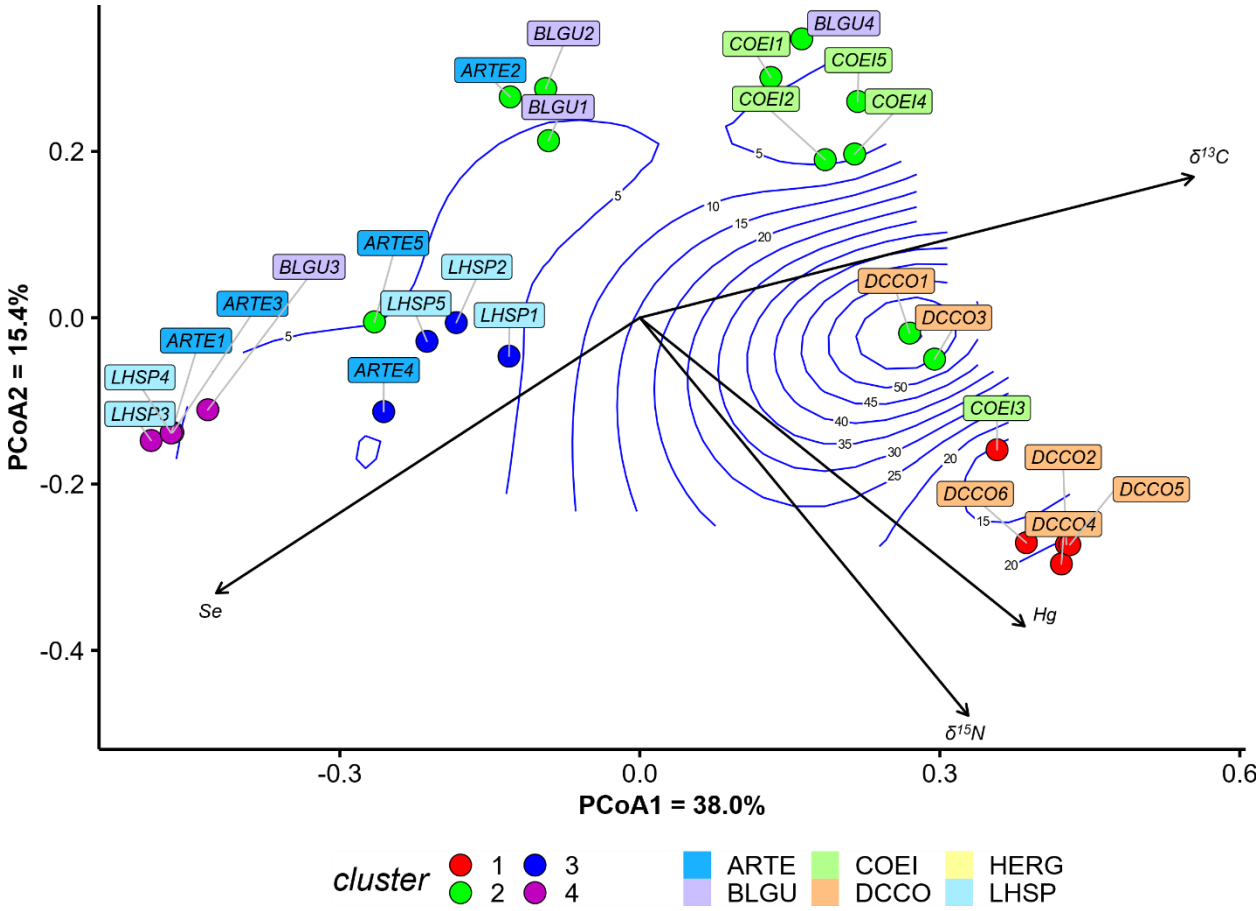

Figure 5.5 – Principal coordinate analysis of physiological and environmental variable body burden. An overlay of mercury concentrations measured was drawn as a surface fit. Each cluster is represented by different colour of the data point. Different bird species are indicated by the label box colour.

5.9 Supplemental Table

Table D1 - Summary of metadata collected from seabirds

	n	Mean	Median	StDev	0.25	0.5	0.75
$\delta^{13}C$	26	-20.01	-20.19	1.20	-21.09	-20.19	-18.97
$\delta^{15}N$	26	12.89	12.25	1.56	11.81	12.25	14.44
C.	26	49.59	49.61	2.09	48.22	49.59	50.34
N.	26	12.56	12.79	1.14	12.14	12.79	13.32
C.N	26	3.994	3.89	0.55	3.532	3.89	4.15
Hg	26	11.72	4.79	17.32	3.277	4.785	9.72
Se	26	27.32	16.75	28.62	11.73	16.75	26.17

Chapter 6: Research synthesis

6.1 Summary of research contribution

My thesis' overarching objective was to explore the relationship between mercury (Hg) and the gut microbiome of animals using a multi-model approach and evaluate whether a framework could be developed to utilize the gut microbial structure as a biomarker for Hg and metal exposure. In chapter 2, my goal was to investigate the effect of diet on human gut microbiota and, subsequently, methylmercury (MeHg) transformation. My findings suggest that diet change promoted MeHg-degrading microbe and, ultimately, increase MeHg degradation. To my knowledge, this is the first study to identify and isolate the gut microbiota as responsible for MeHg degradation in the gut environment. Moreover, this study also showed a link between nutrient addition in diet (protein) to microbial-mediated MeHg degradation. In chapter 3, I showed that known MeHg demethylators (methanogens, methanotrophs and sulfate-reducing bacteria) were not involved in the MeHg degradation in the human gut environment. By comparing the metagenomes of a gut microbiome capable of MeHg degradation to one that does not, I identified *menG* as potentially involved in a novel microbially-mediated pathway for MeHg degradation. This study is the first to propose a potential MeHg degradative pathway. Both these chapters provided significant insight into the demethylation of MeHg in the human gut environment.

Chapter 4 explored the relationship between river otters' gut microbial structure residing surrounding the Athabasca Oils Sand Region and found no correlation. However, to my knowledge, I was the first to describe the river otter gut microbial structure. Moreover, I have provided a framework for further studies into developing the gut microbiota as a biomarker for freshwater ecosystem health. In chapter 5, using the same framework established in chapter 4, I found that

prey selection is significantly correlated with seabirds' gut microbial structure, affecting Hg body burden in seabirds. In these two chapters, I was the first to investigate and provide meaningful insight into the relationship between environmental contaminants and wildlife gut microbiota into the relationship between wildlife gut microbiota and environmental contaminant exposure.

My thesis's central theme revolves around the relationship between the host's diet and its associated gut microbiome. Findings from Chapter 2 showed a significant increase in MeHg degradation due to protein amendment in the medium. Moreover, the addition of carbohydrates significantly decreased MeHg degradation and altered the gut microbiome. Chapter 5 described how seabirds' gut microbiota clustered based on prey's location (littoral vs pelagic). These observations are in concordance with our current understanding that environmental factors such as diet play a significant role in altering the gut microbial structure [1,2]

Overall, my thesis's findings highlighted the importance of environmental influence, such as diet and prey selection on the gut microbial structure and MeHg degradation in the gastrointestinal environment. Moreover, I have identified menaquinone biosynthesis as a plausible pathway involved gut microbial transformation of MeHg. Lastly, my work also provides an exploratory framework for utilizing the gut microbiota as a biomarker for Hg or other contaminants exposure among wildlife in different ecosystems.

6.2 Mercury and human gut microbiome: key findings

In Chapter 2, I tested the hypothesis that diet can increase MeHg degradation in host-associated microbiota's human gut environment. In this Chapter, I developed and optimized an *in vitro* assay to screen the gut microbiota for MeHg transformation using stable isotope MeHg tracers. I have identified one fecal donor that exhibited high MeHg degradation and another that did not.

Furthermore, I have discovered that peptone addition significantly increased MeHg degradation in Individual A, and this phenotype was conserved when fecal samples from Individuals A and B are mixed. It suggested that gut microbiota collected from Individual B is not inhibiting MeHg degradation; instead, those collected from Individual A contained microbial elements that promote this phenotype, and these elements were transferable to Individual B. This is the first study to show the human gut microbiota capable of degrading MeHg and increased dramatically with protein addition. Other studies have done fecal transfer from humans to rat models; however, the results could be influenced by the host's immunity [3–6]. Moreover, my *in vitro* experimental set-up was optimized and replicable, rendering it possible to investigate the microbially-mediated MeHg degradation pathway.

In the follow-up study presented in Chapter 3, I tested the hypothesis that known demethylators (methanogens, methanotrophs and sulfate-reducing bacteria) were involved in the MeHg degradation observed in the human gastrointestinal environment. With no prior knowledge of the MeHg degradation mechanism in the human intestinal environment, I tested whether the mechanism is similar to one of the three known actions reported for marine and aquatic MeHg demethylators using inhibition assays (Oremland et al. 1991; Lu et al. 2017; Kronberg et al. 2018). I showed that none of the known MeHg demethylators were involved in MeHg degradation, suggesting a novel pathway. Using comparative metagenomic analysis, I observed significant differences in taxa, genes and functions in the fecal microbiome collected from Individual A compared to that collected from Individual B. Pathway analysis revealed menaquinone biosynthesis as a potential pathway for MeHg degradation. The discovery of a potential mechanism for MeHg degradation in the human gut environment can lead to a more accurate

physiological-based pharmacokinetic model to extrapolate Hg risk, reduce interindividual variability in population modelling and, ultimately, lead to better risk management. This study was first to provide a novel mechanism for MeHg degradation by the human gut microbiota.

6.3 Mercury and sentinel species of aquatic ecosystem gut microbiome: key findings

Chapters 4 explored the relationship between Hg and the gut microbiota of river otters surrounding the surface mining activities in Athabasca Oil Sands Region. The river otter is a sentinel species for freshwater ecosystem health, and its gut microbiota has yet to be characterized, making it an ideal candidate for this project. My findings showed that the river otter gut microbiota is similar to those reported in other mammalian carnivores [10–12]. Next, I clustered the gut microbiota with similar microbial profiles, and I have identified four clusters with distinct microbial community structures that could provide some evidence on the host diet and health status. Once I have established the different microbial profiles, I investigated the correlation between environmental factors (metal body burden, health indices) and the four clusters. This methodology is an important first step in developing a framework where the gut microbiota can be utilized as a biomarker for early biological effect. This study is the first to describes the gut microbial community of river otters.

Chapter 5 explored the relationship between prey selection, Hg body burden, and the gut microbiome of seabirds. Seabirds are marine predators and have evolved many foraging strategies to successfully prey on marine life and at different oceanic zones, which makes for an ideal sentinel species for marine ecosystem health [13]. I hypothesized that seabirds consuming at higher trophic position will exhibit higher Hg body burden. I clustered the gut microbiome and identified four clusters based on the feeding ecology of the respective seabirds. My findings suggested that the

gut microbiome of seabirds was primarily clustered based on their prey selection. Seabirds preying on higher trophic fishes carried the highest Hg body burden in our dataset. Moreover, the feeding location (littoral vs pelagic, surface vs benthic) significantly impacted the seabird gut microbial structure and liver selenium concentration. Selenium concentration is higher in pelagic-feeding seabirds and is correlated with lower liver Hg concentration. Moreover, I have identified a taxa representative of each cluster which could be further developed into a biomarker for prey ecology and contaminant exposure. This study has established the importance of feeding ecology on the gut microbial structure of seabirds. It is also the first to explore the interaction between diet, environmental contaminant, and seabirds' gut microbiota.

6.4 Limitations and future directions

Some of the more challenging aspects of gut microbiota research were obtaining, transferring and maintaining the microbial structure of the fecal microbiota. Exposure to oxygen can negatively impact strict anaerobe and its potential involvement in MeHg transformation. First, I obtained samples from only two volunteers, and thus, I can not extrapolate my results on a population level. Despite this challenge, I optimized an *in vitro* experimental method that showed a remarkable and replicable difference in two individuals' gut microbial ability to degrade MeHg, repeatably over several years. This experiment led to identifying a novel MeHg degrading mechanisms in the human gut microbiota discussed in Chapter 3. Nevertheless, a larger sample size is necessary to infer the prevalence of *menG* and MeHg degradation in the human population. Future works should assess the involvement of *menG* in MeHg degradation using phenyl amide (a *menG* inhibitor) in an *in vitro* inhibition experiment. If the link between *menG* and MeHg degradation is real, the development of rapid and cost-effective screening tools using digital droplet polymerase chain

reaction (ddPCR) or an immunoassay test would greatly help assess the prevalence of this gene in individuals that can degrade MeHg and provide crucial for population risk management.

Chapters 2 and 3 *in vitro* batch set-up is a closed system resulting in a lack of media turnover. Metabolites and wastes remained in the media and could affect downstream microbial activities. Future experimentation using bioreactors will solve both challenges. Working toward this path, I built a twin-**S**imulated **H**uman **I**ntestinal **M**icrobial **E**cosystem (SHIME®) to mimic the gastrointestinal tract, which incorporates the stomach, small intestine, and large intestine [14]. This multi-compartment bioreactor allows for long-term monitoring of microbial population dynamics to a specific treatment. By having a twin system, one could compare long-term protein amendment on gut microbial steady-state and MeHg degradation.

It is still not understood how protein addition can increase MeHg degradation. Fecal samples collected were representative of the colonic region [15,16], which is also the major site for fermentation of exogenous and endogenous substrate, which benefits the host [17]. Microbial fermentation of protein produces numerous essential metabolites (e.g., short-chain fatty acids and amino acids) [18] and involves numerous microbes members of genera in the Firmicutes, Bacteroides, and Actinobacteria phyla [19]. An increase in microbial diversity and macromolecules will lead to metabolic diversity and increase the chance of unintentional transformation of Hg. Performing a targeted metabolomics analysis of microbial fermentative metabolites could elucidate the mechanism behind gut microbial MeHg degradation.

This thesis leaned heavily on sequence-based microbiological approaches using peer-reviewed and open-sourced computational tools. One needs to be mindful of its caveat from genomic DNA extraction to the interpretation of those results. Biases are introduced at each stage

of the microbiological analysis from DNA extraction, sequencing technology used, and which analysis pipeline used [20,21]. With the addition of more samples, it will provide a more robust picture on genotype of MeHg degradation.

Chapters 4 and 5 provide a framework for developing a biomarker for early biological effect on the sentinel species in aquatic environments. In chapter 4, my dataset lacks a control river otters' population from areas without direct or indirect effects of oil sand activities such as oil pumps and pipelines. Studies have shown that oil sand activities leaked into the watershed, possibly affecting the gut microbiota of the river otter [22,23]. Following studies with broader and more extensive sampling and analyses would shine a light on some of the challenges encountered in chapter 4. In chapter 5, I have encountered similar challenges where sample size was small for each seabird. Moreover, fecal samples only represent the influence of diet on the seabirds' gut microbiome at the time of capture. Future experimentation exploring the metagenome can provide crucial insights into the mechanisms involved in the absorption and metabolism of Hg and selenium. These suggestions would eventually contribute to developing a robust and non-invasive biomarker for marine ecosystem health.

In conclusion, this thesis was, for the most part, exploratory in nature. However, my work has provided an important insight into MeHg demethylation in the human gut environment. I have shown that nutrient amendment to the diet can significantly alter the human gut microbial structure and transformation of environmental contaminant exposure. Moreover, I identified a novel mechanisms for demethylation of MeHg in the human gut environment by microbes. In chapters 4 and 5, I have shown that diet and prey selection played a significant role in shaping the gut microbial structure. I have characterized the gut microbiota of bioindicator species of freshwater

and marine ecosystems. My thesis delved into and explored the gut microbiota role in contaminant exposure, and these contributions are only the first of many steps in the overall understanding of the role of the gut microbiota in ecosystem health.

6.5 Reference Cited

Rothschild, D. *et al.* Environment dominates over host genetics in shaping human gut microbiota. *Nature* (2018). doi:10.1038/nature25973

2. Wu, Y. *et al.* Habitat environments impacted the gut microbiome of long-distance migratory swan geese but central species conserved. *Sci. Rep.* **8**, 1–11 (2018).

3. Seko, Y., Takahashi, M., Hasegawa, T. & Miura, T. Intestinal Absorption of Mercury in Vitro from Intestinal Contents of Methylmercury Administered Mice. *J. Heal. Sci.* **47**, 508–511 (2001).

4. Urano, T., Iwasaki, A., Himeno, S., Naganuma, A. & Imura, N. Absorption of methylmercury compounds from rat intestine. *Toxicol. Lett.* **50**, 159–64 (1990).

5. Nielsen, J. B. Toxicokinetics of mercuric chloride and methylmercuric chloride in mice. *J. Toxicol. Environ. Health* **37**, 85–122 (1992).

6. Nakamura, I., Hosokawa, K., Tamura, H. & Miura, T. Reduced mercury excretion with feces in germfree mice after oral administration of methyl mercury chloride. *Bull. Environ. Contam. Toxicol.* **17**, 528–33 (1977).

7. Lu, X. *et al.* Methylmercury uptake and degradation by methanotrophs. *Sci. Adv.* **3**, e1700041 (2017).

8. Oremland, R. S., Culbertson, C. W. & Winfrey, M. R. Methylmercury decomposition in sediments and bacterial cultures: involvement of methanogens and sulfate reducers in oxidative demethylation. *Appl. Environ. Microbiol.* **57**, 130–7 (1991).

9. Kronberg, R.-M., Schaefer, J. K., Björn, E. & Skyllberg, U. Mechanisms of Methyl Mercury Net Degradation in Alder Swamps: The Role of Methanogens and Abiotic Processes. *Environ. Sci. Technol. Lett.* acs.estlett.8b00081 (2018). doi:10.1021/acs.estlett.8b00081

10. Nelson, T. M., Rogers, T. L. & Brown, M. V. The Gut Bacterial Community of Mammals from Marine and Terrestrial Habitats. *PLoS One* **8**, e83655 (2013).

11. Bahl, M. I. *et al.* The gastrointestinal tract of farmed mink (Neovison vison) maintains a diverse mucosa-associated microbiota following a 3-day fasting period. *Microbiologyopen* **6**, (2017).

12. Sanders, J. G. *et al.* Baleen whales host a unique gut microbiome with similarities to both carnivores and herbivores. *Nat. Commun.* **6**, 8285 (2015).

13. Blévin, P. *et al.* Wide Range of Mercury Contamination in Chicks of Southern Ocean Seabirds. *PLoS One* **8**, e54508 (2013).

14. Van de Wiele, T., Van den Abbeele, P., Ossieur, W., Possemiers, S. & Marzorati, M. The Simulator of the Human Intestinal Microbial Ecosystem (SHIME®). in *The Impact of Food Bioactives on Health* 305–317 (Springer International Publishing, 2015). doi:10.1007/978-3-319-16104-4_27

15. Gill, S. R. *et al.* Metagenomic analysis of the human distal gut microbiome. *Science (80-.).* **312**, 1355–1359 (2006).

16. Eckburg, P. B. *et al.* Microbiology: Diversity of the human intestinal microbial flora. *Science (80-.).* **308**, 1635–1638 (2005).

17. Hillman, E. T., Lu, H., Yao, T. & Nakatsu, C. H. Microbial ecology along the gastrointestinal tract. *Microbes and Environments* **32**, 300–313 (2017).

18. Macfarlane, G. T., Gibson, G. R., Beatty, E. & Cummings, J. H. Estimation of short-chain fatty acid production from protein by human intestinal bacteria based on branched-chain fatty acid measurements. *FEMS Microbiol. Ecol.* **10**, 81–88 (1992).

19. Diether, N. E. & Willing, B. P. Microbial fermentation of dietary protein: An important factor in diet–microbe–host interaction. *Microorganisms* **7**, (2019).

20. Ross, M. G. *et al.* Characterizing and measuring bias in sequence data. *Genome Biol.* **14**, R51 (2013).

21. Xue, M., Wu, L., He, Y., Liang, H. & Wen, C. Biases during DNA extraction affect characterization of the microbiota associated with larvae of the Pacific white shrimp, Litopenaeus vannamei. *PeerJ* **2018**, (2018).

22. Korosi, J. B., Cooke, C. A., Eickmeyer, D. C., Kimpe, L. E. & Blais, J. M. In-situ bitumen extraction associated with increased petrogenic polycyclic aromatic compounds in lake sediments from the Cold Lake heavy oil fields (Alberta, Canada). *Environ. Pollut.* **218**, 915–922 (2016).

23. Schindler, D. W. Unravelling the complexity of pollution by the oil sands industry. *Proc. Natl. Acad. Sci.* **111**, 3209–3210 (2014).

6.6 Figure

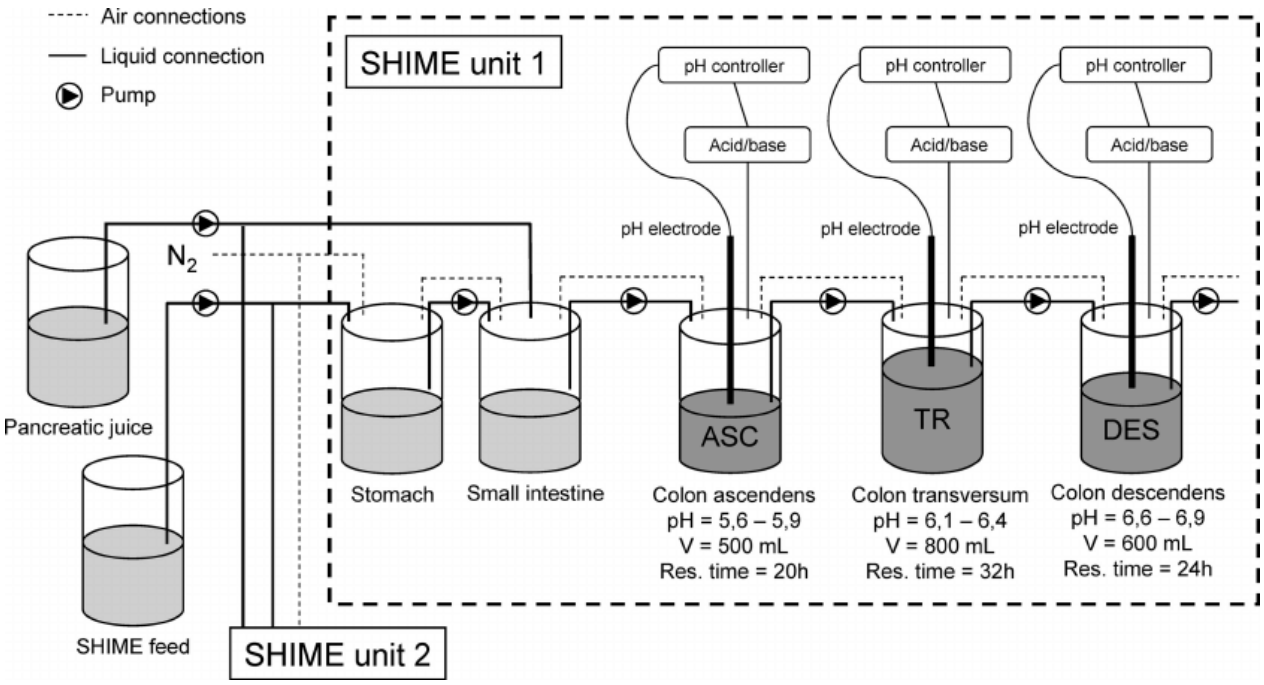

Figure 6.1 - Schematic representation of a Twin-SHIME which consists of two identical SHIME units, SHIME units 1 and 2. Liquid diet medium and pancreatic solution enter the vessel simulating the stomach and small intestine. After a residence time of 4 h in these sterile compartments, the suspension goes to three consecutive colon compartments, the ascending (ASC), transverse (TR), and descending (DES) colon compartments, each characterized by pH and residence times indicated above. With pH probes, acid (HCl 0.5N) and base (NaOH 0.5N) are added to maintain pH within range. These compartments are inoculated with human fecal microbiota (from feces:PBS (1:10) solution). All vessels are continuously stirred, kept anaerobic and at 37°C, and with daily flushing of the headspace with nitrogen.